

THE MORPHOLOGICAL MODELLING OF RIVER INTERVENTIONS

Master Thesis

Civil Engineering & Management

Marthe Oldenhof

April 2021



**UNIVERSITY
OF TWENTE.**

HKV
LIJN IN WATER

Cover picture from Rijkswaterstaat

The morphological modelling of river interventions

Author

M. (Marthe) Oldenhof

Graduation committee

Dr. Ir. D.C.M. Augustijn
Dr. Ir. R.P. van Denderen
Ir. L.R. Lokin

University of Twente
University of Twente / HKV Lijn in water
University of Twente / HKV Lijn in water

Preface

This thesis is the final work of my master programme Civil Engineering and Management at the Water Engineering and Management department of the University of Twente. In the previous months, I worked on the morphological modelling of river interventions. I enjoyed the technical aspects of this research and have gained a lot of new knowledge in the field of river morphology.

This research is done in collaboration with the University of Twente and HKV Lijn in water. I want to thank both organisations for the opportunity to do this master thesis. Despite the situation with Corona, I was able to work a few days at the office of HKV. This gave me the possibility to get to know the company better and meet inspiring people in the field of river and coastal engineering.

I want to thank my daily supervisors Lieke Lokin and Pepijn van Denderen for their feedback and support in doing this thesis. They made me enthusiastic about the topic of river engineering. The critical questions and remarks have made me think more about what I want to achieve with this research. Now, at the end of this thesis, I think there is a nice piece of work that hopefully others can use and further improve. Besides, I want to thank Denie Augustijn for being part of the graduation committee. The meetings with the committee were helpful and there was always a nice atmosphere.

Finally, I want to thank my friends and family for supporting me during the work on my thesis. The conversations about my master thesis let me reflect on what I have been doing.

I hope you enjoy reading my report.

Marthe Oldenhof

April, 2021

Summary

Rivers fulfil an important function in the natural ecosystem. They are a source of drinking water, a popular place for recreation, and they enable transport over water. To maintain these functions and guarantee safety against floods many river projects have been executed. The construction of river interventions affects the river morphodynamics. The interventions generally reduce the discharge that is conveyed within the main channel resulting in a smaller sediment transport capacity, and subsequent aggradation in the main channel. The objective of this research is to gain insight into the morphological effect of river interventions in a quick way. The equilibrium state is split up into a static component and a dynamic component. The static component of the equilibrium is found by a space-marching method. This means that the solution is found by stepping through space without the necessity of computing the transient phase. It significantly reduces the computation time compared to the more "traditional" models. An abridged version of the Backwater-Exner Model is used to find the dynamic component of the equilibrium state. We verified the rapid method with field measurements and the results of a Delft3D computation.

We studied the morphological effect of five different types of river interventions: the construction of a side channel, lowering of the floodplains, lowering of the groynes, widening of the main channel and dike relocation. We chose the size of the river interventions as such that the time-averaged bed level change is similar. However, we see large differences in the dynamic component of the equilibrium state between the river interventions. River interventions that change the geometry of the main channel cause the smallest fluctuations. River interventions in the floodplains are only activated during peak flow when the floodplains are inundated. Once the floodplains are inundated the changes in discharge caused by the river interventions are large, resulting in large bed level fluctuations.

Besides the deterministic model approach, the rapid method makes it possible to look into the uncertainties in morphological modelling and their sensitivity on the bed level. A Monte Carlo Simulation (MCS) is used to quantify the range of bed level fluctuations under seasonal variation in discharge, yearly sediment transport and varying hydraulic roughness. The relationship between discharge and bed level change can be expressed as an exponential fit for which the maximum bed level change reaches a limit by increasing discharges. River interventions that change the geometry of the main channel and the groynes have a small distribution of bed level changes. The distribution of bed level fluctuations is the largest for river intervention in the floodplains. It is recommended to use a MCS with varying discharges to quantify the range of bed level fluctuations for these type of river interventions. In a deterministic approach, the probability of peak flows is very small. Therefore the size and frequency of bed level fluctuations are strongly related to the hydrograph and the frequency of peak flows. The bed level is less sensitive to variations in yearly sediment transport and hydraulic roughness. An increase in these two parameter values results in a slight increase in the size of bed level variations of a couple of centimetres.

We suggest the rapid method as a useful tool in the inventory phase of river projects. The method can be used to make quick estimations of the morphological effect of different types of river interventions separately and combined. Combining river interventions with an opposite morphological effect can reduce the negative effect of a single intervention. The rapid method makes it possible to get insight into the single effect of the river interventions to understand the combined morphological effect of a complex river project, like the Room for Living Rivers. In this way, the rapid method that we developed is a useful tool in river management to gain insight into the morphological effect of river interventions in a quick way.

Samenvatting

Rivieren vervullen een belangrijke functie in het ecosysteem. Ze zijn een bron van drinkwater, een populaire plek voor recreatie en maken transport over water mogelijk. Om deze functies te kunnen onderhouden en om bescherming tegen overstromingen te kunnen waarborgen, zijn er verscheidene rivierprojecten uitgevoerd. De aanleg van rivierinterventies beïnvloedt de riviermorfologie. De maatregelen verminderen in het algemeen de hoeveelheid water dat door het zomerbed afgevoerd wordt, wat resulteert in een vermindering van de sedimenttransportcapaciteit. Dit leidt tot aanzanding in het zomerbed. Het doel van dit onderzoek is om op een snelle manier inzicht te krijgen in de effecten van rivierinterventies op de bodemhoogte. We splitsen de evenwichtstoestand van de rivierbodem op in een statische en een dynamische component. De statische component van het evenwicht wordt berekend met een space-marching methode. Dit betekent dat de oplossing bepaald wordt door ruimtelijke stappen zonder dat de overgangsfase tussen het initiële evenwicht en het nieuwe evenwicht berekend hoeft te worden. Het vermindert de rekentijd aanzienlijk in vergelijking met de meer "traditionele" modellen. Een verkorte versie van het Backwater-Exner model wordt gebruikt om de dynamische component van de evenwichtstoestand te vinden. We hebben deze snelle methode geverifieerd met metingen en de resultaten van een Delft3D-berekening.

We hebben van vijf verschillende rivierinterventies het morfologische effect bestudeerd: de aanleg van een nevengeul, het verlagen van de uiterwaarden, het verlagen van de kribben, het verbreden van het zomerbed en het verleggen van de dijk. De dimensie van de ingreep is zodanig bepaald dat de tijds-gemiddelde verandering in de bodemhoogte gelijk is. Echter, er zijn grote verschillen in de dynamische component tussen de rivierinterventies. Rivierinterventies die de geometrie van de hoofdgeul veranderen veroorzaken de kleinste bodemfluctuaties. Rivierinterventies in de uiterwaarde spelen alleen een rol bij piekafvoeren, wanneer de uiterwaarden meestromen. Indien de uiterwaarden meestromen dan veroorzaakt de lokale verandering in afvoer grote bodemfluctuaties.

Naast de deterministische modelaanpak biedt de snelle methode mogelijkheden om naar de onzekerheden bij het morfologisch modelleren en de gevoeligheid daarvan op de bodemhoogte te kijken. Een Monte Carlo Simulatie (MCS) is gebruikt om de mate van bodemfluctuaties bij veranderingen in afvoer, jaarlijkse sedimenttransport en variaties in bodemruwheden te kwantificeren. De relatie tussen afvoer en bodemhoogte kan uitgedrukt worden in een exponentieel verband waarbij de bodemhoogte een limiet bereikt bij een toename in afvoer. De rivierinterventies die de geometrie van de hoofdgeul en kribben aanpassen veroorzaken de kleinste veranderingen in bodemhoogte. De spreiding van bodemfluctuaties is het grootste voor rivierinterventies in de uiterwaarde. Voor dit type rivierinterventies raden we aan om een MCS te gebruiken met variërende afvoeren om de mate van bodemfluctuaties te kunnen kwantificeren. In een deterministische aanpak is de kans op piekafvoeren klein. De grootte en de frequentie van bodemfluctuaties hangt dus erg af van de reeks afvoeren die gebruikt wordt. De bodemhoogte is in mindere mate gevoelig voor veranderingen in jaarlijks sedimenttransport en bodemruwheden. Een toename in een van deze parameters veroorzaakt een kleine toename van enkele centimeters in de mate van bodemfluctuaties.

We doen de suggestie dat deze snelle methode een handig hulpmiddel is in de verkenningsfase van rivierprojecten. We gebruiken deze tool om snelle schattingen te maken van het morfologische effect van afzonderlijke rivierinterventies als ook gecombineerde interventies. Door rivierinterventies met een tegenovergesteld morfologisch effect te combineren, kan het negatieve effect van een enkele ingreep worden verminderd. De snelle methode maakt het mogelijk om inzicht te krijgen in het afzonderlijke effect van de rivierinterventies om het gecombineerde morfologische effect van een complex rivierproject, zoals Ruimte voor de Levende Rivieren, beter te begrijpen. Op deze manier is de door ons ontwikkelde methode een handig instrument in het rivierbeheer zodat er op een snelle manier inzicht verkregen worden kan in het morfologische effect van rivierinterventies.

List of Abbreviations

| Abbreviation | Description |
|---------------------|---------------------------|
| BWE | Backwater-Exner |
| BWS | Backwater segment |
| Fp | Floodplain |
| Gr | Groyne |
| Mc | Main channel |
| MCS | Monte Carlo Simulation |
| QNFS | Quasi-normal flow segment |
| rkm | River kilometer |
| RfLR | Room for Living Rivers |
| RftR | Room for the River |
| Sc | Side channel |
| std | standard deviation |
| UBS | Upstream boundary segment |

Contents

| | |
|---|------------|
| Preface | i |
| Summary | ii |
| Samenvatting | iii |
| List of Abbreviations | iv |
| 1 Introduction | 1 |
| 1.1 Background | 2 |
| 1.2 Problem formulation | 3 |
| 1.3 Research objective and questions | 4 |
| 1.4 Report outline | 4 |
| 2 Theory | 5 |
| 2.1 Schematisation of a river | 5 |
| 2.2 River Modelling | 7 |
| 2.3 Morphological effect of river interventions | 7 |
| 2.4 Uncertainties in river modelling | 8 |
| 2.5 River projects | 9 |
| 3 Model description | 11 |
| 3.1 Backwater-Exner Model | 11 |
| 3.2 Space-marching model | 12 |
| 3.3 Implementation river interventions | 14 |
| 4 Method | 17 |
| 4.1 Model testing and verification | 18 |
| 4.2 Morphological impact of river interventions | 20 |
| 4.3 Uncertainties in bed level fluctuations | 22 |
| 4.4 Multiple river interventions | 26 |
| 5 Model testing and verification | 29 |
| 5.1 Model choice | 29 |
| 5.2 Model verification | 31 |
| 5.3 Conclusion | 34 |
| 6 Morphological impact of river interventions | 35 |
| 6.1 Average bed level change | 35 |
| 6.2 Dynamic impact of river interventions | 36 |
| 6.3 Conclusion | 40 |
| 7 Uncertainties in bed level fluctuations | 41 |
| 7.1 Generating discharge series | 41 |
| 7.2 Results Monte Carlo Simulation | 41 |
| 7.3 Conclusion | 46 |
| 8 Multiple river interventions | 47 |
| 8.1 Combining river interventions | 47 |
| 8.2 Sequential river interventions | 49 |
| 8.3 Conclusion | 50 |

| | |
|---|-----------|
| 9 Discussion | 51 |
| 9.1 Reflection on method & reliability of results | 51 |
| 9.2 Value of this research | 54 |
| 10 Conclusion & Recommendations | 56 |
| 10.1 Conclusion | 56 |
| 10.2 Recommendations | 56 |
| References | 58 |
| Appendices | 61 |
| A List of Symbols | 61 |
| B Study area river Waal | 62 |
| C Model Testing and Verification | 64 |
| D Uncertainties in bed level fluctuations | 68 |
| E Combination of river interventions | 71 |

1 Introduction

Rivers fulfil an important function in the natural ecosystem. They are a source of drinking water, a popular place for recreation, and they enable transport over water. To maintain these functions and guarantee safety against flooding many river projects have been executed, resulting in regulated rivers with dikes, groynes and floodplains. The river training measures that were introduced in the 19th and 20th century, such as dikes, width constrictions and bend cutoffs, made the river system lose its hydrological resilience (Frings et al., 2009; Havinga, 2020). To mitigate the effect of the reduced hydrological resilience, new river projects were implemented. Until the end of the 20th century, it was thought that the construction of even higher dikes and more powerful pumping stations would be the only solution (Havinga, 2020). This insight gradually shifted towards a more sustainable and ecological approach. Instead of putting rivers in straitjackets by constricting them between dikes, we should give them more space (Drenthen, 2009). In the Netherlands, this resulted in the Room for the River project with a set of different river interventions to improve the river functions and increase flood safety (Van Alphen, 2020). But the need for sustainable solutions to maintain the safety level, and meanwhile optimise the navigation and ecological functions, poses complex questions (Schielen and Havinga, 2010). The different functions of a river lead to large conflicts of interests. For example, when measures in the floodplains are planned, habitats often need to be mitigated (Havinga et al., 2010). To prepare for the right long-term decisions, proper morphological analysis are needed (Schielen and Havinga, 2010).

In this research, we look into the morphological effect of different river interventions. The study focuses on one of the river branches of the river Rhine, the river Waal in the Netherlands (Fig. 1.1). The river Waal is a distributary of the river Rhine and, by discharge, the largest river in the Rhine-Meuse-Scheldt Delta. With a rapid method, we study the effect of single and combined interventions. This tool allows for identifying potential bottlenecks for shipping or flood safety already during the inventory phase.



Figure 1.1: Dutch rivers, including the river Waal running from the Pannerdensch Canal into the Merwede (Klijn et al., 2018)

1.1 Background

A river is characterised by its channel slope, channel width and grain size distribution of the bed surface sediment (bed surface texture). These river characteristics are controlled by the hydrograph, sediment flux and the downstream base level (Arkesteijn et al., 2019). The hydrograph represents the distribution of discharges over a large time scale. Under normal-flow conditions, the three controls are sustained, meaning that there are only small temporal and spatial variations that do not have a long-term impact (Blom et al., 2017). The river system can correct for these small changes by a negative feedback that will bring the characteristic values of a river back to their original balance point (Bolla Pittaluga et al., 2014). This balance point between erosion and deposition is the equilibrium state (Ahnert, 1994). There are four types of equilibrium states defined (Arkesteijn et al., 2019). If there are no changes in bed level over time, a static equilibrium establishes (Fig. 1.2a). Although the bed level of many rivers is time-averaged stable, there are fluctuations in the bed level due to variations in discharge and sediment supply on the short time scale (De Vries, 1993). The local differences in discharge and the corresponding sediment transport cause temporal accumulation and erosion. This is called a dynamic equilibrium (Fig. 1.2b). If the river controls change slowly relative to the response timescale of a channel, the channel geometry keeps pace with the changing controls (Arkesteijn et al., 2019). This is called a static quasi-equilibrium state, because the time-averaged bed level changes slowly corresponding to the changes in river controls (Fig. 1.2c). If the quasi-equilibrium state shows temporal fluctuations in bed elevation, it is a dynamic quasi-equilibrium (Fig. 1.2d). This research is limited to the dynamic equilibrium states.

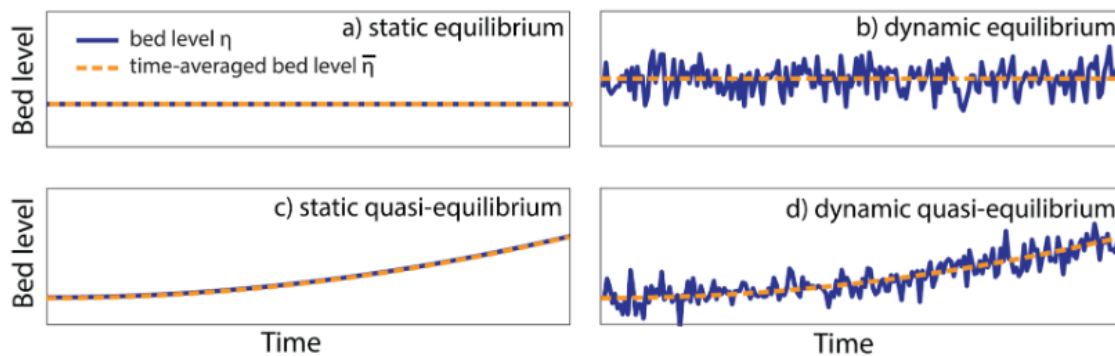


Figure 1.2: Schematisation of different types of equilibria (Arkesteijn et al., 2019)

Variations to the equilibrium state can be distinguished by their spatial scale. This research focuses on the intermediate scale in which bed level fluctuations are caused by changes in the geometry of the river. The small and large scale are not included in this research. The small scale corresponds to river dunes. Variations in the large scale are caused by subsidence and uplift.

The construction of a river intervention changes the river geometry. This results in large changes in the river controls. The changes are too large for the river system to go back to its initial equilibrium state. Over time the river system will find a new balance point between erosion and deposition. For most river interventions, like the construction of a side channel or lowering the floodplains, the initial morphological response is aggradation at the upstream end of the intervention and degradation at the downstream end. Over time, the sediment hump and scour hole migrate downstream and disperse over space. The bed slope alters and the water level upstream of the intervention increases. The increase in bed elevation can cause bottlenecks for shipping. To maintain the shipping routes, large amounts of sediment need to be dredged. As an example, computations have shown that the Room for the River project results in excessive maintenance cost for shipping purposes due to an increase in dredging volumes (Havinga et al., 2013; Van Vuren et al., 2015).

For a sustainable river approach, it is necessary to study the effect of river interventions. There are several methods to study the flow and sediment transport in a river. Field measurements provide insight into the actual hydrodynamics and morphology. Historical data makes it possible to map morphological developments of the past, like the development of the bed profile. Another tool for studying flow and sediment transport is computational modelling (El kadi Abderrezzak and Paquier, 2009). Much effort has been put into the development of numerical model systems, like the one-dimensional model SOBEK and the two- and three-dimensional model systems WAQUA and Delft3D (Van der Klis, 2003). The choice of a certain model depends on the objective of the study, the nature and complexity of the problem itself, and available time and budget for solving the problem (Papanicolaou et al., 2008). A one-dimensional model approach applies to rivers in which the horizontal length scale of the flow is much larger than the one normal to the direction of the flow. If the focus is on small and intermediate spatial scales the preference is given to the use of multi-dimensional models (Van Vuren, 2006). The disadvantage of these complex numerical models is the long computation time. For that reason, rules of thumb, like WAQmorf (Sieben, 2011), can be applied to get a quick insight into morphological changes. These rules of thumb make use of an idealised and simplified view of the processes in a river on a local scale with the assumption of uniform and steady flow conditions (Paarlberg, 2009). Arkesteijn et al. (2019) developed a rapid method to determine the quasi-equilibrium geometry. With the use of a space-marching method, the computational time is considerably reduced compared to the complex numerical models like SOBEK and Delft3D. The model is strongly simplified, but it gives a better representation than applying rules of thumb since the dynamic component of the equilibrium is included.

1.2 Problem formulation

Recent river management studies in the Netherlands have focused on three topics: flood safety, navigability and environmental issues (Lambeek et al., 2004). These three topics can lead to large conflicts of interest (Havinga et al., 2010). As part of the Room for the River project, many river interventions were carried out that affect the river morphology. The interventions generally reduce the discharge that is conveyed within the main channel resulting in a smaller sediment transport capacity, and subsequent aggradation in the main channel (Van Denderen et al., 2020; Van Vuren et al., 2015). Additionally, variations in discharge cause temporal bed level changes. These bed level fluctuations might have negative consequences on navigability and result in large dredging volumes (Havinga et al., 2013). But the bed aggradation can compensate for the ongoing bed erosion caused by the river training works executed in the previous century (Havinga, 2020; Rudolph, 2018). Proper morphological analysis needs to be carried out from the very beginning to ensure that in the final design the negative effects on the river functions are minimal (Havinga et al., 2010).

In the inventory phase, time and budget are limited. Existing morphological models that can be used to investigate bed level changes due to river interventions are complex and have long computation times (like WAQUA and Delft3D). These models are not suitable for calculating a set of different scenarios since computation times are too long. Besides, predicting future morphological effects entails uncertainties. For example, the weather, that influences the amount of discharge, cannot be deterministically predicted more than a few days ahead (De Vriend, 2002). The recommended practice is to quantify the uncertainty of model predictions (Berends, 2020). This calls for a stochastic method that enables us to indicate ranges of possible morphodynamic states, and the estimation of undesired morphological effects (Van Vuren, 2005b). Rules of thumb, like WAQmorf, can be used to make calculations with variations in input variables to include the stochastic behaviour of the river system. These rules make use of an idealised situation in which only a static equilibrium is calculated (Sieben, 2011). However, in the idealised view of WAQmorf the dynamics at the downstream end of a river caused by the backwater effect are not included (Paarlberg, 2009).

So, already in the inventory phase more and quick insight is needed into the morphological effect of river interventions such that interventions can be compared based on their effect. This knowledge will help us to make smart use of river interventions and to improve the river system in the future.

1.3 Research objective and questions

In this research, we are looking into the morphological effect of several river interventions. In this way, we want to meet the general research objective. To do so, we formulate a research question with a set of sub-questions. The answers to these sub-questions will eventually lead to a solution to the problem statement of this research.

Research objective

The objective of this research is to gain insight into the morphological effect of various types of river interventions and investigate how we can use this knowledge on bed level fluctuations in the inventory phase of complex river projects.

Main research question

What is the morphological effect of various types of river interventions, using a rapid method?

Sub-questions

To answer the research question presented above we use a rapid method, based on the principles of the space-marching model of Arkesteijn et al. (2019). The space-marching model consists of a set of sub-models. We look for the best sub-model to use to investigate bed level changes due to river interventions. A set of four sub-questions will guide us through this research and make sure that at the end we can successfully meet the research objective.

1. What is the best model to use to make accurate and rapid calculations for temporal and spatial bed level fluctuations caused by river interventions?
2. How does the distribution of bed level fluctuations for various types of river interventions change under variable flow discharges?
3. How large is the uncertainty in the distribution of bed level fluctuations for various types of river interventions?
4. What is the effect of combined river interventions on the distribution of bed level fluctuations?

1.4 Report outline

The thesis is structured in the following way. In Chapter 2, the most essential background information about the characteristics and morphology of rivers is given. Chapter 3 describes the principles of the space-marching model of Arkesteijn et al. (2019) and the more traditional Backwater-Exner Model. In Chapter 4, the method of this research is clarified. The result of the first sub-question is presented in Chapter 5. For the model testing, we verify the model with measurements and with the results of the computations of a more complex numerical model, Delft3D. Chapter 6 gives the results of the second sub-question. It shows the distribution of bed level fluctuations caused by different river interventions. With a Monte Carlo Simulation, we quantify the uncertainties in bed level fluctuations, corresponding to sub-question 3. These results are presented in Chapter 7. Finally, in Chapter 8 we look into multiple river interventions of the Room for Living Rivers project to study the combined effect on the bed level change, to find a solution to sub-question 4. Chapter 9 gives a discussion about the obtained results. Finally, in Chapter 10, the conclusion is formulated that solves the research question and meets the research objective. Based on this conclusion, recommendations are given for the application of this research in the work field.

Flume experiments and model simulations (Wong and Parker, 2006; Viparelli et al., 2011; An et al., 2017) have shown that the three segments respond differently to variations in discharge. The bed elevation and bed slope in the QNFS and BWS are invariant with changing discharges, while in the UBS, the bed elevation fluctuates cyclically with the variations in discharge (Wong and Parker, 2006). The discordance between constant feed rate from the upstream boundary condition and varying discharge leads to cyclic aggradation and degradation (Wong and Parker, 2006). Figure 2.2 shows the behaviour of the bed slope and grain size over a river reach with an upstream boundary segment, quasi-normal flow segment and a backwater segment, obtained by a model simulation of the Trinity River by Viparelli et al. (2011).

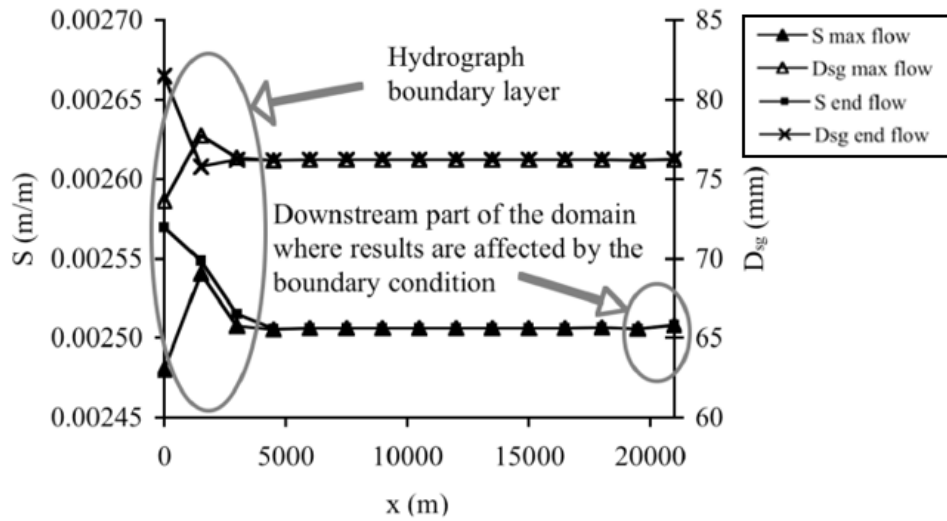


Figure 2.2: Illustration of the nature of the hydrograph boundary layer for the bed slope (S) and the grain size (D_{gs}) as a result of a model simulation. Here, "max" refers to the maximum flow of the hydrograph, and "end" refers to the end of the hydrograph (Viparelli et al., 2011)

The length of the UBS depends on the sediment feed rate and the hydraulic and morphological response time. The hydraulic response time is much shorter than the morphological adjustment time. The morphological adjustment time depends on the characteristics of the river (Arkesteijn et al., 2019). The boundary layer δ [m] extends from $x = 0$ to $x = \delta$, with (Wong and Parker, 2006):

$$\frac{\delta}{L} \sim \mathcal{E}^{1/2} \quad (2.1)$$

Here, L [m] is the total length of the river reach and \mathcal{E} [-] is a dimensionless time ratio between the hydrograph duration (T_h) [s] and the characteristic morphodynamic response time (T_m) [s]. The morphodynamic response time is calculated as:

$$T_m = \frac{(1 - \epsilon)S_0 L^2}{q_{bf}} \quad (2.2)$$

with ϵ [-] the bed porosity which is typically 0.4 for Dutch rivers (Ribberink, 2011), S_0 [-] the initial bed slope, and q_{bf} [m^2/s] the constant feed rate of sediment per unit width.

2.2 River Modelling

The interaction between water movement and sediment movement in a river is a complex process since there is interaction in all three dimensions (De Vries, 1975). For model purposes, simplifications and assumptions are made to formulate the problem as a simplified three-dimensional case or a reduced one- or two-dimensional case. For models that study the large spatial scale, one-dimensional situations are often used, whereas preference is given to the use of multi-dimensional models if the focus is on the small and intermediate spatial scale (Van Vuren, 2006). Since we are focusing on human interventions on the large scale, a one-dimensional model is used. Therefore, the further theory is based on a one-dimensional model situation.

The morphodynamic processes in a river can be described by the continuity- and momentum equation for water and sediment. For a small element of the river Δx , the mass and momentum of the water are conserved. The conservation of mass (Eq. 2.3) and momentum (Eq. 2.4) in a one-dimensional situation are given by (Parker, 2004):

$$\frac{\partial h}{\partial t} + \frac{\partial(uh)}{\partial x} = 0 \quad (2.3)$$

$$\frac{\partial(uh)}{\partial t} + u \frac{\partial(u^2h)}{\partial x} = -\frac{1}{2}g \frac{\partial h^2}{\partial x} - gh \frac{\partial \eta}{\partial x} - c_f u^2 \quad (2.4)$$

The water depth is given by h [m], u [m/s] represent the depth-averaged flow velocity, η [m] the bed elevation, and c_f [-] the bed friction coefficient. g represents the acceleration due to gravity and is equal to 9.81 m/s^2 . The conservation of mass between sediment at the river bed of a channel and sediment that is being transported, is described by the Exner equation (Exner, 1920):

$$(1 - \epsilon) \frac{\partial \eta}{\partial t} + \frac{\partial q_s}{\partial u} \frac{\partial u}{\partial x} = 0. \quad (2.5)$$

Here, q_s [m^2/s] the sediment transport per unit width.

In case of a steady gradually varied flow ($\partial h/\partial t = 0$), the mass and momentum equation can be reduced to get the backwater equation:

$$\frac{dh}{dx} = \frac{S - S_f}{1 - Fr^2}. \quad (2.6)$$

Here, S [-] is the bed slope, given as $-\partial \eta/\partial x$, S_f [-] denotes the friction slope defined as $S_f = c_f Fr^2$ and Fr [-] the Froude number defined as $Fr = u/\sqrt{gh}$.

2.3 Morphological effect of river interventions

After the construction of a river intervention, the hydrodynamic and morphodynamics will change. Depending on the size and type of the intervention, a certain fraction of the discharge in the main channel will be extracted by the river intervention. As an example, we take the construction of a side channel (see Fig. 2.3). At the upstream end, water is extracted from the main channel to the side channel. The sudden decrease in discharge in the main channel results in a decrease in water depth (h). As a consequence, the flow velocity decreases which results in a decrease in the capacity of sediment transport. Less sediment can be transported by the flow, resulting in sediment deposition. So, at the upstream end of the intervention, a sediment hump develops. At the downstream end of the intervention, the processes are inverse. The discharge suddenly increases downstream of the intervention. As a consequence, the sediment transport capacity increases resulting in erosion. A scour hole develops and migrates downstream. Over time, the perturbations in bed elevation migrate downstream and disperse over space. A new equilibrium is found in which water depth and bed elevation are in balance. Between the upstream and downstream end of the river intervention, the bed elevation has been increased by a couple of centimetres. Upstream of the river interventions, the water slope and bed slope are altered.

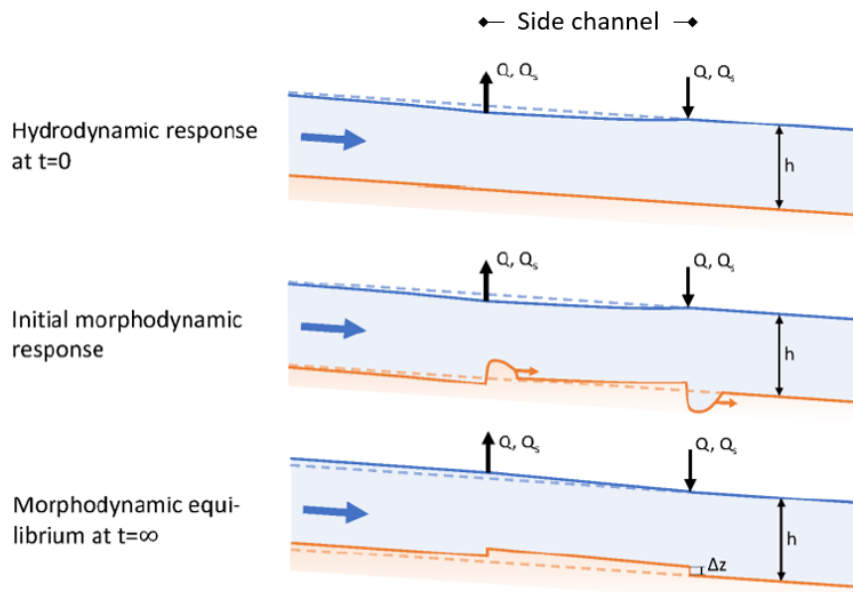


Figure 2.3: Longitudinal profile with initial and long-term morphodynamic response for the implementation of a side channel with constant sediment transport and discharge (Paarlberg and Schippers, 2020)

2.4 Uncertainties in river modelling

Modelling the behaviour of river systems entails a lot of uncertainty. Not only the river system behaviour itself is inherently uncertain (Van Vuren, 2005b), also the assumptions and simplifications made for model purposes result in uncertainties in the outcome. Understanding the uncertainties is important to make a meaningful interpretation of this model outcome (Pappenberger et al., 2006). In river modelling, much effort is put into quantifying confidence intervals. This is done for water levels during floods (Straatsma and Huthoff, 2011; Warmink et al., 2013), but also for long-term morphological changes (Van der Klis, 2003; Van Vuren, 2005b).

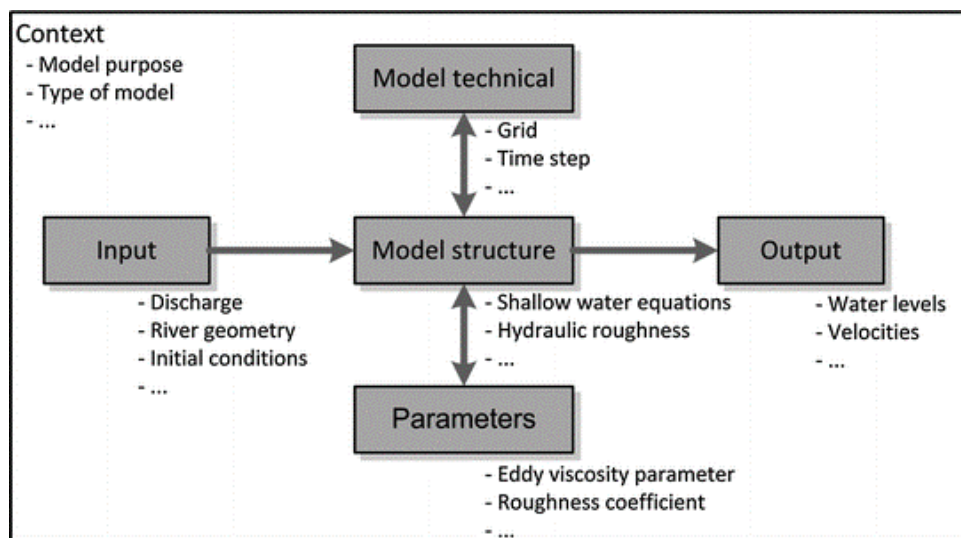


Figure 2.4: Example of the global identification of uncertainties for a river model (Warmink and Booij, 2015)

For river modelling, the uncertainties can be classified into five categories (Van Vuren, 2005b; Warmink and Booij, 2015) (Fig. 2.4): the context, input, model structure, model technical, and parameters. Based on the model purpose, a choice is made for a certain model. This model includes model uncertainties due to assumptions, simplifications and schematisations. In addition, model uncertainties can be induced by the technical set-up of the model, which includes the numerical approximation of mathematical processes (Van Vuren, 2005b). In this research, we are only looking into the statistical uncertainties caused by the input, including boundary conditions, initial conditions, and model parameters. These uncertainties are caused by variability and limited knowledge (Van Asselt and Rotmans, 2002). For example, the extreme conditions that we are dealing with are rare. In principle, this uncertainty can be reduced by waiting for more statistical information. In practice, we do not have the time to wait so long (De Vriend, 2002).

Examples of input uncertainties in river morphological models are (Van der Klis, 2003):

- Future water discharge
- Future sediment supply
- River geometry
- Initial bed level
- Grain size bed material
- Hydraulic roughness

2.5 River projects

Rivers fulfil an important ecological and economical function. However, they constitute a risk of flooding. In the 18th century, every generation in the Netherlands experienced several floodings (Sieben, 2009). With the rise of relatively large scale industrial activities in the 19th century, the importance of large rivers as shipping routes increased as well (Smit, 1985). This resulted in large-scale river training aiming for better navigation and safety of the rivers (Smit, 1985). Rivers were straightened and dredged and groynes were placed to give the river a narrow uniform width (Le et al., 2020). The morphological response of the river to these training works resulted in an incision process that reached a rate of two centimetres per year (Sieben, 2009). The erosion of the river bed has a negative impact on navigation since the bed level at locations with non-erodible layers, and the foundation of bridges and groynes does not change. River projects are prepared and executed to increase discharge capacity for flood defence and maintaining and improving navigability at low flow.

Room for the River

The Room for the River (RftR) programme is an integral project to ensure the required level of protection against river flooding and contribute to the improvement of spatial quality in the river area (Zevenbergen et al., 2015). It marks the transition from dike improvement to an integrated approach with hydraulic effectiveness, ecological robustness, and cultural meaning as core values (Van Alphen, 2020). A set of river interventions (Fig. 2.5), including the construction of a side channel and widening of the main channel, leads to more room for the river. In the short term, the water level decreases (Fig.2.3). But, in the long-term, the decrease in water level results in a decrease in flow velocity which leads to a drop in sediment transport. This causes bed level aggradation which forms a bottleneck for shipping during low water levels. To guarantee sufficient water depth for shipping the bed level needs to be dredged. This results in high maintenance costs. Van Vuren et al. (2015) have shown that, due to the river interventions in the river Waal, dredging amounts will be increased by about 10% compared to the present situation. The sediment transport gradient decreases due to human intervention, resulting in less bed degradation. This leads to smaller equilibrium depths resulting in increasing dredging quantities.

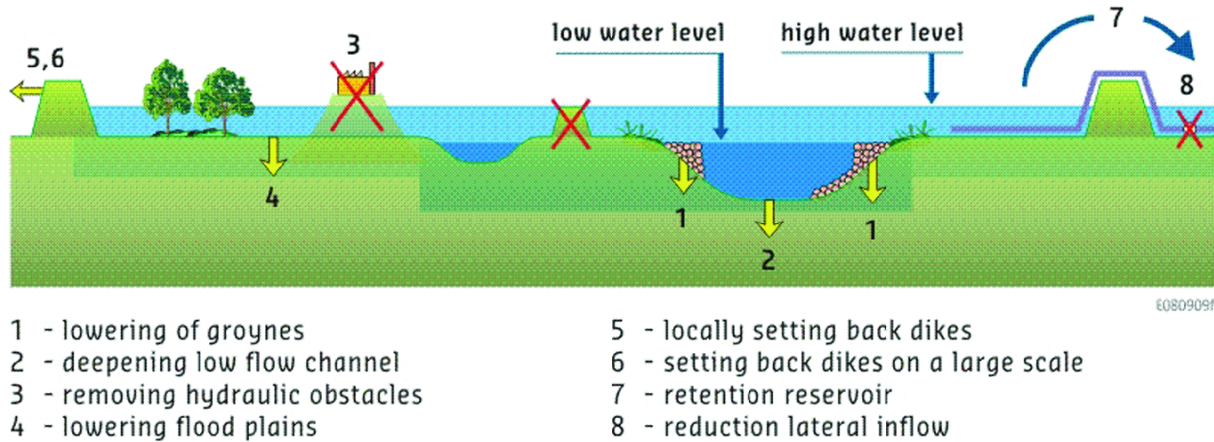


Figure 2.5: Eight different Room for the River measures (Silva et al., 2001)

Room for Living Rivers

Since the normalisation of the rivers, the river systems are relatively uniform with two basic functions; discharging water and navigation (Smit, 1985). The diversity of the ecosystem around the rivers, which is also one of the functions of natural streams, has been declined. The project Room for Living Rivers (RfLR) aims for living and climate-resilient rivers in which nature can flourish and people can live, work and recreate safely. The project focuses on the mitigation of the ongoing erosion of the bed level. By creating more room for the river, the flow velocities will decrease which result in a decrease in the sediment transport capacity. The interventions of RfLR focus on the mean water discharges where a large part of the annual sediment transport takes place (Barneveld et al., 2019). The river interventions of this project are based on river widening. The interventions are lowering floodplains, removing summer dikes, and lowering groynes. To compensate for the possible low water levels during drought periods, longitudinal dams can be placed. Barneveld et al. (2019) investigated whether (a combination of) measurement of the river widening plans of RfLR contribute to stop or decrease the erosion of the bed level of the river Waal in the Netherlands. They concluded that the widening of the river has a positive effect on the decrease in the sediment transport capacity and erosion in the long-term.

3 Model description

This research focuses on the use of a simple and rapid method to calculate the changes in bed elevation due to river interventions. We use the principles of the model of Arkesteijn et al. (2019) and adapt it to make the model applicable for river interventions. Arkesteijn et al. (2019) use a space-marching model that is significantly different from the traditional time-marching Backwater-Exner Model. With a time-marching model, the solution is found by walking through time. For each time step a hydrodynamic and morphodynamic update is made (Fig. 3.1). This results in many computations. In a space-marching model, the solution is found by walking through space. Per spatial step, the weighted averaged discharge over time is calculated. Based on this value, the equilibrium characteristics are calculated. This reduces the computation time since the transient phase between two equilibrium states is not needed.

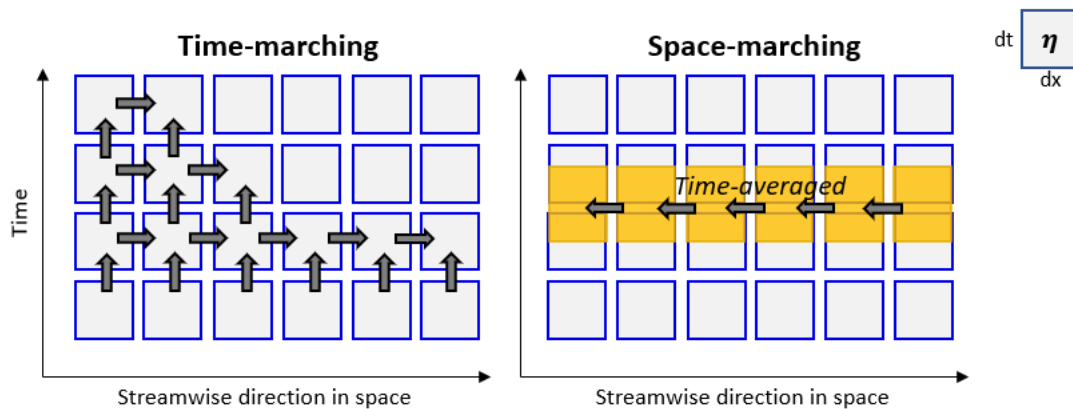


Figure 3.1: Time-marching versus space-marching. The arrows indicate the direction of marching. The squares represent the value of the bed elevation in a grid cell for a certain time step. In a space-marching model, first, the weighted-averaged discharge is calculated. Then, the time-averaged bed elevation is found.

In this chapter, an explanation of the principles of Arkesteijn’s model and the additions to it are given. First, the traditional Backwater-Exner Model (BWE) is explained. Second, the space-marching method of Arkesteijn et al. (2019) is discussed including the assumptions and simplifications that are made. Then, the implementation of river interventions into the model is explained.

3.1 Backwater-Exner Model

The BWE Model can be seen as a traditional and robust time-marching model that solves a system of partial differential equations through time. The initial condition follows from Model A (Fig. 3.2), which is part of the space-marching model of Arkesteijn et al. (2019) and calculates the static component of the equilibrium state. The result of Model A can be seen as a first estimation for the equilibrium state such that the computation time of the BWE model reduces. Further explanation about Model A is given in section 3.2.2. Arkesteijn et al. (2019) use the BWE model to verify their space-marching method. The BWE Model is part of the one-dimensional numerical research code Elv (Blom et al., 2017; Chavarrías et al., 2018). It solves the flow, bed elevation, and grain size distribution in a decoupled manner. The water level is updated using the backwater equation (Eq. 2.6). The bed elevation is updated with the Exner equation (Eq. 2.5). The model also includes an update on grain size distribution. However, this update is ignored in this research because the analysis is limited to uni-sized sediment and bed-material load only (Arkesteijn et al., 2019).

The original BWE model uses a cycled hydrograph and repeats it 1000 times. It is assumed that after 1000 repeated hydrographs, corresponding to a simulation of 100 000 years, the river system is in an equilibrium state. Taking this equilibrium state, the dynamics in bed elevation due to variation in dis-

charge can be calculated. The disadvantage of this original BWE model is the long computation time. To run 100 000 years takes about a day. Since we are interested in a rapid model, we use an abridged version of the BWE model. Instead of running 1000 repeated hydrographs, the model uses one single hydrograph. We assume that the initial estimation by Model A is accurate enough to produce reliable results after one hydrograph.

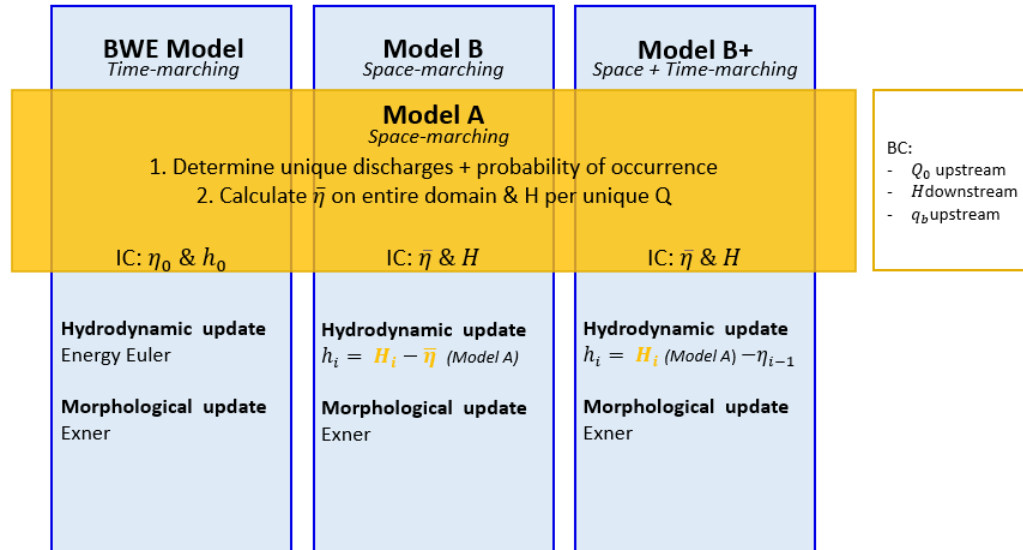


Figure 3.2: Schematisation of the BWE Model, Model B and B+ that all three the results of Model A as initial condition (IC). The time-averaged or static component of the equilibrium calculated by Model A uses a set of boundary conditions (BC). Part of the hydrodynamic of Model B and B+ follows from Model A.

3.2 Space-marching model

Arkesteijn et al. (2019) developed a one-dimensional numerical space-marching model that simulates the evolution of the bed level of a river for a dynamic quasi-equilibrium. The model makes a distinction between the quasi-static and the dynamic component of the equilibrium state. First, the time-averaged or static component of the equilibrium state is calculated with Model A (Fig. 3.2). The result is based on the weighted average discharge obtained from the hydrograph. Second, the fluctuations in bed elevation, or dynamic component of the equilibrium state, is calculated with Model B. The size of fluctuations is determined per discharge level. The results of both components can be superimposed to reproduce similar results as the BWE Model.

3.2.1 General model principles

With a space-marching method, the solution is found by stepping through space, without the necessity of computing the transient phase between two equilibrium states. This results in a decrease in computation time, which makes the model suitable as a rapid assessment tool for bed level variations. The equilibrium state (or quasi-equilibrium state) is characterised by (quasi-)static and dynamic components. These components define the characteristic timescale at which the dynamics average out. For the bed level η [m] a distinction is made between the quasi-static component ($\bar{\eta}$) and the dynamic or fluctuating component ($\Delta\eta$):

$$\eta = \bar{\eta} + \Delta\eta. \quad (3.1)$$

The quasi-static component equals the time-averaged elevation. The time-averaged value of the dynamic component equals zero, since the fluctuations in bed level average out.

Similar to the bed level, the bed slope S [-] can be divided into a quasi-static component (\bar{S}) and a dynamic component (ΔS):

$$S = \bar{S} + \Delta S. \quad (3.2)$$

Arkesteijn et al. (2019) showed that irrespective of the dynamics, the bed slope of a backwater or quasi-normal flow segment can be approximated as quasi-static. In other words, the dynamic component of the bed slope approximates zero. Therefore, the bed slope is calculated as $S = \bar{S}$. This is called the static slope approximation. This approximation is only valid if the short-term fluctuations of the bed slope are small compared to the slowly varying slope \bar{S} .

The relation between the temporal changes in bed level and the bed slope is given by a modified Exner equation. This equation combines the Exner equation (Eq. 2.5) with the backwater equation (Eq. 2.6).

$$\frac{\partial \eta}{\partial t} = \lambda(\bar{S} - S_f). \quad (3.3)$$

Here λ [m/s] denotes the characteristic celerity of the changes in bed elevation. This indicates the speed at which a perturbation in the bed level, for instance a sediment hump, propagates downstream. λ is expressed as

$$\lambda = \frac{1}{1 - \epsilon} \frac{1}{1 - Fr^2} \frac{u}{h} \frac{\partial q_s}{\partial u}. \quad (3.4)$$

3.2.2 Model A

Model A computes the static component of the equilibrium state. The solution is found by averaging the modified Exner equation over time (Eq. 3.3). This results in

$$\frac{\partial \bar{\eta}}{\partial t} = \bar{\lambda} \bar{S} - \lambda \bar{S}_f. \quad (3.5)$$

In a static equilibrium there are no changes in bed level over time. In a quasi-static equilibrium the changes in bed level average out over time. So, in both cases it can be assumed that $\partial \bar{\eta} / \partial t = 0$. This results in a simplification of equation 3.5.

$$\bar{S} = \frac{\lambda \bar{S}_f}{\bar{\lambda}} \quad (3.6)$$

Here, the time-averaged bed slope (\bar{S}) is given as a function of the time-averaged friction slope (\bar{S}_f) times the bed celerity (λ) divided by the time-averaged bed celerity ($\bar{\lambda}$). The time-averaged bed slope is used to calculate the static component of the bed elevation ($\bar{\eta}$). The system of equations for bed slope and bed level is solved by marching through space, which means that quasi-equilibrium channel geometry is solved from downstream to upstream. The bed slope is found by the weighted average discharge and is used to calculate the bed level in the upstream grid cell. The spatial step is 10 metres which is small with respect to the spatial scale of the problem, which is more than one hundred kilometres, to ensure the stability of the system.

For calculations of the sediment transport, the bedload transport relation of Meyer-Peter and Müller (Meyer-Peter and Müller, 1948) is used. For the friction coefficient, the relation of Manning (Manning et al., 1890) is used.

3.2.3 Model B

The dynamic component of the bed level is found by the numerical solution that builds on the quasi-static component that is found by Model A (Fig. 3.2). The dynamic component is found by marching

through space from downstream to upstream, similar to Model A. The dynamic bed elevation is found by the difference in sediment transport between two successive grid cells. The sediment transport is calculated with the water depth obtained from model A. The modified Exner equation (Eq. 3.3) with $\eta = \bar{\eta} + \Delta\eta$ is used to the short timescale. In this situation, the quasi-static bed elevation, ($\bar{\eta}$), does not vary at the short timescale ($\partial\bar{\eta}/\partial t = 0$):

$$\frac{\partial\Delta\eta}{\partial t} = \lambda(\bar{S} - S_f). \quad (3.7)$$

Here, the bed celerity λ and friction slope S_f depend on time and follow from Model A. The time-averaged bed slope \bar{S} (Eq. 3.6) follows from Model A as well. The dynamic component of the bed elevation is calculated using the Exner equation (Eq. 2.5) to the short timescale:

$$\frac{\partial\Delta\eta}{\partial t} = -\frac{\partial q_s}{\partial x} \frac{1}{1 - \epsilon}. \quad (3.8)$$

3.2.4 Model B+

In the original model of Arkesteijn et al. (2019) the water depth, h [m], is calculated with the time-averaged bed level obtained from Model A. Using only the time-averaged bed level to calculate the water depth, gives a good approximation in situations where the fluctuations of the bed elevation are relatively small. However, if the fluctuations in bed elevation are relatively large, these variations will affect the water depth and in turn, the water depth will affect the temporal bed elevation.

The water depth that is calculated in Model A and used in Model B, is only dependent on the discharge. At the upstream boundary segment and at the location of the river intervention, the temporal changes of the bed elevation are of such an order of magnitude that the fluctuations do influence the water depth (h). Therefore, the assumption that the water depth does only depend on the discharge is not valid for the purpose of modelling river interventions. As a consequence, Model B has been adapted to include the time-dependent component of the water depth such that the water depth is dependent on the dynamic component of the bed elevation instead of the static component obtained by Model A. This adapted model is called Model B+ to indicate the difference between the original Model B provided by Arkesteijn et al. (2019).

Model B+ uses the static component of the bed level calculated by Model A as an initial condition (Fig. 3.2). This is similar to Model B. The dynamic component is calculated using a time-loop and marching through space from upstream to downstream rather than from upstream to downstream as the original Model B does. Model B+ is a combination of the BWE Model and Model B (Fig. 3.2). The water level is still calculated with a space-marching method, but the water depth is now a function of time to make it dependent on the bed level fluctuations. Model B+ includes an additional equation:

$$h_i = H_i - \eta_{i-1} \quad (3.9)$$

where i indicates the time step, H [m] the water level obtained from Model A and η [m] the bed elevation calculated in the previous time step with the static component ($\bar{\eta}$) obtained from Model A and the dynamic component ($\Delta\eta$) from Model B+.

3.3 Implementation river interventions

River interventions change the geometry of the river which results in changes in discharge. These changes in discharge can be schematised as an extraction and supply of discharge from and to the main channel. The amount of extracted discharge is dependent on the type of intervention but also on the discharge and corresponding water level.

3.3.1 Schematisation river interventions

A river cross-section can be schematised as a basin with three uniform bed levels: main channel, groynes and floodplains (Initial cross-section river Fig. 3.3). Since we are interested in bed level fluctuations on an intermediate spatial scale, we can simplify the groynes as a rectangular basin. The small spatial scale of fluctuations in bed elevation around the groynes is not part of the scope of this research. For simplicity of the model, we assume that the geometry of the channel is uniform along the river, except for the river intervention. Each river section, meaning the main channel, groynes and floodplains, has its own characteristics. In other words, the sections differ in size and bed roughness. The bed roughness is expressed by the Nikuradse roughness height (k) (Nikuradse, 1933) and is assumed to be uniform over the length of the river.

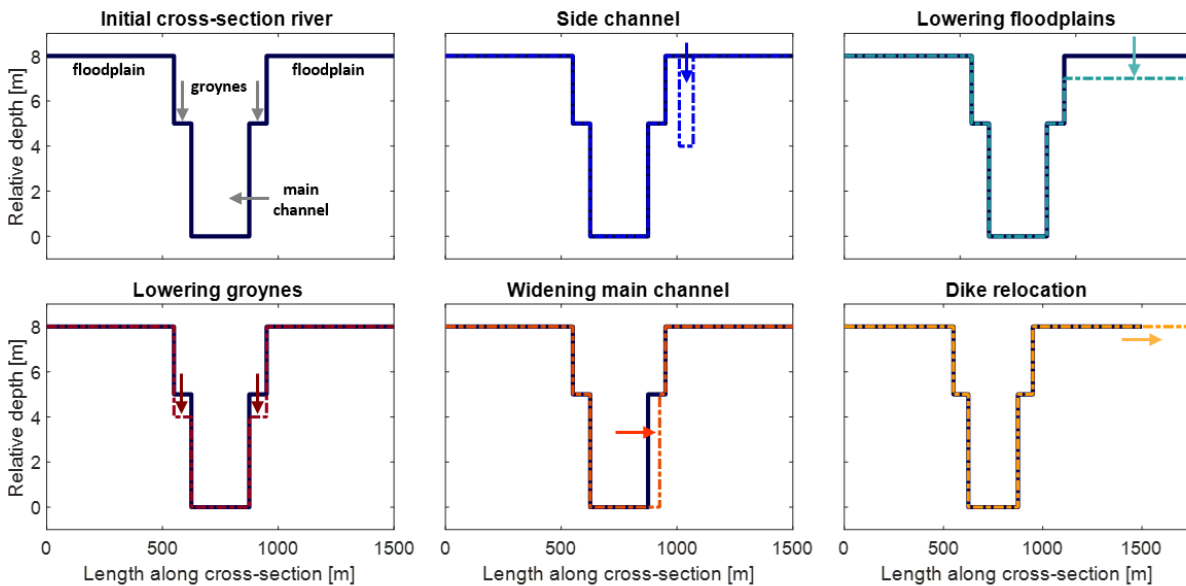


Figure 3.3: Schematisation of the cross-section of the river and the changes in cross-section after different river interventions

The construction of a river intervention results in changes in the channel geometry (see Fig. 3.3). For example, the construction of a side channel changes the size of the floodplains. We look at the morphological impact of the most common river interventions and choose the interventions that are easiest to implement in the space-marching model. In total, five different types of river interventions are investigated:

1. Side channel construction
2. Lowering of floodplains
3. Lowering of groynes
4. Widening the main channel
5. Dike relocation

Each type of intervention is translated to a change in width and/or depth of one of the cross-sectional segments of the river. For the schematisation of the river interventions, some simplifications and assumptions are made. In Table 3.1 the assumptions per river intervention are given. The parameter of interest indicates the variable that determines the size of the intervention.

Table 3.1: Implementations of river interventions

| Type of intervention | Assumption for implementation | Parameters of interest |
|---------------------------|---|-------------------------------------|
| Side channel construction | The side channel is constructed in one of the two floodplains. The side channel has a fixed depth-width ratio of 1/25. The roughness height (k) is set to be 0.3 m. The total width of the river stays the same | Width and depth of the side channel |
| Lowering of floodplains | One of the two floodplains is lowered over its entire width. | Depth of floodplain |
| Lowering of groynes | The groynes on both sides of river are lowered. It is assumed that the roughness of the groynes stays the same. | Depth of groynes |
| Widening main channel | The width of the main channel will change on one side. The length of the groynes will be shorter on this side such that the width of the floodplain stays the same. | Width of main channel |
| Dike relocation | Relocation of the dike on one side. The total width of the channel will change. | Width of floodplain |

3.3.2 Extraction tool

The geometry of a river determines the fraction of the total discharge that flows through the main channel. For example, at peak flow conditions the floodplains are inundated. This means that not the entire discharge is flowing through the main channel. The extraction tool calculates per discharge the water depth. Based on the water depth, it is possible to determine the fraction of the discharge through the main channel. The calculations are done iterative and inverse. And an estimation of the bed slope of 10^{-4} is used. Based on the water depth, which is determined from a predetermined range, the total discharge is calculated. First, for each river section the Chézy value is calculated with the formula of White-Colebrook (Colebrook et al., 1939):

$$C_i = 18 * \log_{10} \left(\frac{12R_i}{k_i} \right) \quad (3.10)$$

with R [m] the hydraulic radius determined by $R = A/O$ in which A [m²] is the flow area, and O [m] the wetted perimeter that is defined as the length of the cross-sectional water-land interface. k [m] is the roughness height. i indicates the cross-sectional segments of the river that are inundated. Based on the Chézy value, the flow velocities of each inundated segment is calculated, using

$$u_i = \sqrt{SR_i C_i^2} \quad (3.11)$$

where S [-] is the averaged bed slope along the river. Now, the total discharge can be calculated as a sum of the discharges of all inundated segments (n):

$$Q = \sum_{i=1}^n u_i A_i \quad (3.12)$$

The fraction of the discharge through the main channel is expressed as a percentage of the total discharge. This is the fraction curve. The effect of a river intervention on the change in discharge can also be expressed as an extraction curve, where the difference in discharge before and after the intervention is expressed as a percentage.

4 Method

To answer the research questions and to fulfil the research objective, we take several steps and actions. In this chapter, the method of this research is presented. We divide the method into four sub-sections corresponding to the four sub-questions. First, we make changes to the model, test the different models to find the best rapid and accurate method, and verify this method with measurements and the results of the computations with Delft3D. Second, we use the verified model to analyse the effect of several types of river interventions on the bed elevation. Third, we look at the uncertainties in the model outcome by performing a Monte Carlo Simulation. Finally, we look at the application of this model in the field by a case study of the Room for Living Rivers project.

For the model calculations, we use the initial parameter settings that Arkesteijn et al. (2019) provided and use additional characteristics that roughly scale to the Middle-Waal (Table 4.1). We consider a 300 km single-branched reach with a uniform channel width of 250 meters. We simplify the sediment transport to uni-sized sediment and bed-material load only. The flow capacity of the floodplains refers to the width of the floodplain. Not the entire width of the floodplain will carry the flow. Based on SOBEK calculations, it is found that on average 70% of the width of the floodplains along the river Waal is carrying the flow during peak discharges (Paarlberg and Schippers, 2020).

Table 4.1: Characteristics Middle-Waal based on Paarlberg and Schippers, 2020

| Symbol | Value | Unit | Description |
|------------|-------|----------|----------------------------------|
| B_{tot} | 1500 | m | Total width of river |
| B_{mc} | 250 | m | Width main channel |
| B_{gr} | 75 | m | Width groynes |
| B_{fp} | 550 | m | Width floodplains |
| fc | 0.7 | - | Flow capacity of floodplains |
| g | 9.81 | m/s^2 | Gravity constant |
| Z_{mc} | 0 | m | Reference bed level main channel |
| Z_{gr} | 5 | m | Reference bed level groynes |
| Z_{fp} | 8 | m | Reference bed level floodplains |
| c_f | 0.007 | - | Friction coefficient |
| k_{mc} | 0.22 | m | Roughness height main channel |
| k_{gr} | 1 | m | Roughness height groynes |
| k_{fp} | 0.96 | m | Roughness height floodplains |
| k_{sc} | 0.3 | m | Roughness height side channel |
| D | 1.3 | mm | Grain size diameter |
| ϵ | 0.4 | - | Porosity of the bed |
| ρ_s | 2650 | kg/m^3 | Sediment density |
| ρ_w | 1000 | kg/m^3 | Water density |
| S_{yr} | 0.624 | Mt/year | Yearly sediment transport |

The 20th-century hydrograph measured at Lobith is used for the simulations. We multiply the record by 2/3, as approximately 2/3 of the water of the river Rhine flows into the Waal branch. The mean discharge over the period from 1900-1999 is $1480 m^3/s$. The average annual peak discharge is $4130 m^3/s$. The range of discharges varies between a minimum of $830 m^3/s$ and a maximum of $8190 m^3/s$. The hydrograph is reduced to a frequency of one data point every five days (see Fig. 4.1). Over the five days, the discharge is assumed to be constant.

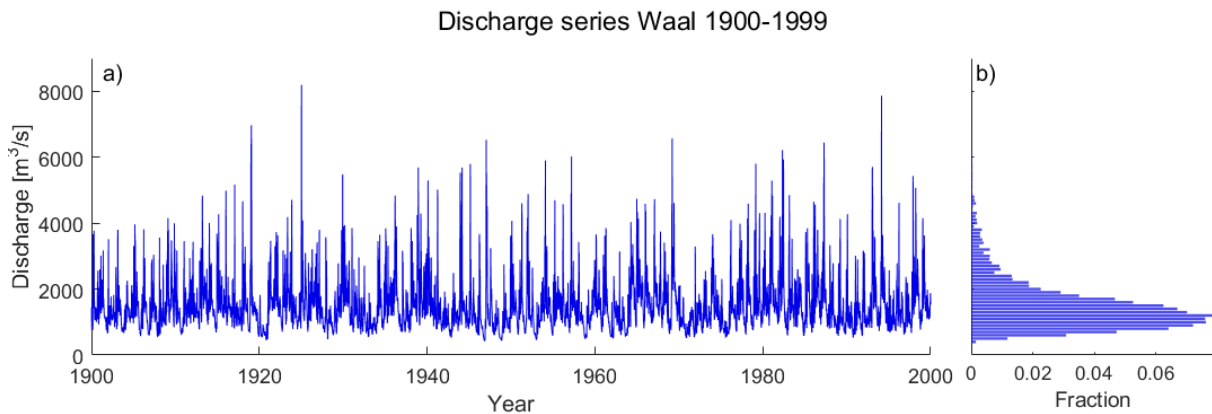


Figure 4.1: (a) 5 days discharge of the river Waal from 1900-1999, (b) The discrete probability density function of the discharge of the river Waal based on the measurements between 1900-1999

4.1 Model testing and verification

In this research, we want to analyse the impact of river intervention on the bed elevation in a quick way. Therefore, we are looking for an accurate, and simple method to describe the morphological changes due to river interventions. We use the principles of the space-marching model of Arkesteijn et al. (2019) and further develop it to make it applicable for river interventions. In addition, we use an abridged version of the Backwater-Exner model to make rapid calculations of bed level changes. We test both models on their performance and verify the outcomes with measurements and the results of the more complex numerical model Delft3D. With this verification we answer the first research question:

What is the best model to use to make accurate and rapid calculations for temporal and spatial bed level fluctuations caused by river interventions?

We divide this section into two parts. First, we make a choice for a rapid method. Second, we verify the implementation of a river intervention into the model.

4.1.1 Model choice

We look at three different options for the rapid method that calculates the equilibrium state of the bed elevation (Table 4.2). All three options use the result of the space-marching Model A (section 3.2.2) as an initial condition. The first model is the original space-marching Model B of Arkesteijn et al. (2019). The second option is the adjusted version of Model B, Model B+, that includes an additional time-loop to make the water depth dependent on the bed level fluctuations. Finally, we look at an abridged version of the BWE Model that computes the bed elevation for only one hydrograph instead of 1000 cycled hydrographs as the original version of the BWE Model does. We base our model choice on the correctness of the model output and on the computation time since we are looking for an accurate and rapid method to calculate bed level changes. For the testing of the three different models, we use a straight channel without floodplains and groynes and without river interventions. We are interested in the general performance of the models before we implement a river intervention into the model. The best model will be used for further investigations.

Table 4.2: Three different options for a rapid method to calculate the equilibrium state of the bed elevation

| Model Name | Description |
|--------------------|--|
| Model B | Original model Arkesteijn et al., 2019 |
| Model B+ | Adapted version of Model B with an additional time-loop |
| Abridged BWE Model | Backwater-Exner Model calculated for a single hydrograph |

4.1.2 Model verification

We use the model selected in the previous step to investigate bed level changes due to river interventions. We verify the implementation of a river intervention into the model with field measurements and with the results of a more complex numerical model, Delft3D. Due to limited available data, we are only able to verify the implementation of a side channel. We look at two case studies: the side channel at Hurwenen and the side channel at Passewaaij. For the location of both side channels see Appendix B. For the side channel at Hurwenen, bi-weekly field measurements are available. For the side channel at Passewaaij, a two-dimension model in Delft3D is established to assess the morphological effect of reconnecting a side channel to the main channel. We use both case studies to verify the model performance on its average bed level change, and the dynamic component. We look at the bandwidth of fluctuations representing the 90% confidence interval. This bandwidth consists of the 5th to the 95th percentile, such that outliers are disregarded. It should be said, that the percentiles represent the distribution of bed level fluctuations over space and not over time. So, the 95th percentile upstream of an intervention will not occur at the same time as the 95th percentile downstream of the intervention. We state that the model performs well compared to the case studies if the average bed level change is in the same order of magnitude and if the temporal changes show a similar trend over the length of the intervention.

Comparison with measurement: case study Hurwenen

From 2004 till 2020, the bed level of the navigation channel in the river Waal is measured bi-weekly. Van Denderen (2021) used a wavelet transform to disentangle the bed level variation that is related to small-scale, medium-scale and large-scale bed level changes. These medium-scale bed level changes correspond to the bed level fluctuations that are caused by changes in the geometry of the river. In 2015, a side channel at the location of Hurwenen was constructed. The side channel is located in an inner bed of the river Waal between river kilometres (rkm) 929 to 932. In the nineties, just upstream of the intervention, a non-erodible layer was constructed in the outer bend to reduce the aggradation in the inner bend. This has resulted in a large scour hole just downstream of the non-erodible layer that extends almost to the entrance of the side channel. Additional to the non-erodible layer, the height of the groynes in the river was reduced and the floodplain opposite to the one with the side channel was excavated. Both interventions lead to aggradation in the main channel. The side channel at Hurwenen is implemented in the model with the extraction curve (Fig. 4.2a) based on the design values provided by Driesen & De Jong (2011). This curve indicates the percentage of discharge that is drained by the side channel. Other changes in geometry are neglected. For the model computations, the characteristics of the Middle-Waal are used as given in Table 4.1.

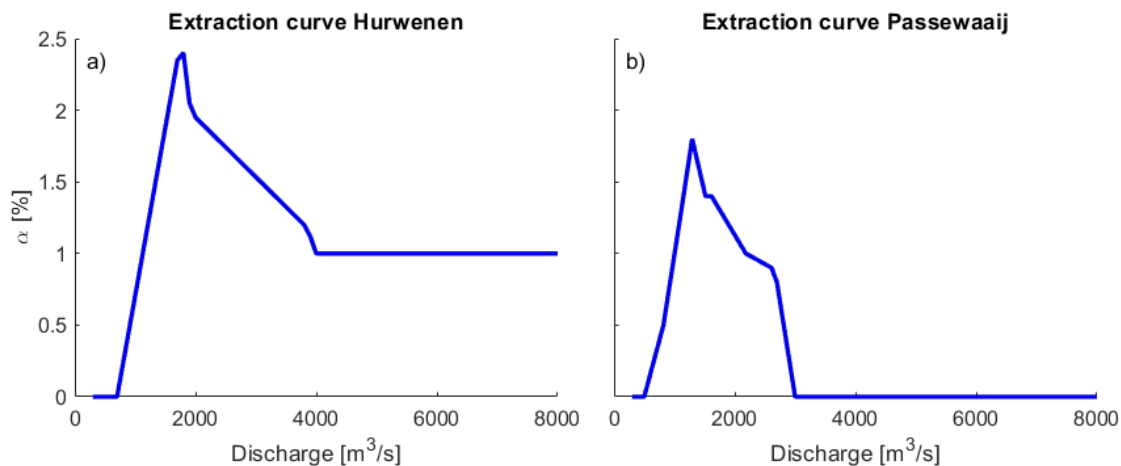


Figure 4.2: Extraction curves side channels at (a) Hurwenen and (b) Passewaaij

Comparison with complex numerical model: case study Passewaaij

The existing channel in the floodplain at Passewaaij, which was only connected to the river Waal at the downstream end, was to be reactivated with a connection at the upstream end. In 2012, Paarlberg (2013) studied the hydrological and morphological impact of connecting the upstream end of the channel by a culvert to the river Waal. The project also included raising the quay and looking at dredging options once per five years, but these additions are not taken into account in this analysis. The side channel is located between the rkm 916 and 917. In the study, model computations in Delft3D are made. The initial bed elevation for the model is based on the Baseline reference database. Already before the construction of the side channel, the location is a bottleneck for shipping, because the rkm 916 to 918 are located in the transition area between two successive river bends. Regularly, dredging activities are carried out which results in more dynamics on the river bed. The model is run for a period of 20 years with schematised discharge series of the Upper-Rhine with eight discharge levels. The discharge is multiplied by 2/3 to represent the discharge of the river Waal. The extraction curve of this side channel is given in Figure 4.2b. For discharges above 3100 m³/s, the culvert is filled to the top. Paarlberg (2013) assumed that at these discharge levels no additional discharge can flow through the side channel. It can be discussed whether this is indeed the best representation, but in order to be able to compare the model results, we also assume no additional extraction for discharges above 3100 m³/s.

The two-dimensional model results need to be width-averaged to compare the results with the one-dimensional rapid method. We chose three gridlines located at the middle of the main channel, and assume that the average bed level change at these three grid lines is representative of the full channel. Figure 4.3a shows the grid that is used for the Delft3D computations. The three red lines in Figure 4.3b are the three chosen grid lines. The green line indicates the location of the side channel.

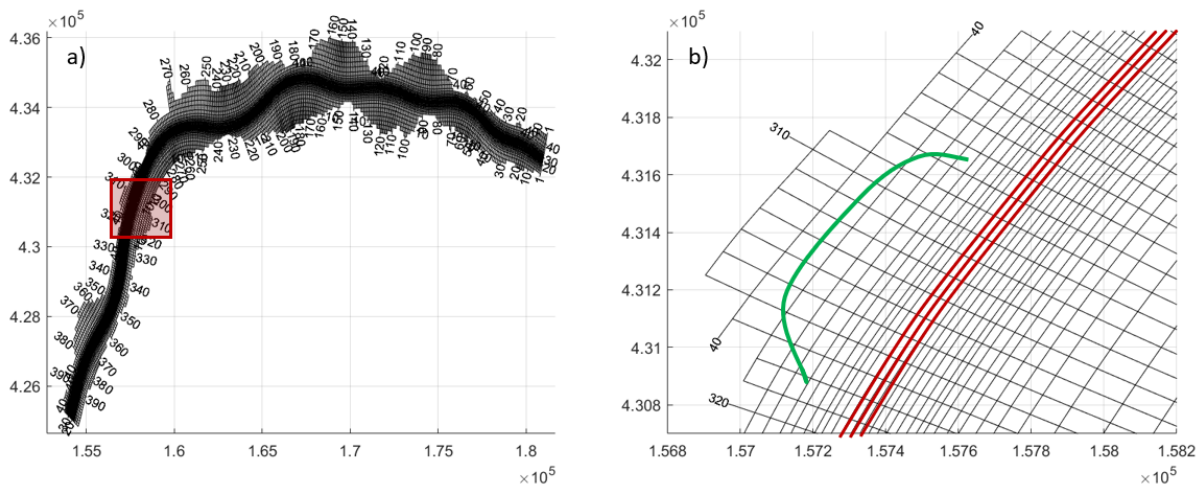


Figure 4.3: Two-dimensional grid near Passewaaij used for the computations in Delft3D, given with its x and y-coordinates. (a) The numerical domain with the red square indicating the location of interest. The numbers indicate the number of grid line in the total grid. (b) The grid lines over which the bed level change is averaged. The numbers indicate the number of grid line in the total grid.

4.2 Morphological impact of river interventions

With the verified model the impact of river interventions on the bed elevation is investigated. We look at five different river interventions and how the bed elevation changes due to varying discharges. This leads to the answer of the second sub-question:

How does the distribution of bed level fluctuations for various types of river interventions change under variable flow discharges?

The implementation of river interventions in the model is explained in Chapter 3. In this section, we explain how we use the model to study the fluctuations in bed elevation for five different types of river interventions.

The size and type of intervention determine the degree of bed level changes. To compare the different intervention types, we chose the size of each intervention in such a way that the initial bed level changes at the downstream side of the intervention are the same for each river intervention. The size is determined by an iterative process using the time-averaged bed elevation obtained from Model A. The initial bed elevation at the downstream end of the intervention is found by the results of Model A. By changing the geometry of the channel, a new equilibrium bed elevation is determined. This equilibrium state is based on the yearly sediment flux, similar to the initial bed level. Each intervention results in a time-averaged increase in bed elevation of 20 cm. The sizes of the different types of river interventions are presented in Table 4.3.

Table 4.3: Size of river interventions based on an average aggradation of 20 cm, implemented over a length of 5 km

| Intervention | Size |
|-----------------------|-----------------------------|
| Side channel | 73.5 m width & 2.94 m depth |
| Lowering floodplains | -1.15 m |
| Lowering groynes | -0.61 m |
| Dike relocation | 7.37 km |
| Widening main channel | 8.14 m |

Based on the sizes of the river interventions, we calculate the fraction curves with the extraction tool. The black solid line in Figure 4.4 represents the initial situation. In the initial situation, the groynes are flooded at a discharge level of $1500 \text{ m}^3/\text{s}$ and the floodplains start to inundate above discharges of $3000 \text{ m}^3/\text{s}$. All types of river interventions lead to a decrease in the fraction of discharge that flows through the main channel. In other words, the river interventions extract water from the main channel. Only the widening of the main channel results in an increase in the flow capacity of the main channel and therefore an increase in the fraction of the total discharge that flows through the main channel. For the dike relocation, it can be seen that there is no effect of the intervention until the floodplains are inundated. But once the floodplains start to inundate, there is a significant decrease in the fraction of discharge that flows through the main channel.

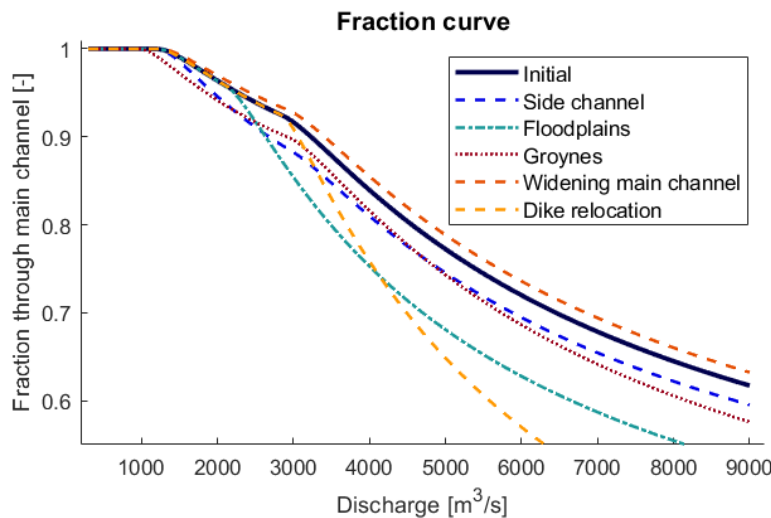


Figure 4.4: Fraction of discharge flowing through the main channel for different river interventions. The sizes correspond to the sizes presented in Table 4.3

The river interventions are implemented over a length of five km, which is in the same order of magnitude as the river interventions in the field. The model is run on a domain of 300 km. We implement the river interventions between the river kilometres 150 and 155 based on the 300 km model domain, such that fluctuations caused by the upstream and downstream boundary conditions do not influence the changes in bed elevation at the location of the river intervention. For the computations, we use the historical discharge series from 1900-1999 (Fig. 4.1).

To assess the morphological impact of the river interventions, a distinction is made between the mean bed elevation and the dynamic component of the bed level. For the dynamic component, we look at the distribution of temporal bed level changes. Since the bed level changes are largely influenced by the discharge, the discharge is divided into three levels: low ($<1500 \text{ m}^3/\text{s}$), intermediate ($1500 \text{ m}^3/\text{s}$ to $3000 \text{ m}^3/\text{s}$) and high discharge ($>3000 \text{ m}^3/\text{s}$). These correspond with base flow, bankfull flow and peak flow conditions, respectively.

4.3 Uncertainties in bed level fluctuations

Due to limited observations of extreme events and the challenges related to predicting future conditions, computing the effect of river interventions entails large uncertainties. The recommended practice is to quantify these uncertainties of model predictions (Berends, 2020). At locations with a non-uniform geometry, like river interventions, the morphological response is sensitive to seasonal variations in discharge (Van Vuren, 2005b). Besides, the sediment transport model, which is an important part of studying morphological developments, consists of a set of uncertainties (Jansen et al., 1979). It includes methodological uncertainties in the choice of the particular transport model and technical uncertainties in the transport model parameters. We quantify the range of uncertainties using a Monte Carlo Simulation (MSC). The outcome of this simulation helps us to define the uncertainties and answer the third sub-question:

How large is the uncertainty in bed level fluctuations for various types of river interventions?

In this section, first we describe how we generate discharge hydrographs. Second, the use of MSC is explained and the probability distributions corresponding to the discharge, yearly sediment transport and hydraulic roughness are given. These are the three variables that we used for MSC. Finally, an estimation of the sample size is made.

4.3.1 Generating discharge series

The long-term morphological changes can only be simulated realistically if a representative range of discharges is used in the calculations, rather than a uniform discharge (Huthoff et al., 2010). We use the historical discharge series from 1900-1999 of the river Waal to draw new discharge series that show seasonal variations. To reproduce these variations we split a year into 36 decads (see Appendix D.1) (Duits, 1997; Van Vuren et al., 2005a). Note that this is different than the 5-days discharges that we use in the reduced historical hydrographs. For a MCS, a set of 36 decad-discharges per year represents the seasonal variations well (Duits, 1997). Per decad, we make a probability distribution of the decad-discharge based on the observations. The probability distribution of decad-discharges of the river Waal can be described as a shifted log-normal distribution (Duits, 1997):

$$f(x|\mu, \sigma, a) = \frac{1}{\sqrt{2\pi}\sigma(x-a)} \exp\left(-\frac{(\ln(x-a) - \mu)^2}{2\sigma^2}\right) \quad (4.1)$$

with $\mu = \text{mean}(\ln(x))$, $\sigma = \text{std}(\ln(x))$, a the parameter that indicates the shift in the log-normal function. This value corresponds with the lowest observed discharge in the set of historical decad-discharges. The range of input values, in this case the input discharges, is given by x . The values of μ and σ are based on the historical discharge series from 1900-1999 (see Fig. 4.1 and Appendix D.1 for the corresponding parameter values). Figure 4.5, that shows the observed exceeding frequency of the first decad and

the corresponding log-normal distribution, proves that a log-normal distribution corresponds with the observations of the discharges in the river Waal.

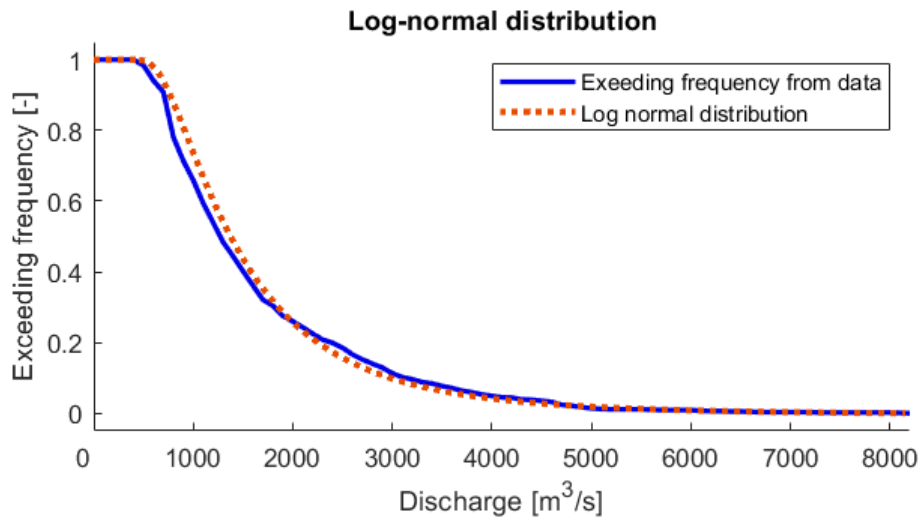


Figure 4.5: Empirical exceeding frequencies of discharges in the first decad of the river Waal observed from 1900-1999 compared with exceeding frequencies generated using a shifted log-normal function

Between decads, there is a strong correlation in discharges. With an autocorrelation function, the dependence between successive decads can be determined. Duits (1997) has shown that the discharge in a decad is most strongly determined by the discharges of the previous two decads (Fig. 4.6). For larger differences between decads the autocorrelation becomes less than 0.5. We use the dependence of the previous two decads to include the dependency of more than one decad, without making the process of discharge generating too complex.

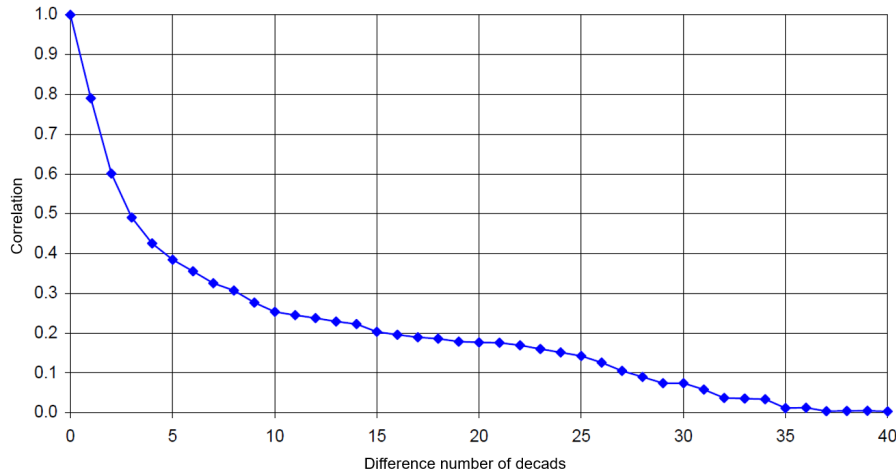


Figure 4.6: Values of the autocorrelation-function of the decad-discharges of the river Waal (Duits, 1997)

The dependency of discharges of subsequent decads can be expressed with a log-normal multivariate distribution (Duits, 1997). The discharge in the first decad is calculated by a log-normal distribution,

similar to Equation 4.1. Here q [m^2/s] gives the range of input unit discharge.

$$f_1(q_1) = f_1(q_1|\mu_1, \sigma_1, a_1) = \frac{1}{\sqrt{2\pi}\sigma_1(q_1 - a_1)} \exp\left(-\frac{(\ln(q_1 - a_1) - \mu_1)^2}{2\sigma_1^2}\right) \quad (4.2)$$

The unit discharge of the second decadal (q_2) is dependent on the discharge in the first decadal (q_1):

$$f_2(q_2|q_1) = \frac{1}{\sqrt{2\pi}\sigma_2\sqrt{1-\rho}(q_2 - a_2)} \exp\left(-\frac{1}{2\sigma_2^2(1-\rho)} \left[\ln(q_2 - a_2) - \mu_2 - \frac{\rho\sigma_2}{\sigma_1}(\ln(q_1 - a_1) - \mu_1)\right]^2\right) \quad (4.3)$$

All the other decadal-discharges are calculated using the log-normal multivariate distribution that uses the dependency of the previous two decadal-discharges. The index i indicates the index of the decadal of interest.

$$f_i(q_i|q_{i-1}, q_{i-2}) = \frac{1}{\sqrt{2\pi}\tilde{\sigma}_i(q_i - a_i)} \exp\left(-\frac{(\ln(q_i - a_i) - \tilde{\mu}_i)^2}{2\tilde{\sigma}_i^2}\right) \quad (4.4)$$

With $\tilde{\mu}_i$ expressed as

$$\tilde{\mu}_i = \mu_i - \frac{\rho_1\rho_2 - \rho_1}{1 - \rho_1}\sigma_i\tilde{q}_{i-1} - \frac{\rho_1\rho_1 - \rho_2}{1 - \rho_1}\sigma_i\tilde{q}_{i-2} \quad (4.5)$$

in which \tilde{q}_{i-1} and \tilde{q}_{i-2} are defined as

$$\tilde{q}_{i-1} = \frac{\ln(q_{i-1} - a_{i-1}) - \mu_{i-1}}{\sigma_{i-1}} \quad \text{and} \quad \tilde{q}_{i-2} = \frac{\ln(q_{i-2} - a_{i-2}) - \mu_{i-1}}{\sigma_{i-2}}. \quad (4.6)$$

And with $\tilde{\sigma}_i$ expressed as

$$\tilde{\sigma}_i = \sigma \frac{\sqrt{1 + 2\rho_1\rho_2\rho_1 - \rho_1^2 - \rho_2^2 - \rho_1^2}}{\sqrt{1 - \rho_1^2}}. \quad (4.7)$$

The variables ρ_1 and ρ_2 represent the correlation between the discharge in respectively the previous decadal and the one before the previous decadal. From Figure 4.6 it reads that these values are 0.79 and 0.6.

With the probability distribution of all 36 decads we generate discharge series by draws. Within a decadal we assume the discharge to be constant. This might result in an over or underestimation of the discharge level for the decadal since in reality the discharge is not constant over a period of 10 days. Because we are generating 20 years of 36 decads per year the over and under estimation using constant decadal-discharges average out. We use repeated cycled hydrographs of 20 years to generate discharge series of 100 years. With this set of discharge series, we perform the Monte Carlo Simulation.

4.3.2 Monte Carlo Simulation

Monte Carlo Simulation is a universal method to compute model output uncertainty in river modelling (Berends, 2020). It is used to quantify the confidence intervals of long-term morphological changes (Van der Klis, 2003; Van Vuren, 2005b). The principle behind MSC is to run a large number of deterministic simulations, where the uncertain model input is randomly generated according to prescribed probability distributions.

One of the most important sources of uncertainty is the future discharge hydrograph (Van der Klis, 2003; Van Vuren et al., 2002). The probability distribution is explained in the previous section. In addition to the variabilities in discharge, we look at variations in yearly sediment transport (Frings et al., 2015). It is

one of the boundary conditions of the morphological model. Another uncertain and sensitive variable is the hydraulic roughness (Berends, 2020; Van Vuren, 2005b; Warmink et al., 2013). Other uncertain variables like particle size, critical Shields parameter and the exponent of the bed shear stress are not taken into account in this analysis, since previous studies have shown that morphological changes are less sensitive for variations in one of these parameters (Van der Klis, 2003; Van Vuren, 2005b).

The uncertainty is often expressed using the coefficient of variation (c_v) (Johnson, 1996). This coefficient is defined as the ratio of standard deviation to the mean ($c_v = \sigma/\mu$). The yearly sediment transport entails an uncertainty of about $\pm 50\%$ (Frings et al., 2015). We estimate the standard deviation such that c_v is approximately 0.15. For the hydraulic roughness we use also a fixed c_v of 0.15, similar to Van Vuren (2005b). We use the same coefficient of variation for all three cross-sectional segments; main channel, groynes, and floodplains. The c_v of 0.15 corresponds with an uncertainty of $\pm 25\%$. In Table 4.4 the variables that we use in the MCS are given, including their distribution and corresponding properties.

Table 4.4: Distribution of uncertainties in model variables

| Variable | Distribution | Properties |
|--|--|---|
| Yearly sediment transport (S_{yr}) | Truncated normal (Van Vuren, 2005b) | $\mu = 0.624$ Mt/year $\sigma = 0.104$ Mt/year domain: [0.312, 0.936 Mt/year] |
| Roughness height (k) | Uniform (Van Vuren, 2005b; Johnson, 1996) | main channel: [0.165, 0.275 m] groynes: [0.75, 1.25 m] floodplains: [0.72, 1.2 m] |

The accuracy of MCS is dependent on the sample size. An increasing sample size results in an increase in accuracy. However, pointless computational effort should be avoided. Morgan & Henrion (1990) describe a method to estimate the sample size required for a specific degree of accuracy. This degree of accuracy is given as a confident α that the actual p^{th} percentile, Y_p , lies between the estimates of the $p - \Delta p^{\text{th}}$ and $p + \Delta p^{\text{th}}$ percentiles. The associated sample size is given by:

$$N = p(1 - p) \left(\frac{c_\alpha}{\Delta p} \right)^2. \quad (4.8)$$

Here, N is the sample size, p the percentile of interest, c_α the deviation that encloses probability α of a random variable with unit normal distribution ($P(-c_\alpha < \Phi < c_\alpha) = \alpha$), and Δp the allowed deviation in terms of an interval of percentiles. To make this method correspond better with the present river management practice, the desired accuracy can be expressed as an allowed deviation from the estimated percentile in metres of bed level change (Van der Klis, 2003). We use a Gaussian distribution as a first assumption for the model output. To estimate the required sample size, we make the next steps (Van der Klis, 2003; Van Vuren, 2005b):

1. Specify the desired degree of accuracy of a percentile p that should be estimated and the width of the α confidence interval should contain the actual value of p .
2. Roughly estimate the statistical parameters of the Gaussian distribution based on a small sample of outputs, that is in the order of a few tens of runs.
3. Estimate the percentile (p_1, p_2) of the assumed output distribution that corresponds to the confidence interval defined in step 1, and determine the percentile interval of width $2\Delta p = p_2 - p_1$.
4. Estimate the sample size using equation 4.8.

We want to be 95% confident that the actual 90th Y_p of the maximum accretion ($p=0.90$) has a precision of plus or minus 2.5 cm (similar to Van der Klis, 2003 and Van Vuren, 2005b). Based on a small sample size of 50 runs we determine the percentile interval Δp . The 90th percentile of maximum accretion is different per intervention type (see Fig. 4.7). For the construction of a side channel, the 90th percentile of maximum accretion equals 0.55 meters. Taking a confidence interval with a precision of ± 2.5 cm corresponds with the fractions $p_1 = 0.87$ and $p_2 = 0.97$. The allowed deviation Δp becomes 0.11. Using a value of $c_a = 2$ (Van der Klis, 2003) results in a sample size (N) of 30. The sample size can also be determined based on the lowering of floodplains. The allowed deviation Δp is only 0.03. This results in a sample size of 400. Since we are investigating five different types of river interventions we want to make sure that the sample size is sufficient for all five interventions. Actually, the sample size should be based on the dike relocation since the deviation in bed level fluctuations is largest for this type of river intervention. However, the size of river intervention is unrealistic and the sample size is very large. This results in undesirable long computations times. Therefore we consider using a sample size of 400 runs that gives for at least four types of river interventions a good representation.

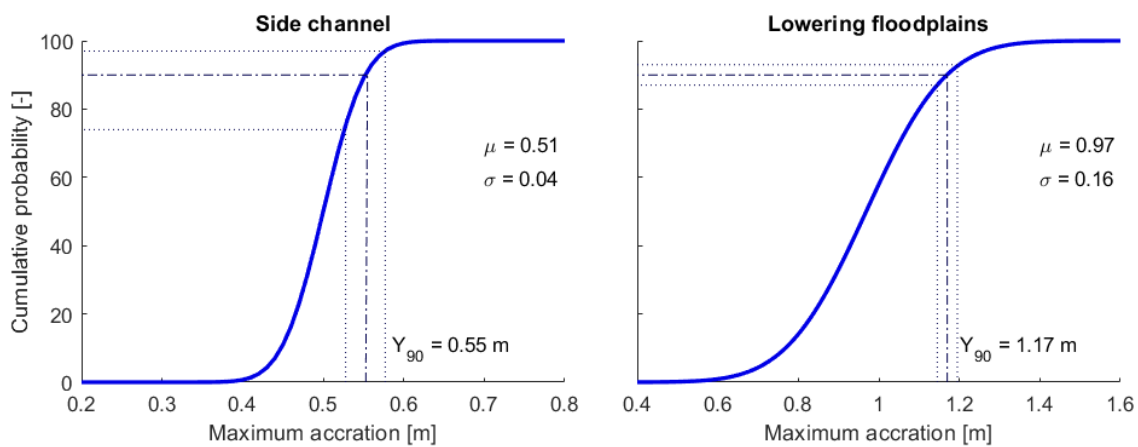


Figure 4.7: Cumulative probability distribution of Gaussian distributed maximum accretion for the construction of a side channel and lowering of floodplains for a small set of 50 runs

4.4 Multiple river interventions

River interventions change the morphology of the river system. Some interventions, like narrowing the main channel or longitudinal dams, result in a decrease in bed elevation. Other interventions, like floodplain lowering or the construction of a side channel, lead to an increase in bed elevation. Combining interventions with an opposite effect leads to smaller bed level fluctuations since the increase in bed elevation caused by a certain intervention is compensated by the decrease in bed elevation caused by the other intervention. In the project Room for Living Rivers (RfLR), combinations of interventions are investigated to give more room to the nature, but still provide sufficient water depth for shipping. We use the case study of the RfLR project along the Middle-Waal, between Oosterhout and IJzerdoorn (rkm 880 - 912) to investigate the effect of a combined river intervention on the bed elevation. The result of this investigation helps us to answer the last sub-question:

What is the effect of combined river interventions on the fluctuations in bed elevation?

Paarlberg and Van Lente (2021) performed a test case of the RfLR plan between Oosterhout and IJzerdoorn that includes eleven floodplains in the Middle-Waal. The RfLR plan is a combination of several types of river interventions: narrowing the main channel by means of filling up the groyne fields, raising the embankments, construction of side channels, lowering the quay, and removing obstacles from the floodplains. The interventions are designed alternately left and right. The aim of the project was

to extract water from the main channel earlier than in the original situation, but at the same time to maintain the water depth at low water levels. Paarlberg and Van Lente (2021) made calculations in the two-dimensional model WAQUA to study the changes in discharge through the main channel and the effect of the interventions on the bed level.

We chose two simplified case studies to implement in the model. We look only at the combination of a side channel and narrowing the main channel by filling up the groyne fields (Fig. 4.9), and instead of looking at eleven sequential side channel, we limit it to two side channels. So, we distinguish two situations:

1. Two river interventions at the same location: a side channel in combination with narrowing the main channel.
2. Two sequential river interventions: two side channels, one after the other.

We use the WAQUA calculations to estimate the extraction curves (Appendix E), based on the difference between the reference and test situation. We adjusted the curves manually to make them smooth and correspond better to reality (Fig. 4.8a). The plan RfLR affects the discharge partitioning at the Pannerdense Kop. This effect, varying between -2 and -50 m^3/s , is not taken into account in the extraction curves. Besides, we use the extraction tool (Chapter 3) to compare the extraction curve obtained by the calculations in WAQUA with basic calculations (Fig. 4.8b). The advantage of the use of the simple extraction tool is that not only the combined effect but also the effect of a single intervention can be investigated. We assume that the extraction curves of single river interventions can be superimposed, presuming that the upstream and downstream end of both river interventions are at the exact same location.

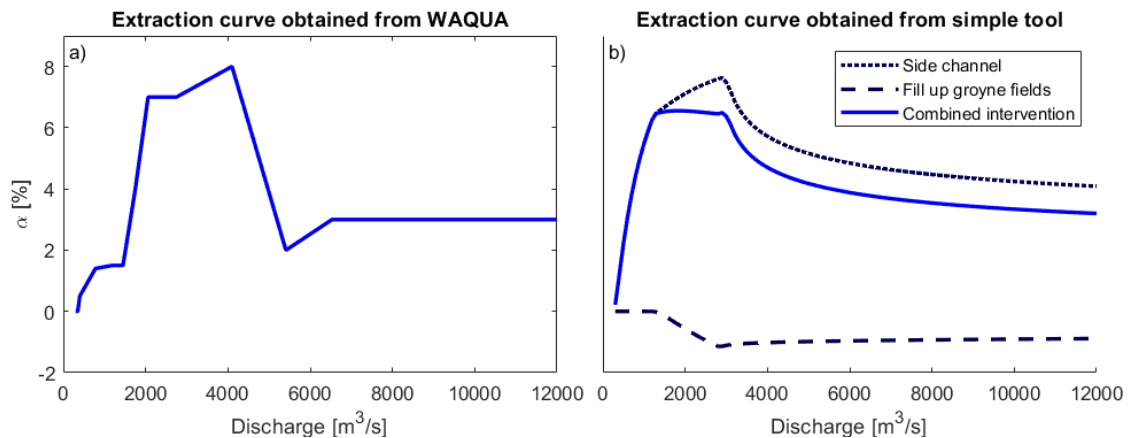


Figure 4.8: Extraction curve of a combined intervention with a side channel and filling up the groyne fields. (a) Extraction curve obtained from WAQUA and (b) calculated with the extraction tool including the extraction curves of each intervention separately

The dimensions of the side channel and the change in groyne fields are based on the RfLR project. The changes in geometry are shown in Figure 4.9. For both case studies, we use the following dimensions:

- A side channel with a width of 50 meters and with a bed level located two meters above the river bed level.
- Narrowing the main channel by filling up the groyne fields.

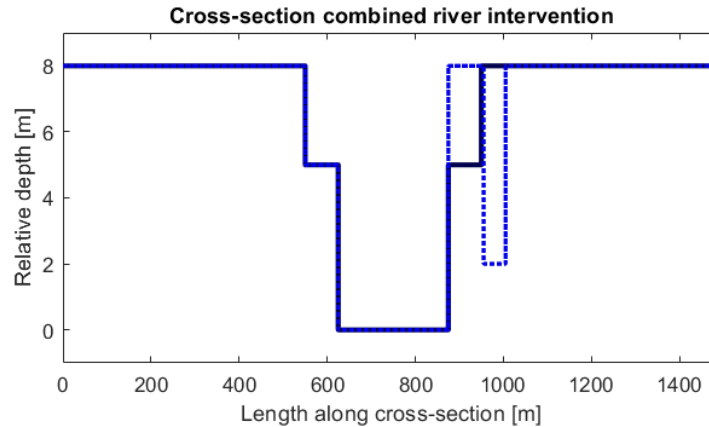


Figure 4.9: Cross-section for a combination of a side channel and filling up the groyne fields

For the two sequential side channels, we use the extraction curve obtained by WAQUA calculations and assume that both side channels have the same extraction curve. A distinction can be made between three different situations of how the two side channels are aligned (Fig. 4.10). The downstream end of the first side channel and the upstream end of the second side channel can be exactly at the same location. In this case, we can assume that there is one large side channel with one extraction curve. In a second situation, the upstream end of the second side channel can be located just upstream of the downstream end of the first side channel. There is an overlap between both side channels. Finally, the upstream end of the second side channel can be located just downstream of the downstream end of the first side channel. There is a small gap between both side channel. We will look at the last two situations. For the first situation, it is recommended to use a two-dimensional model to investigate local bed level changes. In a one-dimensional model, the effect of two successive side channels that are perfectly aligned will be negligible. The length of the side channels is similar to the plan of RfLR, which is 1.5 and 2.5 kilometres for the first and second side channel, respectively. We will use the historical discharge series from 1900-1999 of the river Waal and use a deterministic approach for the calculations. The dimensions of the river are based on the dimensions of the Middle-Waal.

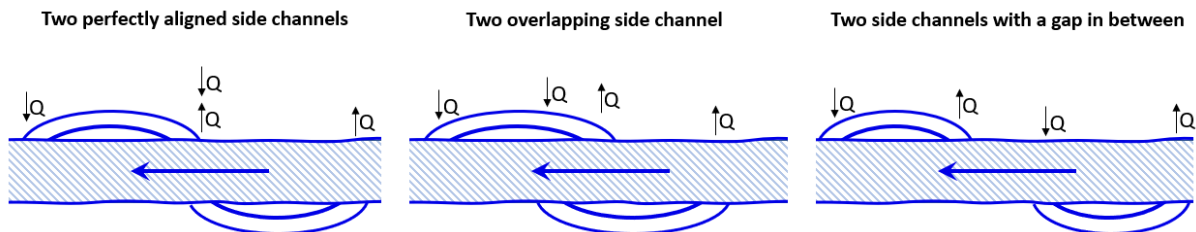


Figure 4.10: Three different situations for the alignment of two successive side channels

5 Model testing and verification

We are looking for a rapid method that describes the bed level fluctuations adequate and can be used to study the morphological effect of river interventions. To find the best method, we first test the performance of three rapid methods without the implementation of a river intervention. Second, we take the best method and add the implementation of river interventions. We verify the model application of a side channel with measurements and the results of a Delft3D computation.

5.1 Model choice

We test three different types of rapid methods that determine the equilibrium state of the bed elevation. We assume that the BWE Model shows accurate model results. We use these results to see if another method exists that has the same level of accuracy for the model outcome, but a reduction in computation time. The three different models, Model B, Model B+, and the BWE Model are described in Chapter 3 and are used to compute bed level fluctuations over a period of 100 years based on the historical discharge series from 1900-1999 of the river Waal.

5.1.1 Comparison by model output

We compare the results of the three models by the bandwidth of bed level fluctuations 5.1. We see that at the upstream boundary, the bed elevation computed by Model B+ and the BWE Model shows much more fluctuations than the bed elevation computed by Model B. Looking more in detail at the variations in bed elevation at a fixed point at the upstream end, we see that the BWE Model shows perturbations in bed elevation up to 5 centimetres. Model B+ also gives bed perturbations but these are one centimetre

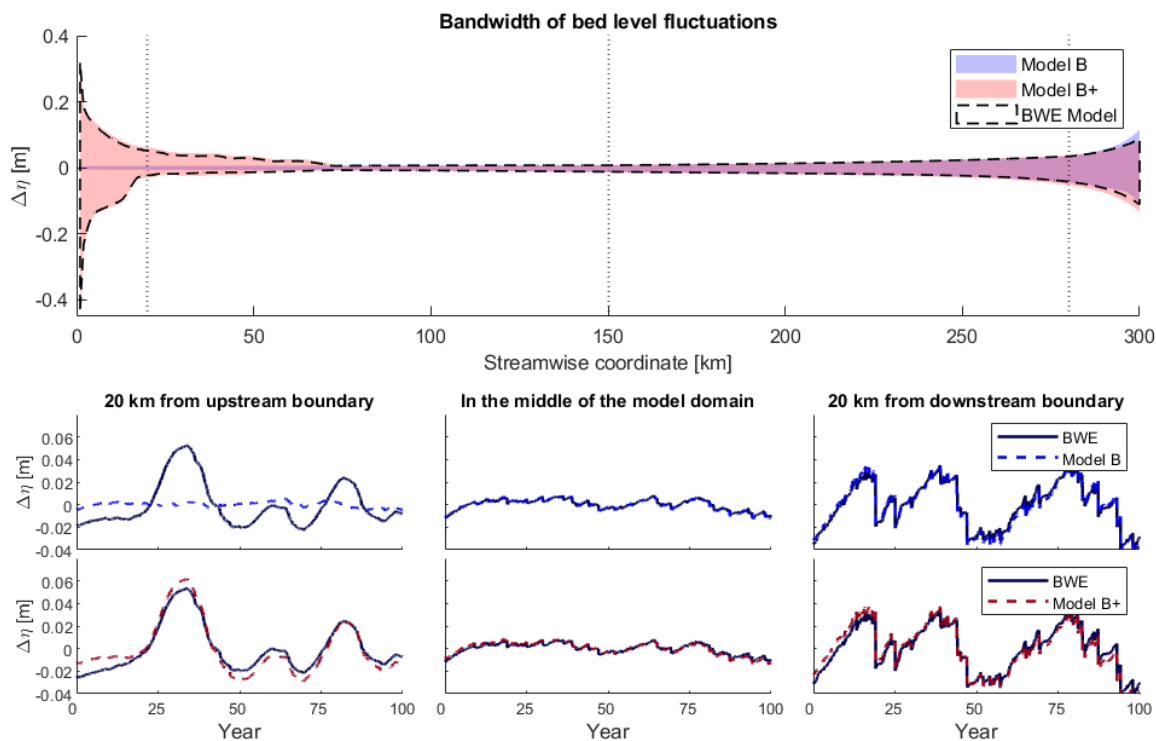


Figure 5.1: Fluctuations in bed elevation calculated with Model B, Model B+ and the BWE Model over the entire model domain (top figure), and on three fixed locations (bottom figures): 20 km downstream of the upstream boundary, in the middle of the model domain, at the location $x = 150$ km, and 20 km upstream of the downstream boundary.

larger than the fluctuations calculated with the BWE Model. Model B shows almost no bed level fluctuations at the upstream end. In the middle of the model domain, the variations in bed elevation are small. Model B, Model B+ and the BWE Model show bed level variations around one to two centimetres. Looking at the variations over time, we see that the results of the three models are practically the same. At the downstream end, the fluctuations in bed level become larger. For all three models, the variations in bed elevation vary between ± 5 centimetres. Over time, the trends of bed level variations are similar for the three models, but it seems like Model B and Model B+ are lagging behind the BWE Model.

The difference between Model B and the BWE Model at the upstream part of the river reach can be explained by the absence of an upstream boundary condition for the sediment supply. The BWE Model uses a yearly sediment flux of 0.62 Mt. For model B there is no sediment flux defined at the upstream boundary. The large fluctuations in bed elevation are caused by a mismatch between the boundary condition and the calculated sediment transport, which is usual for morphological models (Viparelli et al., 2011; Wong and Parker, 2006). In Model B+, the upstream boundary condition for sediment flux is added. This makes the difference in bed level fluctuations at the upstream end between Model B+ and the BWE Model smaller than the difference between Model B and the BWE Model. Although, there are still some differences between Model B+ and the BWE Model at the upstream end. These differences can be explained by the static slope approximation (Fig. 5.2). For the quasi-normal flow segment and the backwater segment, it can be concluded that the static slope approximation is a valid simplification. The quasi-static component of the BWE Model and Model A are similar (Fig. 5.2a) and the short-term fluctuations of the bed slope are small compared to the slowly varying slope (\bar{S}) (Fig. 5.2b). This is in line with the findings of Arkesteijn et al. (2019). However, for the upstream boundary segment, the static slope approximation does not hold. The fluctuations in bed elevation at the upstream boundary are one order of magnitude larger than the slowly varying bed slope. The consequence of using the static-bed slope approximation for the upstream boundary segment is an error in the calculations in Model A. At the upstream end, this error equals one to two centimetres. In the middle of the river reach, corresponding to the QNFS, there are almost no differences between the bed slope and bed level calculated with Model A and the BWE Model. At the downstream end, there is a small error caused by the downstream boundary condition (Fig. 5.2).

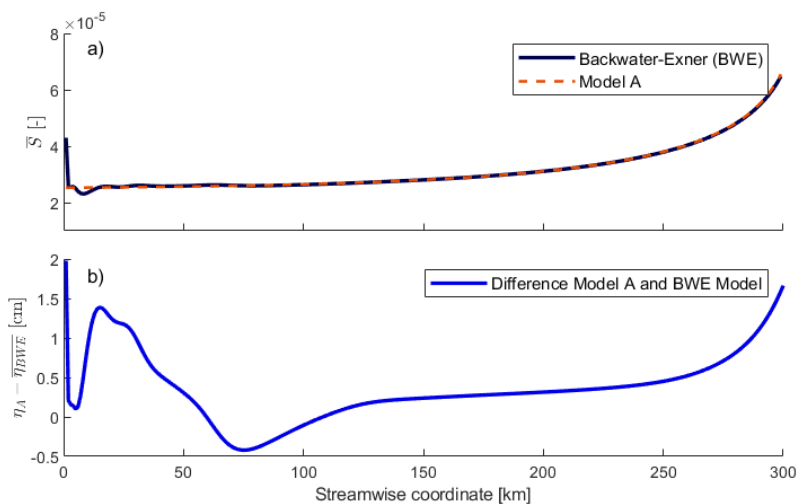


Figure 5.2: (a) The quasi-static component of the bed slope calculated with the BWE Model and Model A, (b) Difference in the quasi-static component of the bed level between Model A and the BWE model

5.1.2 Comparison by computation time

Besides the performance of the models, we can compare the models by computation time. The advantage of the space-marching model is that the transient phase does not need to be computed (Arkesteijn et al., 2019). This should save time. However, in model B+ an additional time loop is added to make the water depth dependent on the fluctuations of the bed elevation. In Table 5.1 the computation times are given. All three cases need input from Model A. For large spatial and temporal steps, the run time for Model B(+) and the BWE model are almost the same. However, for smaller time steps, especially for a simulation time of 100 years, the run time of model B+ becomes significantly longer than the original Model B. It should be stated that Model B+ is not optimised such that the computation times showed in Table 5.1 might be an overestimation. However, it can be concluded that the advantage of the space-marching model does not hold for the adapted version of model B.

Table 5.1: Computation time given in MM:SS for different parts of the model and different simulation characteristics

| Simulation characteristics | Model A | Model B | Model B+ | BWE Model |
|----------------------------------|---------|---------|----------|-----------|
| 20 year, dx = 1000m, dt = 5 day | 00:14 | 00:04 | 00:04 | 00:06 |
| 20 year, dx = 100m, dt = 1 day | 00:18 | 00:04 | 01:10 | 00:46 |
| 100 year, dx = 1000m, dt = 5 day | 00:25 | 00:09 | 00:19 | 00:00:34 |
| 100 year, dx = 100m, dt = 1 day | 00:29 | 00:10 | 09:47 | 04:02 |

To conclude, the models B and B+ are based on a static slope approximation that is not valid in the upstream boundary segment. However, this approximation results in a reduction of computation time. This does no longer hold if an additional time-loop is added. Since the abridged version of the BWE Model gives the most accurate results and the computation time is even shorter than the adjusted version of the space-marching model, we choose to use the BWE Model in further computations in this research.

5.2 Model verification

The model verification is very limited. We verify the model results of the implementation of a side channel with field measurements and with model results of a Delft3D computation.

5.2.1 Comparison with measurements: Case study Hurwenen

In 2015, the side channel at Hurwenen was constructed. It is assumed that after 2018 a new equilibrium has been reached. Measurements show that the side channel causes an average bed level change of about 15 cm (Fig. 5.3b). The model computed a bed level change of 17 cm (Fig. 5.3a). In the model results, the dynamics of the bed elevation are virtually absent before the implementation of the side channel. We used a uniform geometry to compute the initial situation. So, there are locally no large differences in discharge that could cause large bed level fluctuations. After 2018, the bed level fluctuations are still relatively small. The field measurements show a time-averaged bed level change of zero metres, which is equal to the model results. However, the bed level fluctuations are much larger. In previous years, several human interventions have been implemented in the river Waal that resulted in more fluctuations in the bed elevation. The scour hole around rkm 928 can be explained by the non-erodible layer at St. Andries constructed in the nineties.

For a better comparison between the model results and the field measurements, the situation before 2014 is adjusted in such a way that the model results and the measured data show the same initial bed fluctuations. Since the measured bed level fluctuations correspond to a historical discharge hydrograph it is not possible to look at the difference between the bed level fluctuations before and after the implementation of the side channel. The measured data before 2014 includes eight peak discharges with discharge levels above 6000 m³/s (Van Denderen et al., 2021). The data set after 2018 is much smaller and includes only one peak discharge.

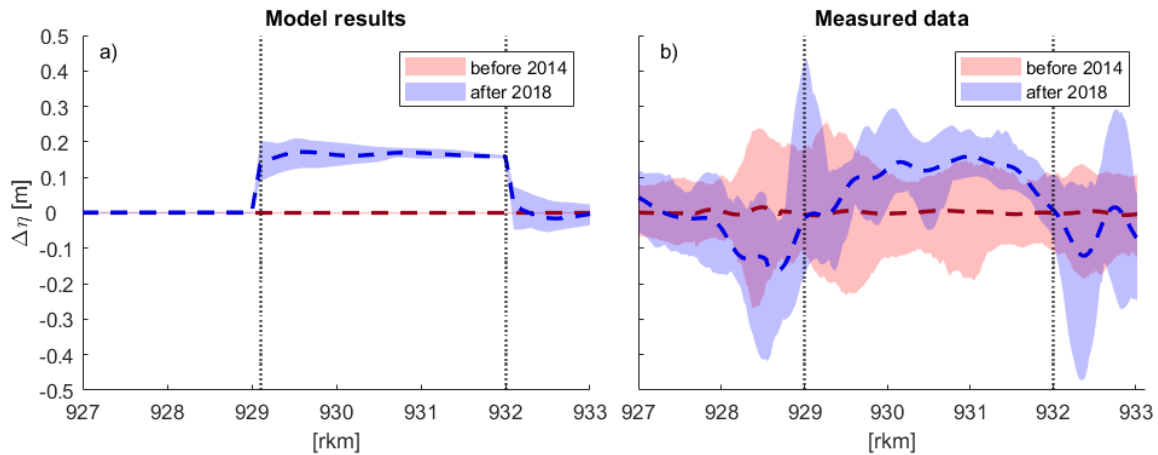


Figure 5.3: 5th and 95th percentile of bed level variations before and after the side channel, located between rkm 929 - 932, at Hurwenen. (a) BWE Model. (b) Results from bi-weekly measurements (Van Denderen et al., 2021)

Figure 5.4 shows the adjusted model results and the measured data after 2018. In the middle of the river intervention (between rkm 930-931) the mean bed level change is approximately the same for the measured data and the adjusted model. The difference between both bed level changes is one to two centimetres which equals a deviation of 10% from the mean bed level change. For the purpose of the rapid method, this deviation of the model results from the measurements is relatively small. However, the shape of the equilibrium state is different for both cases. The model results show a clear jump in bed elevation at the beginning and end of the side channel. This is the point where the discharge is extracted and supplied from and to the main channel. In reality, there is not one point where the water flows into the side channel. The extraction of water is distributed over the length of the beginning of the side channel. Therefore, the field measurements show a gradual change in bed elevation. In the field, several processes influence the bed profile resulting in a less steep transition of bed elevation at the location of the intervention. The largest differences between both cases are just downstream of the intervention. The mean bed level change computed by the model equals zero while the measurements show a scour hole of 10 cm. The bed level fluctuations calculated by the model range from 20 cm to minus 20 cm. The measurements show bed level fluctuations between 10 cm and minus 40 cm. An elaborated explanation of these differences is given in the discussion.

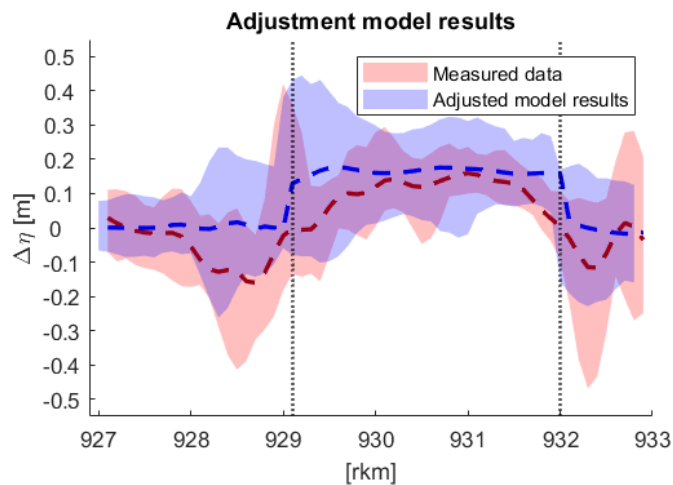


Figure 5.4: 5th and 95th percentile of bed level variations after implementing a side channel at Hurwenen. The model results are adjusted such that the dynamics before the construction of the side channel are included.

5.2.2 Comparison with complex numerical model: Case study Passewaaij

Besides the comparison with measurements, the model results are compared with the results of a more complex numerical model, Delft3D. Calculations with Delft3D show an average bed level change of 10 cm (Fig. 5.5b). The BWE model gives a bed level change of 12 cm (Fig. 5.5a). Looking at the dynamic component, we see that, similar to the results of Hurwenen, the dynamics in bed elevation before the implementation of the side channel are virtually absent. The results of the Delft3D simulation do show fluctuations in bed elevation in the initial situation. It uses the bed level obtained from Baseline that represents the actual local bed level. This initial bed level shows some irregularities (Appendix Fig. C.6). In Figure 5.5b it can also be seen that before the implementation of the side channel there is a hump at rkm 916 and a scour hole at rkm 916.5. We do not have an explanation for this sediment hump and scour hole. The scours hole at rkm 917 is caused by the side channel which is already present in the initial situation but which is not yet connected to the river Waal at the upstream end.

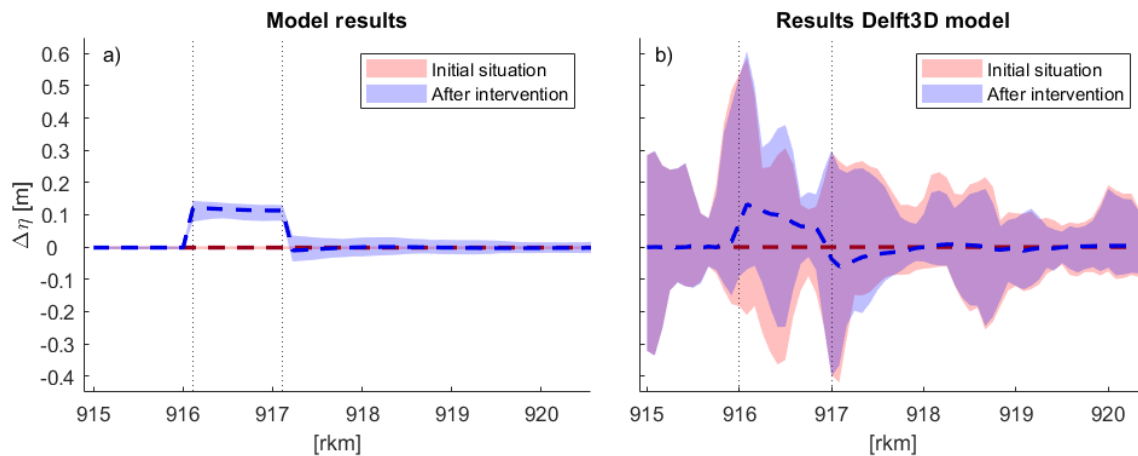


Figure 5.5: 5th and 95th percentile of bed elevation before and after the implementation of a side channel at Passewaaij. The dashed line indicates the mean bed. The side channel is located between rkm 916 - 917. (a) BWE Model. (b) Results of the Delft3D study side channel Passewaaij (Paarlberg, 2013)

To compare both models, the difference in bed level changes before and after the implementation of the side channel is taken (Fig. 5.6). Both models used the same hydrograph to compute the situation before and after the implementation of a side channel. This makes it possible to subtract the initial bed level changes from the bed level changes caused by the river intervention. It can be seen that the results of the Delft3D model show much more variation in bed level than the BWE model. The Delft3D computation is done by a characteristic hydrograph with eight uniform discharge levels. This might result in larger bed level fluctuations since a uniform discharge results in a constant sediment rate. A historical hydrograph shows more variations in discharge such that the sediment humps that develop during high discharges mitigate downstream and fade out during low discharge. In the project of Passewaaij also a quay is included to assure higher water depths in the navigation channel. This means that the threshold for the floodplains before inundating is increased. Although the Delft3D model is more complex and takes several processes into account that the simple one-dimensional model does not, we can compare both trend lines of bed level changes. At the upstream end, the time-averaged bed level change calculated with the rapid method resembles the result of the Delft3D computation. Further downstream we see that the mean bed level change computed with the rapid method stays approximately the same while the bed level change computed by Delft3D decreases. It seems like the bed elevation computed by Delft3D has not yet reached its equilibrium state. Over time, we see that the bed level shows a small gradient (Appendix Fig. C.2). Similar to the case study at Hurwenen, the largest differences are found just downstream of the river intervention. We expect a scour hole, similar to the Delft3D results, but the rapid method shows aggradation and degradation downstream that cancel each other out over time.

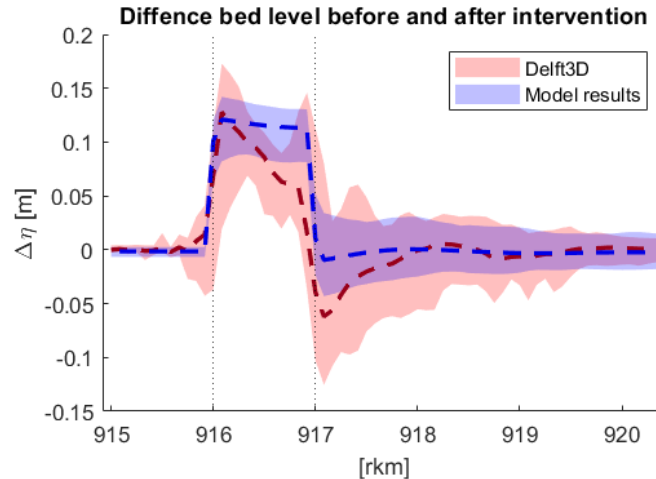


Figure 5.6: The morphological effect of the side channel at Passewaaij with a bandwidth between the 5th and 95th percentile

5.3 Conclusion

In this research, we are looking for a rapid method that can be used in the inventory phase of river projects to make an estimation of the morphological effect of river interventions. Already, analytical models of quasi-equilibrium channel geometry exist. However, these tools are not applicable to backwater-dominated river segments. By definition, a river intervention causes additional backwater effects. The space-marching model of Arkesteijn et al. (2019) is a rapid tool to calculate the equilibrium state in backwater and quasi-normal flow segments. However, we have shown that the model for the dynamic component of the equilibrium state is based on two assumptions that are not valid for river interventions. First, the model uses a static slope approximation, which is not valid in the upstream boundary segment (An et al., 2017). Second, the hydrodynamic update is done by stepping through space. River interventions cause large bed level changes that influence the water level. This process is not included in a space-marching hydrodynamic update. Thus, we choose an abridged version of the traditional Backwater-Exner Model and assume that this gives a correct estimation of the equilibrium state.

The verification of the model is very limited. We only verified one of the five types of river interventions. We verified a side channel with measurements at Hurwenen and with model results of Passewaaij computed with Delft3D. Despite the limited amount of reference material, we can still say something about the performance of the model. The mean bed level change at the location of the river intervention calculated with the abridged version of the BWE model approximates the measured and calculated mean bed level change. At the downstream end of the river intervention, we expect a scour hole since the discharge is supplied from the side channel into the main channel. This expectation is confirmed by the measured data and the Delft3D computation. However, the mean bed level change calculated by the rapid method does not show a scour hole. For the rapid method, we use an extraction tool that determines the fraction of discharge that flows through the main channel prior to the computation. Due to the river intervention the bed level changes and therefore, the geometry of the river changes. This results in a re-distribution of the discharge between the main channel and the floodplains. In fact, the discharge extraction is not constant, but a function of the morphological change in the main channel (Van Vuren, 2005b). In practice, the initial erosion downstream of the river intervention induces a re-distribution of the river discharge between the main channel and the floodplains. A higher percentage will flow via the main channel. This feedback results in more erosion. The same occurs at the upstream end of the river intervention but can be seen less clearly by the comparison of the case studies. Besides, the measurements and Delft3D show much more bed level fluctuations since the irregularities in river geometry are included in the initial situation. Nevertheless, the rapid method is an appropriate tool to compute the bed level changes just upstream of a river intervention.

6 Morphological impact of river interventions

We use a combination of the space-marching model A and the abridged version of the BWE Model to investigate the morphological effect of five different types of river interventions. First, we look at the time-averaged bed level change. Second, we look at the dynamic impact of the river interventions.

6.1 Average bed level change

To compare the different types of interventions, we choose the sizes of the intervention in such a way that the initial condition at the downstream end of the interventions, obtained from Model A, is similar (see Table 4.3). However, for dike relocation, this leads to an unrealistic value for the size of the intervention. A dike relocation only has an effect on the peak discharges. Just a few days per year, the effect of the river intervention is noticeable. Therefore, the size of the intervention is relatively large to compensate for the short period that the intervention is active.

Results Model A

For each of the river interventions, the mean bed level is computed over a period of 100 years. We use Model A to find the sizes of the river interventions. The sizes are based on a time-averaged bed level change of 20 cm. The results of Model A show that the five types of river interventions indeed result in aggradation of 20 cm (Fig. 6.1). Upstream of the river intervention there are some very small differences between the river intervention but these are not significant compared to the bed level change of 20 centimetres. Also at the upstream end of the river interventions there are some very small differences. We do not know what causes these small differences, but these differences are only a few millimetres. So, we can assume that the bed elevation computed by Model A is similar for all five types of river interventions.

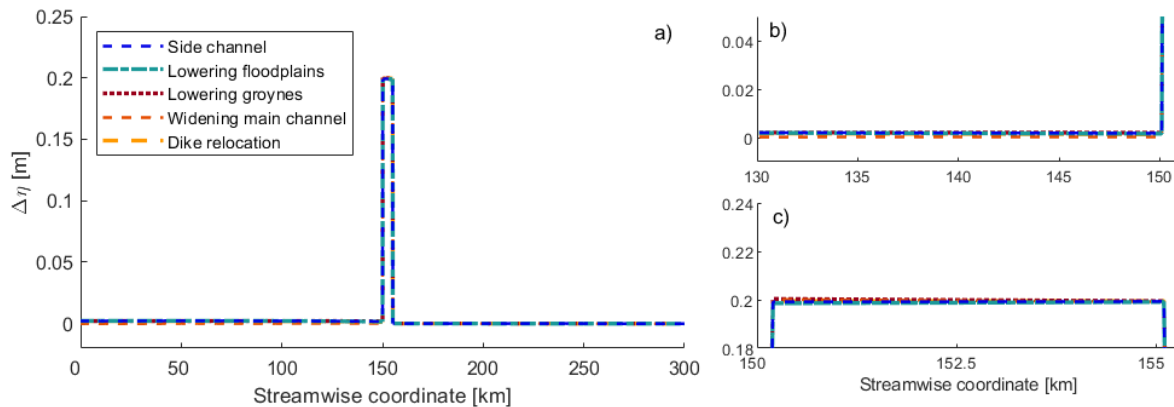


Figure 6.1: Time-averaged change in bed elevation obtained from Model A. (a) Change on the full domain. (b) Detailed bed level change at the upstream side of the intervention. (c) Detailed bed level change along the river intervention.

Time averaged results BWE Model

As explained in the model description (see Chapter 5.3) the result of Model A is used as an initial condition for the BWE Model. Therefore, we would expect that the time-averaged bed elevation computed by the BWE Model would approximate the result of Model A. However, the results show that the static-component of the equilibrium state computed by Model A is different than the time-averaged bed elevation obtained by the BWE Model (Fig. 6.2). All five river interventions show perturbations in bed elevation downstream of the intervention (Fig. 6.2c). The largest perturbations are caused by dike relocation,

followed by the lowering of floodplains and the construction of a side channel. At the downstream end of the river intervention, the average bed level change is for all five types of river interventions approximately 21 centimetres instead of 20 centimetres as calculated by Model A (Fig. 6.2b). The perturbations in bed elevation make it seem like the bed elevation calculated by the BWE Model has not yet reached the equilibrium state. However, the variations in time-averaged bed elevation over space show a maximum deviation of one centimetre compared to the static equilibrium computed by Model A, except at the upstream end of the intervention where the deviation is about two centimetres for widening the main channel.

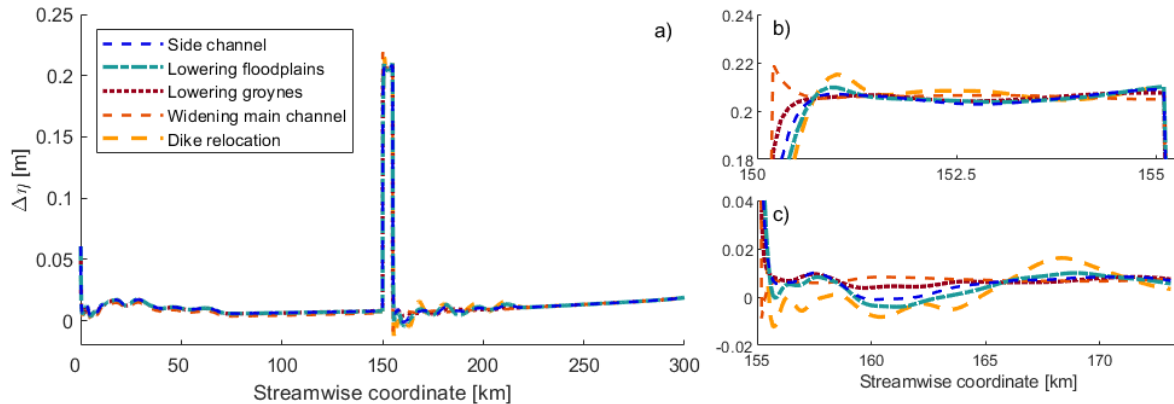


Figure 6.2: Time-averaged change in bed elevation obtained from the BWE Model. (a) Change on the full domain. (b) Detailed bed level change along the river intervention. (c) Detailed bed level change downstream of the river intervention.

6.2 Dynamic impact of river interventions

The initial bed level computed by Model A is approximately the same for all five types of river intervention. Looking at the temporal bed level changes, we see that the variation in bed elevation is distributed differently per type of intervention (Fig. 6.3). Some river interventions have only a small effect on the bed level fluctuations downstream whilst others cause large migrating bed level perturbations (Fig. 6.4). We discuss the main findings for each type of river intervention, one by one.

Side channel construction

The general morphological effect of the construction of a side channel is aggradation at the upstream end of the intervention and erosion at the downstream end. The largest bed level fluctuations can be found just upstream and downstream of the intervention and are around 0.5 meters (Fig. 6.3). The fluctuations in bed elevation, caused by the construction of a side channel, migrate downstream and fade out over space. Only one-third of the bed level fluctuations is still visible 15 kilometres downstream of the intervention (Fig. 6.4). Low discharge levels, corresponding with the base flow, cause little effect on the bed level (Fig. 6.5). The side channel is not yet active at these low discharge values (Fig. 4.4). For discharges above $1500 \text{ m}^3/\text{s}$, water from the main channel is extracted by the side channel. We see that the bed level changes become larger for higher discharge values. At the upstream end, there is a clear correlation between the discharge in the previous time step and the bed level change in the next time step (Fig. 6.5). Peak discharges cause, on average, bed level changes of 0.4 meters. At bankfull discharge, the bed level changes are approximately 0.2 meters, similar to the static component of the equilibrium state. At the downstream end, the correlation between discharge levels and the size of bed level change is reverse. Peak discharges result in large amounts of erosion. At base flow and bankfull discharge erosion and aggradation occurs such that the average bed level change equals zero metres.

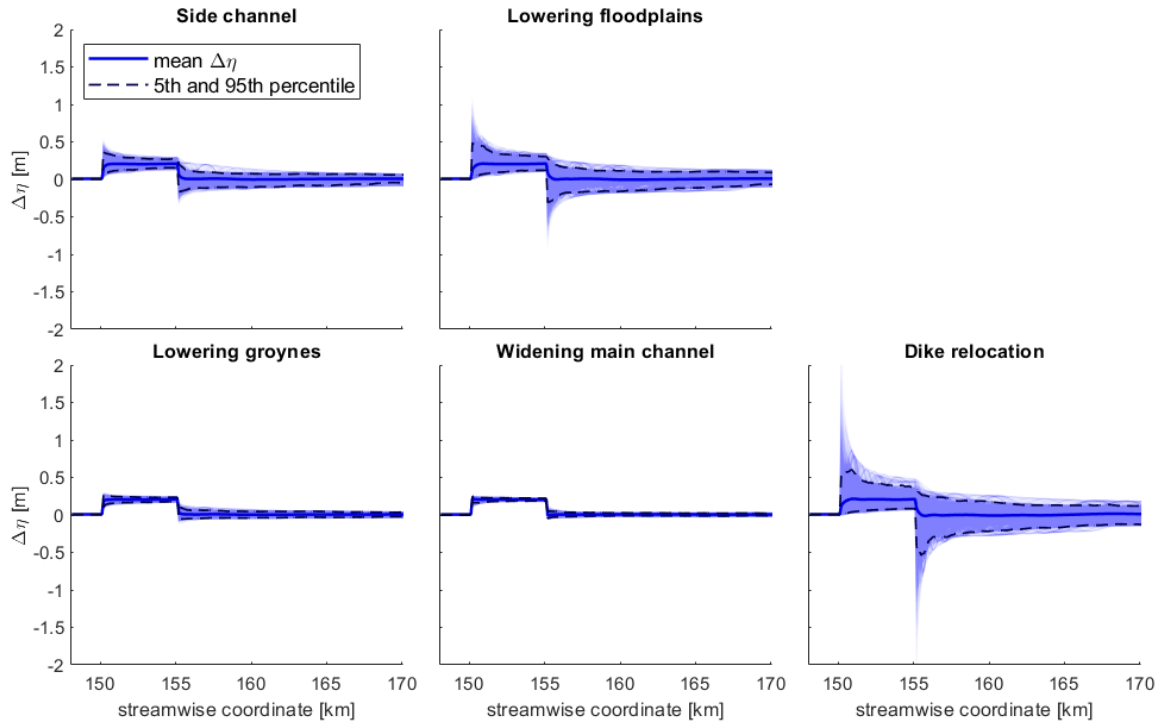


Figure 6.3: Variations in bed level change for different river interventions with the mean bed level change and the 5th and 95th percentile over space

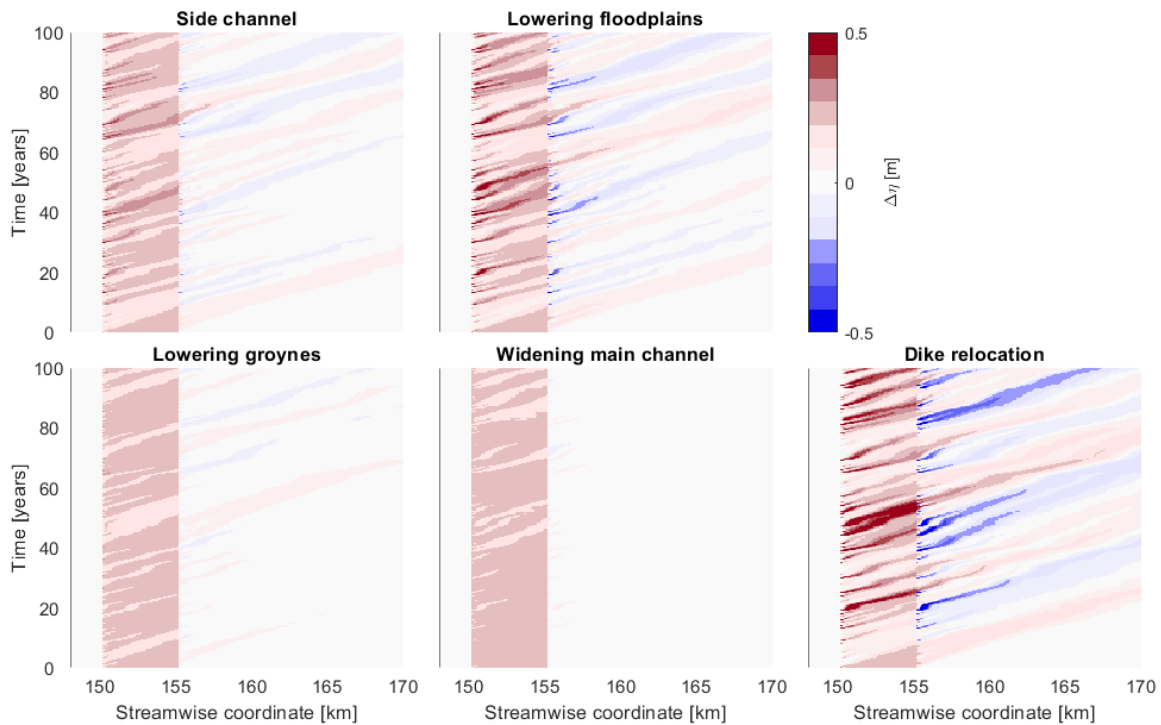


Figure 6.4: Temporal bed level changes over space (x-axis) and time (y-axis). The river intervention is located between 150 and 155 km. Blue areas indicate erosion. Red areas indicate aggradation. For lowering floodplains and dike relocation the maximum temporal bed level changes exceed 0.5 meters but the frequency is very low.

Lowering floodplains

The morphological effect of lowering the floodplains is similar to the effect of the construction of a side channel, only the size of bed level fluctuations is larger. The maximum bed level change at the upstream end of the intervention is 1.0 meter, but the frequency of occurrence is very low. 95% of the time, the bed level change is not more than 0.5 meters (Fig. 6.3). At the downstream end, the largest change in bed elevation is -0.8 meters. The fluctuations in bed elevation, caused by lowering the floodplains, migrate downstream and slowly fade out over space (Fig. 6.4). The bandwidth of bed level fluctuations is still more than 10 centimetres 15 kilometres downstream of the intervention. The distribution of bed level changes upstream and downstream of the intervention is lowest for base flow (Fig. 6.5). The distribution becomes larger for increasing discharge rates. Without lowering the floodplains, the floodplains are inundated only about 20 days a year (based on the fraction curve, Fig. 4.4, and the discharges of the river Waal). By lowering the floodplain, the floodplains are inundated almost twice as much, but this is still only one-tenth of the time. Therefore, the differences in bed level change are relatively large for this type of river intervention. At a discharge level of 4000 m³/s and with a base flow in the previous time step, the bed level change can be zero, but it can also become more than 0.8 meters.

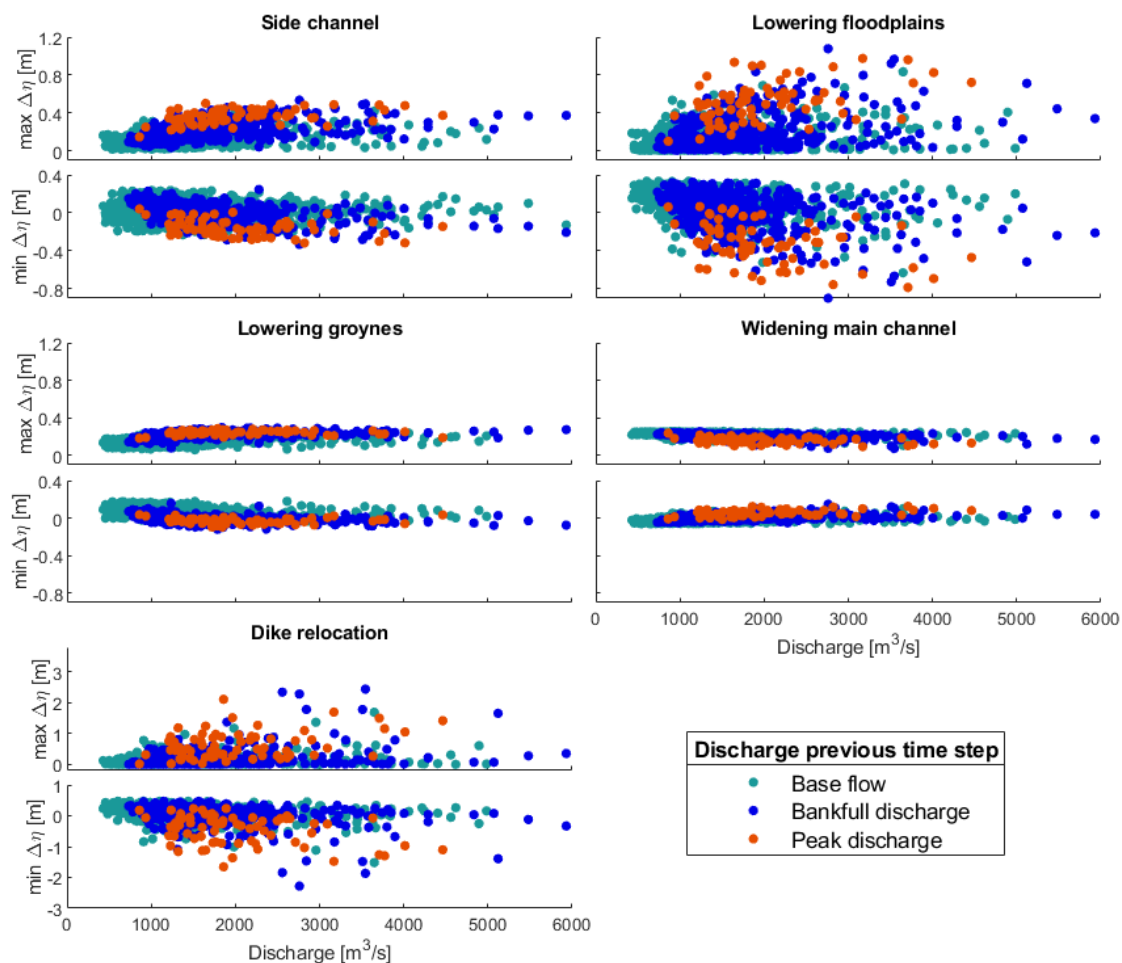


Figure 6.5: Correlation between discharge and bed level change at the upstream end ($\max \Delta\eta$) and downstream end ($\min \Delta\eta$) of the river intervention classified by the discharge level in the previous time step: base flow ($>1500 \text{ m}^3/\text{s}$), bankfull discharge ($>1500 \text{ m}^3/\text{s}$ & $<3000 \text{ m}^3/\text{s}$) and peak discharge ($>3000 \text{ m}^3/\text{s}$)

Lowering groynes

The morphological effect of lowering groynes is relatively small. The fluctuations in bed elevation are centred around 0.2 meters at the upstream end and 0 meters at the downstream end (Fig. 6.3). We see no outliers in bed level change as can be seen for the lowering of floodplains. The bandwidth of bed level variation is less than 20 centimetres. Also, over time, we see less variation in bed elevation (Fig. 6.4). The perturbations in bed elevation that are caused by the river intervention are small and fade out over space relatively quick. We see a clear correlation between the discharge in the previous time step and the bed level change (Fig. 6.5). Low discharge levels with base flow in the previous time step, result in very small bed level fluctuations. However, at the downstream end of the river interventions, these low discharge levels cause bed level aggradation up to 10 centimetres. Higher discharge levels cause more bed level fluctuations. At the downstream end of the intervention, the higher discharge levels are responsible for the erosion of the river bed. An explanation for the relatively small bed level fluctuations, caused by lowering the groynes, can be found by the fact that the lowered groynes are inundated half of the time. There is a relatively constant change in the discharge at the upstream and downstream end of the intervention, such that the local variations in sediment transport are small.

Widening main channel

The morphological effect of widening the main channel is an increase in bed elevation of 20 centimetres. The fluctuations around the time-averaged bed elevation are very small. The magnitude of these fluctuations is only a couple of centimetres (Fig. 6.3). There barely are fluctuations over time and space. Downstream of the intervention, the bed level fluctuations are almost invisible (Fig. 6.4). The perturbations in bed elevation fade out over a few kilometres. 5 kilometres downstream of the river intervention the effect is no longer noticeable. The effect of an increase in discharge on the bed elevation is opposite for the widening of the main channel compared to the other four types of intervention (Fig. 6.5). The bed level fluctuations at the upstream end of the river intervention become less when the discharge increases. On the downstream side, low discharges result in bed erosion, while large discharges are responsible for bed level accretion. The peak discharges result in the smallest bed level changes upstream and the most aggradation downstream. At high discharge levels, the groynes and floodplains are inundated and the effect of the widening of the main channel becomes smaller. Therefore, the effect of the discharge on the river bed is the opposite.

Dike relocation

The relocation of the dike has a large effect on the temporal bed level changes. Whilst the time-averaged bed level change is only 20 centimeters, the fluctuations in bed elevation rise to 2 meters at the upstream and downstream end of the intervention (Fig. 6.3). The frequency of occurrence of these maximum bed level fluctuations is small. 90% of the time, the bed level at the upstream end of the river intervention varies between 0 and 0.6 meters. At the downstream end, the bed level varies between 0.4 and -0.5 meters. Even downstream of the intervention, the bandwidth of bed level fluctuations is large. The time-averaged bed level change is zero, but over time, sediment humps and scour holes with a magnitude of tens of centimetres migrate downstream (Fig. 6.4). Almost all perturbations in bed elevation caused by the dike relocation are still visible 15 kilometres downstream of the intervention. Only the size of the perturbations has slowly decreased over time and space. A large part of the year, the relocation of the dike does not cause an additional effect on the bed level change (Fig. 6.5). At base flow, the floodplains are not inundated and the relocation of the dike has no effect. At peak flow, the floodplains start to inundate and the effect on the bed elevation becomes visible. The distribution of bed level changes becomes larger at higher discharges. Large bed level changes are not caused by a single high discharge, but by two or more successive high discharge levels. The large differences in bed level fluctuations are caused by the large size of the river intervention. At high discharges, almost half of the total discharge is extracted from the main channel (Fig. 4.4).

6.3 Conclusion

We see that, although the time-averaged bed level change is almost similar for the five different types of river interventions, the fluctuations in bed elevation show large differences. It can be concluded that a river intervention that changes the geometry of the main channel causes the smallest fluctuations in bed elevation. The size of these bed level fluctuations is only a couple of centimetres. The river interventions of a side channel and lowering groynes that not directly change the geometry of the main channel, show some more fluctuations. The perturbations caused by the river intervention are larger and migrate further downstream. These fluctuations vary between a couple of centimetres up to twenty centimetres for the side channel. The most and largest fluctuations are caused by interventions in the floodplains, namely lowering the floodplains and dike relocation. Since the floodplains are only part of the time inundated, we see that most of the time the bed level changes are almost zero. But once the floodplains start to inundate large sediment humps and scour holes arise which migrate downstream and slowly fade out over space. The largest bed level fluctuations can become more than one metre. The size of changes in bed elevation is strongly related to the discharge in the previous time step. Peak discharges cause the largest bed level changes, except for widening the main channel where the morphological effect is opposite.

7 Uncertainties in bed level fluctuations

Modelling river interventions is inherently uncertain due to a lack of knowledge and assumptions and simplifications made for model purposes (Van Vuren, 2005b). To investigate the uncertainties in simulated morphological changes for different river interventions, we perform a Monte Carlo Simulation. We look at the uncertainties introduced by variations in river discharge, yearly sediment transport and hydraulic roughness.

7.1 Generating discharge series

We generate a set of 400 discharge series of cycled hydrographs of 20 years based on historical discharge series from 1900-1999. The minimum and averaged generated discharges resemble the observed minimum and averaged discharges of the river Waal (Fig. 7.1). The maximum value of the generated discharges is higher than the observed maximum discharge. The absolute maximum generated discharge is approximately 9000 m³/s. In the historical discharge series, the maximum discharge is limited to 8200 m³/s. The peak discharges are higher in the generated discharge series but are less frequent. This distribution of generated discharges resembles the historical data set. Some small differences can be found in the frequency of low and high discharges (Appendix Fig. D.9), but in general, we can conclude that the generated discharge series represents the observed discharge series well.

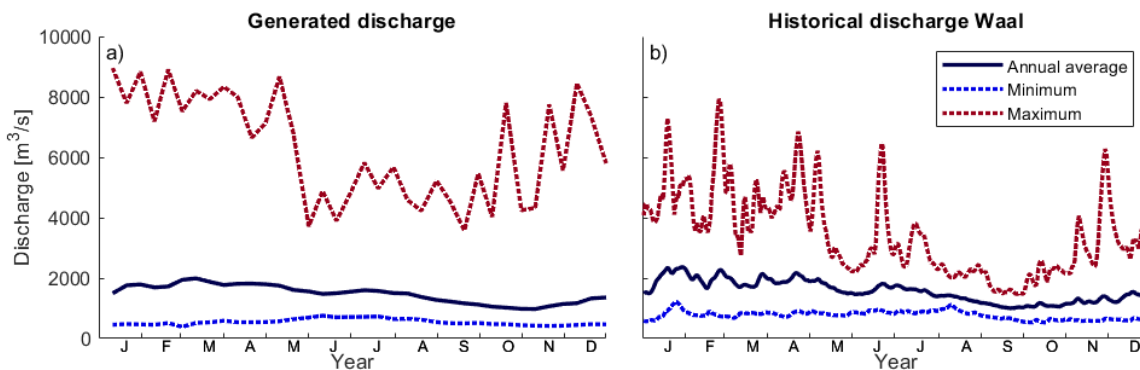


Figure 7.1: Maximum, averaged and minimum values of (a) 400 discharge hydrographs synthesised by random sampling from the multivariate lognormal distribution function and (b) measured historical river Rhine discharge translated to the river Waal over the period 1900-1999.

7.2 Results Monte Carlo Simulation

We perform an MCS with a sample size of 400 which is sufficient to show accurate results (see Appendix D.2). We look at variations in discharge (Fig. 7.2), the yearly sediment transport (Fig. 7.3), and hydraulic roughness of the main channel, groynes and floodplains (Fig. 7.4). Large changes in bed elevation are not caused by a single high discharge but result from a period of high discharges (Fig. 6.5). We use the maximum discharge per month and look at the corresponding maximum aggradation and erosion at the upstream and downstream end of the intervention. The results are similar to the results of a deterministic computation (Fig. 6.5) but have much more data points. For some river interventions, this results in a larger distribution of bed level fluctuations. For the yearly sediment transport and hydraulic roughness, we take the maximum aggradation and erosion per run of the MCS. We are interested in the uncertainty of the maximum bed level fluctuations since these cause the largest bottlenecks for shipping. All five types of river intervention are more sensitive to variations in discharge than yearly sediment transport and hydraulic roughness. The degree of sensitivity and uncertainty differs per type of river intervention.

Side channel construction

Under varying flow discharges, the aggradation at the upstream end of a side channel varies between 0 and 0.7 meters (Fig. 7.2). At the downstream end, the bed level variations vary between 0.5 and -0.5 meters. High discharge values result in more sedimentation upstream of the intervention and erosion downstream of the intervention. At the upstream end, the variations in bed level reach a limit. For discharge values above 2000 m^3/s , the maximum aggradation calculated by the MCS stays approximately the same. The dispersion of data points becomes less as the discharge increases. At the downstream end, we see that at low discharge levels the bed level aggrades. For higher discharge levels the bed level degrades.

The maximum bed level changes caused by the construction of a side channel is less sensitive to changes in yearly sediment transport and hydraulic roughness. An increase in yearly sediment transport results at the upstream and downstream end of the river intervention in a decrease in bed level change (Fig. 7.3). At the upstream end, an increase in sediment transport of 10 kilotonnes per year results in a decrease in bed elevation of 4 mm. At the downstream end, this results in a decrease in bed elevation of 1.5 cm. Thus, the downstream end of the river intervention is more sensitive to variations in yearly sediment transport. An increase in roughness height of the main channel results in an increase in bed level change at both, the upstream and downstream end of the river intervention (Fig. 7.4). This effect is almost one order of magnitude larger than the effect of variations in roughness height of the groynes and floodplains. Besides this effect is opposite compared to the effect at the groynes and floodplains.

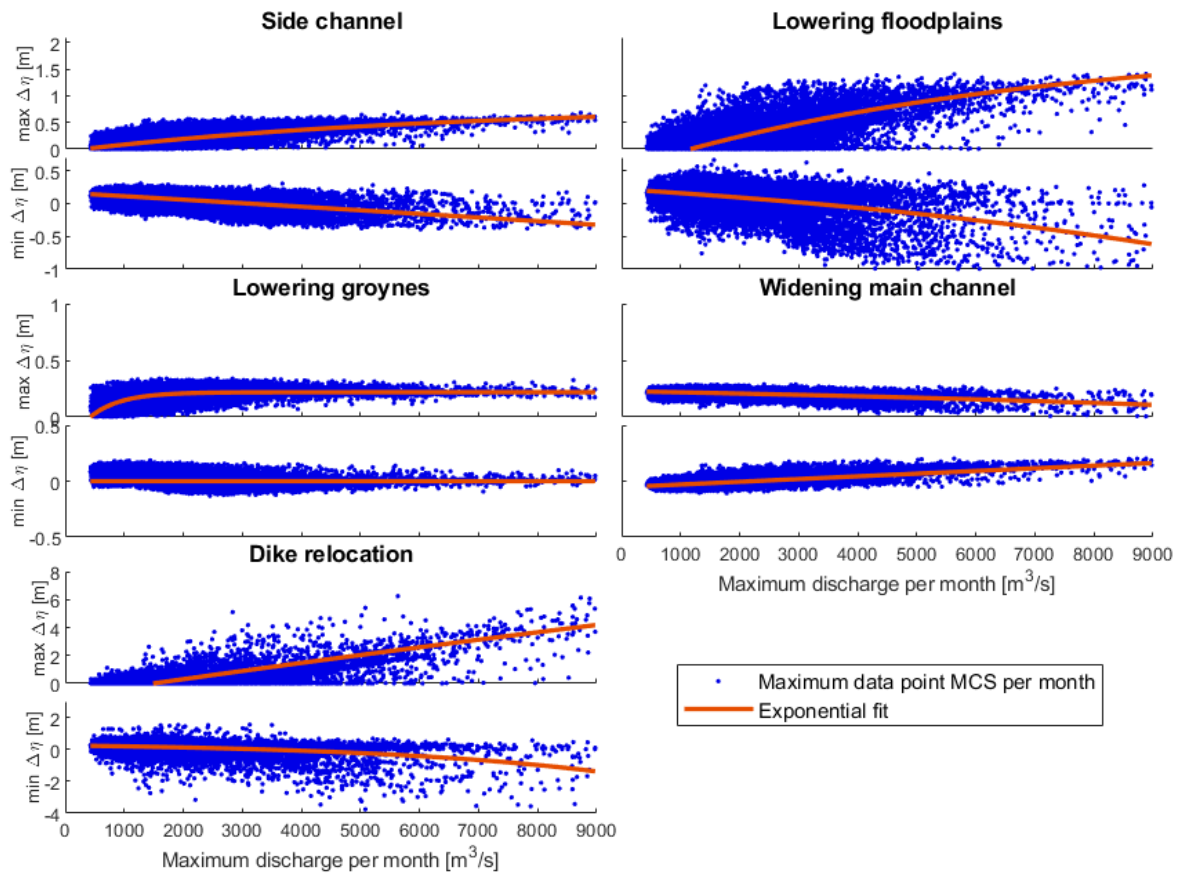


Figure 7.2: Bed level changes at the upstream end ($\max \Delta\eta$) and downstream end ($\min \Delta\eta$) of the river interventions, given in meters, under varying monthly-discharges.

Lowering floodplains

Variation in discharge results in a maximum amount of aggradation at the upstream end of lowered floodplains between 0 and 1.5 meters (Fig. 7.2). At the downstream end, the variations in bed elevation fluctuate between 0.5 and -1 meters. Similar to the effect of the construction of a side channel, the changes in bed elevation at the upstream end reach a limit. Discharge values above $3000 \text{ m}^3/\text{s}$ result in no significant increases in bed level changes. At the downstream end, an increase in discharge results more bed erosion. The dispersion in variations in bed elevation is the smallest for very low discharge levels. Although there are fewer data points for high discharge levels, the dispersion of these data point become larger.

The effect of variations in yearly sediment transport on the lowering of floodplains is similar to the side channel, except the maximum and minimum bed level changes are almost twice as large for the lowering of floodplains (Fig. 7.3). The effect at the upstream end is relatively small. At the downstream end, the effect is almost four times bigger. The effect of variations in roughness height is largest for the main channel at the upstream end (Fig. 7.4). A larger roughness height results in a smaller Chézy value. This leads to higher equilibrium water depth. So, with an increase in roughness height in the main channel, the floodplains will inundate more often resulting in more bed level fluctuations. Remarkably, the sensitivity of the roughness height in the main channel is almost eight times bigger than the floodplains. However, the uncertainty in the floodplains is much larger than in the main channel.

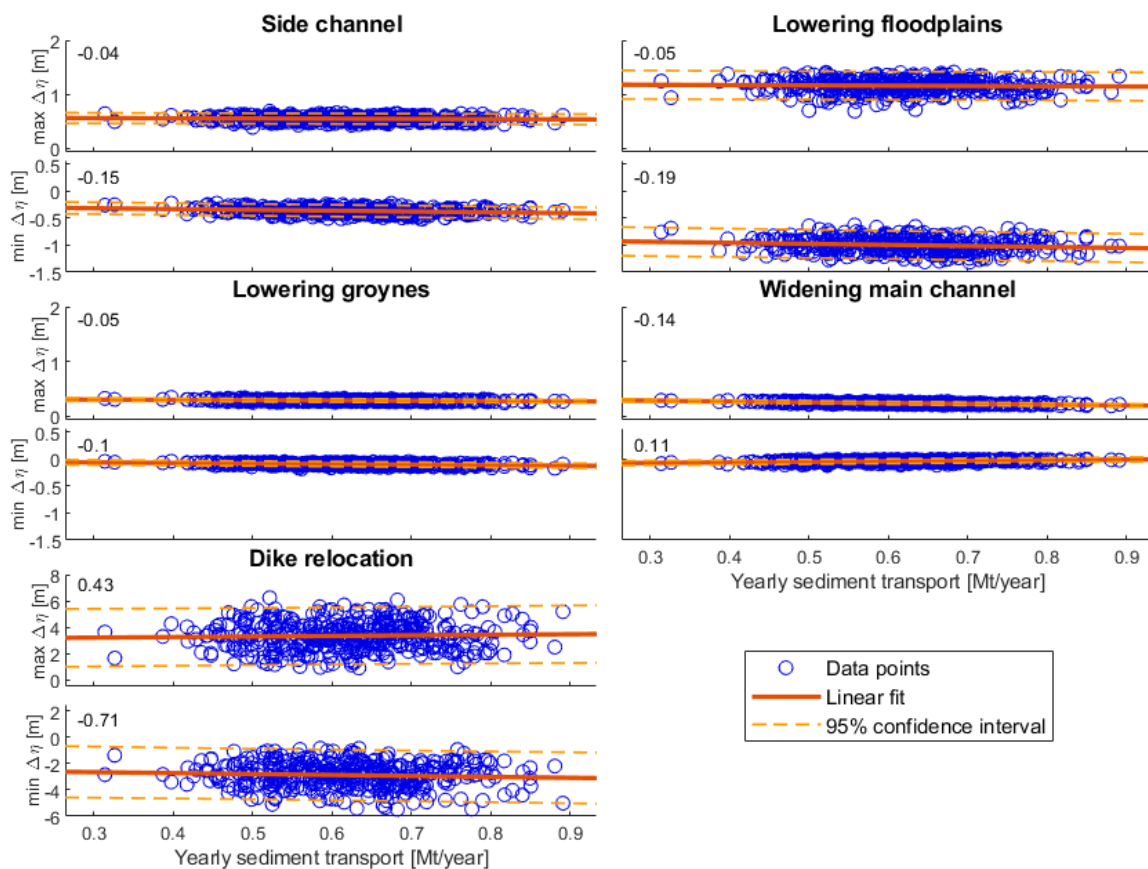


Figure 7.3: Bed level changes at the upstream end ($\max \Delta \eta$) and downstream end ($\min \Delta \eta$) of river interventions for variations in yearly sediment transport. The numbers indicate the slope of the linear fit. It represents the increase or decrease of bed elevation in meters for an increase of 1 Mt/year in yearly sediment transport.

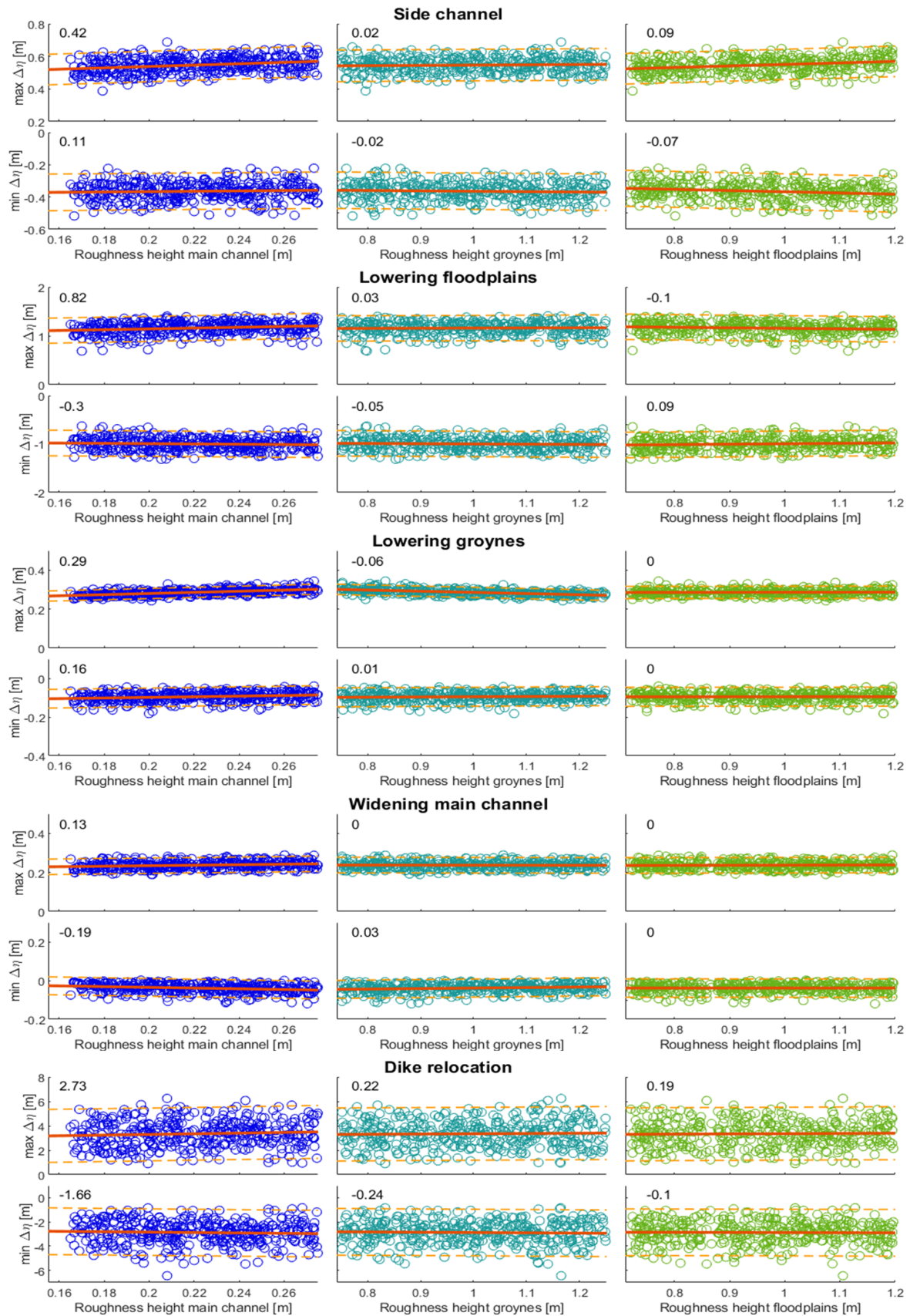


Figure 7.4: Roughness height for main channel (left), groynes (middle) and floodplains (right) at upstream and downstream end, with linear fit (red line) and the 95th confidence interval (orange dotted line). The numbers indicate the slope of the linear fit.

Lowering groynes

The effect of variations in discharge is relatively small for lowering groynes. At the upstream end, the maximum bed level changes vary between 0 and 0.4 meters (Fig. 7.2). The aggradation already reaches its limit at a discharge level of 1500 m³/s. At the downstream end, the exponential fit gives a steady line at 0. This means that the amount of aggradation and erosion average out over all discharge levels. The dispersion of bed level changes is higher at low discharge levels than at high discharge levels.

The effect of variations in yearly sediment transport and roughness height is also relatively small for lowering groynes. An increase in yearly sediment transport results in a decrease in bed level change at both ends of the river intervention (Fig. 7.3). The effect of variations in roughness height is largest in the main channel. An increase in roughness height results in an increase in bed level change at both ends of the river intervention (Fig. 7.4). This effect is similar to the side channel. The effect of variations in the roughness height of the groynes is small, but opposite to the effect of the four other river interventions. An increase in roughness height results in a decrease in aggradation upstream. Higher values in roughness height result in higher equilibrium water depths. This means that less water can be extracted from the main channel to the groyne fields. Therefore the morphological effect becomes smaller. The opposite occurs at the downstream end.

Widening main channel

The effect of variations in discharges has an opposite effect on bed level changes compared to the other types of interventions (Fig. 7.2). Instead of a decrease in the fraction of discharge that flows through the main channel, widening the main channel results in an increase of discharge fraction. An increase in discharge results in a decrease in bed level change upstream of the intervention. Downstream of the intervention, this results in less erosion and for high discharge levels even in more aggradation. The variations in bed level are small, only a few tens of centimetres. At the upstream end, the bed elevation varies between 0.15 and 0.4 meters. At the downstream end, the bed elevation varies between -0.15 and 0.2 metres.

Variation in yearly sediment transport also results in an opposite effect compared to the other four types of river interventions, especially downstream of the river intervention (Fig. 7.3). The effect at the upstream end of the river intervention is almost three times as large compared to the effect of the previous three river interventions. An increase in yearly sediment transport results in smaller bed level changes. The yearly sediment transport determines the bed slope of the river. An increase in yearly sediment transport results in an increase in bed slope. This leads to higher flow velocities and therefore an increase in sediment transport capacity. The effect of variations in roughness height is virtually absent in the groyne fields and the floodplains (Fig. 7.4). Due to the change in geometry of the main channel, the groynes and floodplains will less often be inundated. At the upstream end, an increase in roughness height results in an increase in bed level change. The larger the resistance by the river bed, the smaller the flow velocities.

Dike relocation

We saw already that variations in bed elevation are the largest for dike relocation (see Chapter 6). Also, the uncertainties in bed elevation introduced by variations in discharge are the largest for dike relocation. At the upstream end, the bed elevation varies between 0 and 7 meters (Fig. 7.2). At the downstream end, the variations in bed elevation vary between -4 and 2 meters. This is a factor 10 larger than the variation in bed elevation caused by the construction of a side channel. High discharge levels result in large variation in bed elevation. For the other four types of interventions, we see that there is a limit in bed level change. At the dike relocation, the limit is not yet reached at discharge rates of 7000 m³/s. At the downstream end of the intervention, we also see large variations in bed level change. The exponential fit shows that up to 4000 m³/s, the averaged bed level change is approximately zero. However, the bandwidth of uncertainties is quite large. For example, at a discharge of 4000 m³/s there are periods

without bed level changes. On the other hand, there are also periods with an increase in bed elevation of 4 meters at the upstream end of the intervention.

The variations in yearly sediment transport and roughness height also show large variations in bed elevation (Fig. 7.3). The confidence interval of the maximum bed level changes is almost 5 meters. An increase in yearly sediment transport increases the aggradation upstream and degradation downstream of the intervention. The effect of changes in hydraulic roughness is most pronounced in the main channel (Fig. 7.4). The larger the roughness height in the main channel, the higher the equilibrium water depth. This results in more water extracted by the floodplains and consequently more water supplied back to the main channel at the end of the river intervention.

7.3 Conclusion

Based on deterministic model computations we can already say something about the range of bed level fluctuations, but the MCS helps us to quantify the uncertainty in bed elevation. We looked at variations in discharges, yearly sediment transport and hydraulic roughness. In the previous chapter, we calculated the bed level fluctuations caused by a historical hydrograph of 100 years. The advantage of the MCS is that we have much more data to find correlations and trends. We see that for the river interventions in the main channel, the correlation and trends found by the MCS are similar to the results of the deterministic computation. For river interventions in the floodplains, the MCS shows that the distribution of bed level fluctuations becomes larger. This means that the river interventions in the floodplains are more sensitive to variations in discharge. Besides, the river interventions in the floodplains are only activated if the floodplains are inundated. In the historical hydrograph, the floodplains are on average 10 days per year inundated. This means that the probability of occurrence of peak flows is very small compared to base flow and bankfull discharge. A MCS helps to account for these uncertainties in discharge. Therefore, it is recommended to use a stochastic model approach for river interventions in the floodplains.

The yearly sediment transport shows large uncertainties. Therefore, we looked into the effect of variations in yearly sediment transport on the changes in bed elevation. We see that the effect is larger at the downstream end than at the upstream end. We have no explanation why there is this difference. A possible reason could be the increase in flow velocity that results in more sediment that can be transported by the flow. In general, an increase in yearly sediment transport results in a decrease in bed level change at both ends of the river intervention.

Finally, we looked into the variations in roughness height. We found that variations in the main channel are most dominant for bed level changes. The roughness height in the main channel determines the equilibrium water depth. Larger roughness heights result in larger equilibrium water depth. Based on these equilibrium water depth the fraction of discharge through the main channel is determined. Although the variations in roughness height in the main channel show the largest sensitivity, the roughness height in the floodplains is most uncertain. Based on the vegetation in the floodplains, the roughness height becomes larger or smaller. But because the floodplains are only part of the year inundated their sensitivity on bed level fluctuations is relatively small.

8 Multiple river interventions

After investigating single river interventions, we look at the effect of multiple river interventions. We use the project Room for Living Rivers to formulate two case studies. We look at the combination of a side channel and filling up the groyne fields, and we investigate the effect of two sequential side channels.

8.1 Combining river interventions

At first glance, the two extraction curves obtained from the WAQUA calculations and the extraction tool are not very different (Fig. 4.8). But, the resulting bed level changes show clear differences (Fig. 8.1). The time-averaged bed level change is approximately 0.5 meters based on the extraction curve obtained by the WAQUA calculations. The fluctuations in bed elevation vary around 0 to 0.4 meters. The combined river intervention causes a lot of bed perturbations that migrate downstream over time and fade out over space. Some bed perturbations migrate 15 kilometres downstream. Computations with the extraction curve obtained by the extraction tool, show an averaged bed level change of 0.7 meters. Although the averaged bed level is larger for this extraction curve, the bed fluctuations are less compared to the extraction curve based on the WAQUA calculations. The red band between 150 and 151.5 km in Figure 8.1, bottom right, indicates that there are little bed fluctuations. Compared to the results with the extraction curves based on the WAQUA calculations, there are fewer perturbations and the effect of the river interventions is less noticeable further downstream of the interventions.

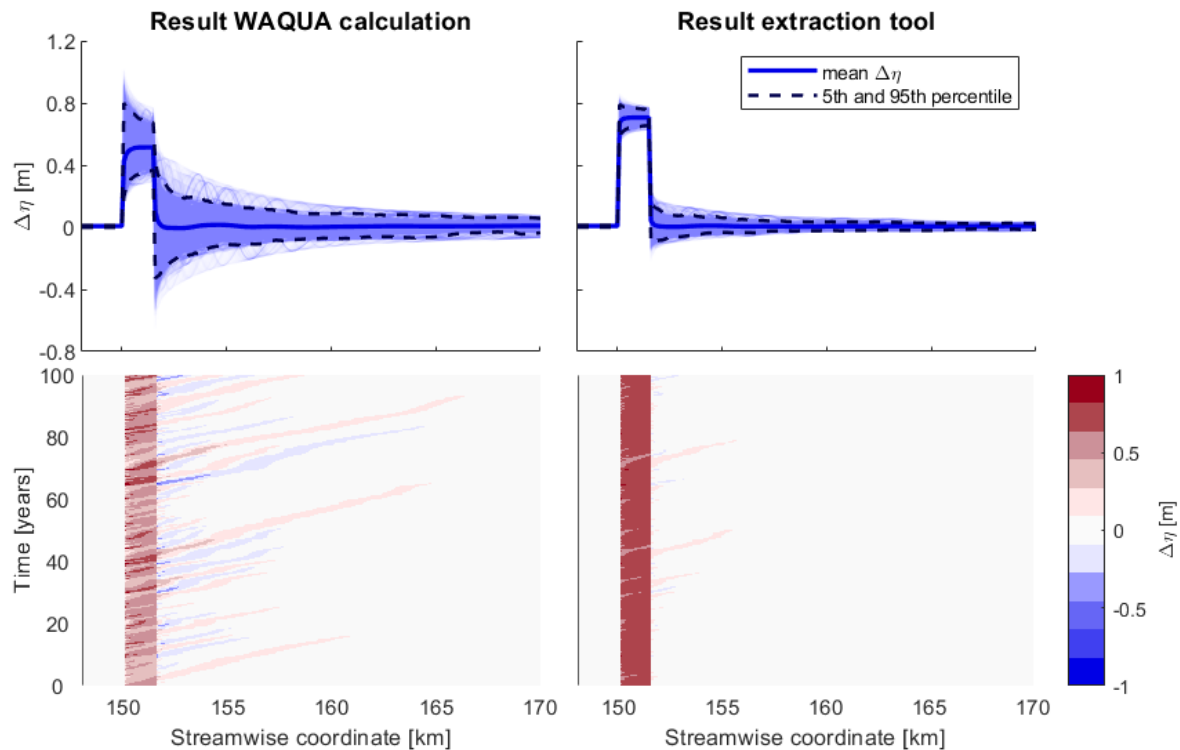


Figure 8.1: Bed level changes with two different extraction curves: obtained by calculations in WAQUA (left) and with the extraction tool (right). Top, time-averaged bed level change and the 5th and 95th percentile. Bottom temporal bed level changes over space (x-axis) and time (y-axis)

The differences in bed level change obtained by the extraction curve based on the WAQUA calculations and the extraction curve computed with the extraction tool are caused by the small differences in the shape of the extraction curves. The extraction curve obtained from WAQUA shows for small discharges

an extraction of approximately 2%. At a discharge level of $1800 \text{ m}^3/\text{s}$ the extraction rises to 7%. The difference in extraction between approximately $1000 \text{ m}^3/\text{s}$ and $2000 \text{ m}^3/\text{s}$ causes the largest fluctuations in bed elevation. The dip at $6000 \text{ m}^3/\text{s}$ is not responsible for the changes in bed elevation since only a small fraction of the discharges exceeds $6000 \text{ m}^3/\text{s}$ (Fig. 4.1). The extraction curve obtained by the extraction tool shows a smooth line from $300 \text{ m}^3/\text{s}$ to $1800 \text{ m}^3/\text{s}$. Since there are no irregularities in the extraction curve, there are no large differences in extracted discharge when the total discharge increases by a small amount. Therefore, the bed level fluctuations are relatively small.

The advantage of the use of the extraction tool is that we can also look at both interventions separately (Fig. 8.2). This helps us to understand the combined morphological effect. The construction of a side channel leads to a time-averaged increase in bed elevation of 0.75 meters. This is compensated by the change in groynes that leads to a decrease in bed elevation of 0.05 meters. The difference in average bed level change can be explained by the difference in extraction discharge. The discharge extracted by the side channel is almost four times as large as the supply of discharge caused by filling up the groyne fields. This also explains the differences in the size of bed level fluctuations. The filling up of groyne fields results in very small bed perturbations of only a couple of centimetres downstream of the interventions, whilst the side channel causes bed level fluctuations up to tens of centimetres. We see that at the times that the bed level increases as a result of the side channel, the bed level decreases as a result of the change in groynes and vice versa (Fig. 8.3). Both perturbations migrate downstream with the same celerity such that the reverse effect holds for the entire river reach. The effect of groynes on the dynamics in bed elevation is smaller than the effect of the side channel. Combining both effects (Fig. 8.1) results in a decrease in fluctuations compared to the situation in which only a side channel would be implemented. So, what we see is that it is possible to reduce the effect of river interventions by combining the interventions in such a way that the effect of a single intervention is compensated by the reverse effect of another type of river intervention.

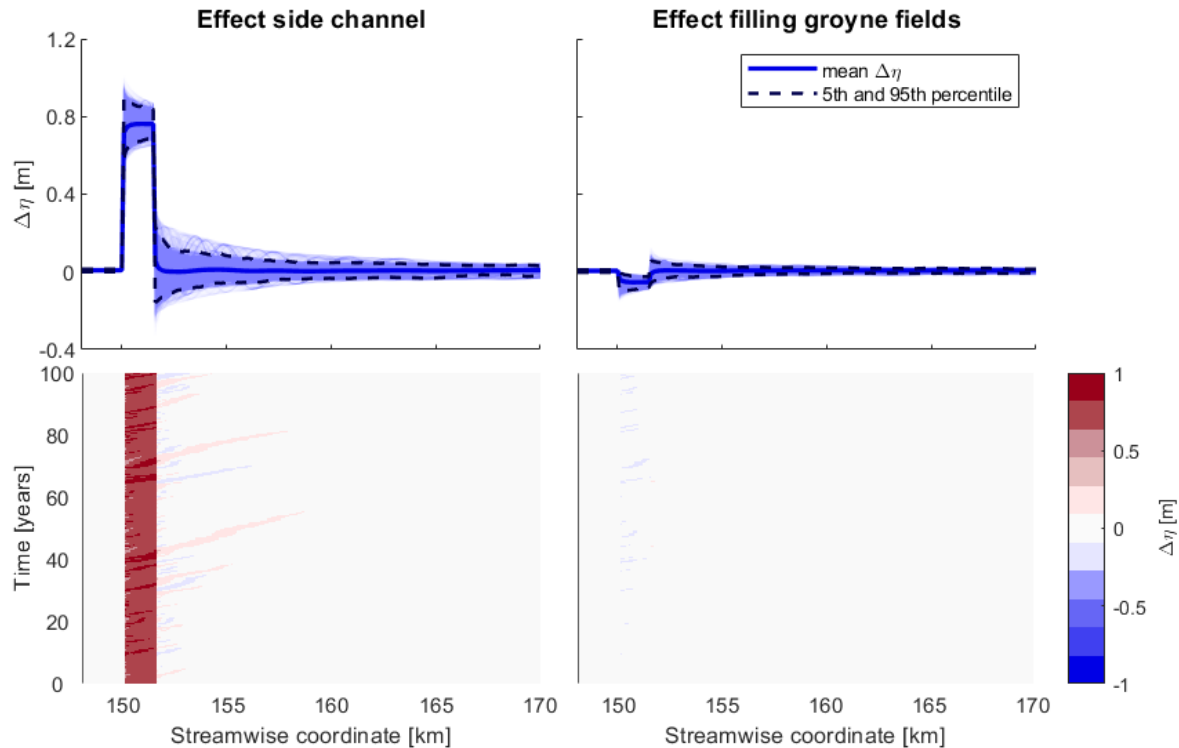


Figure 8.2: Bed level changes for only a side channel (left) and filling up the groyne fields (right). Top, time-averaged bed level change and the 5th and 95th percentile. Bottom temporal bed level changes over space (x-axis) and time (y-axis).

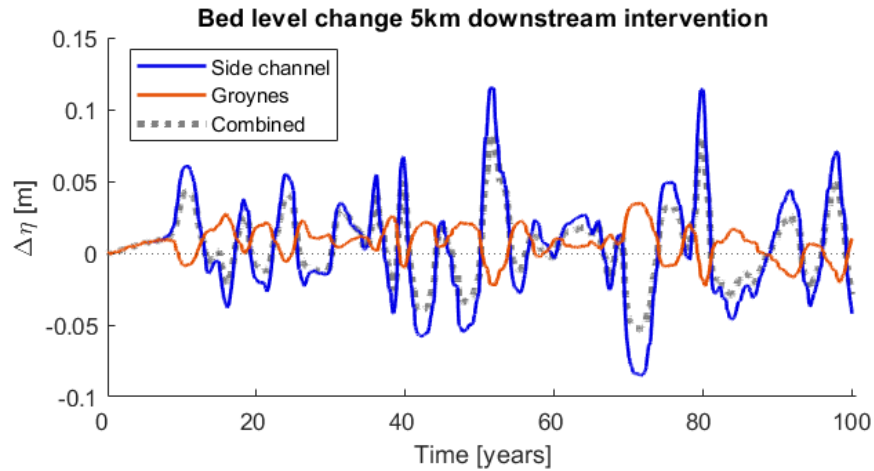


Figure 8.3: Bed level changes over time 5km downstream of the intervention. The single effect of a side channel and filling up the groyne fields have an opposite effect on the bed elevation.

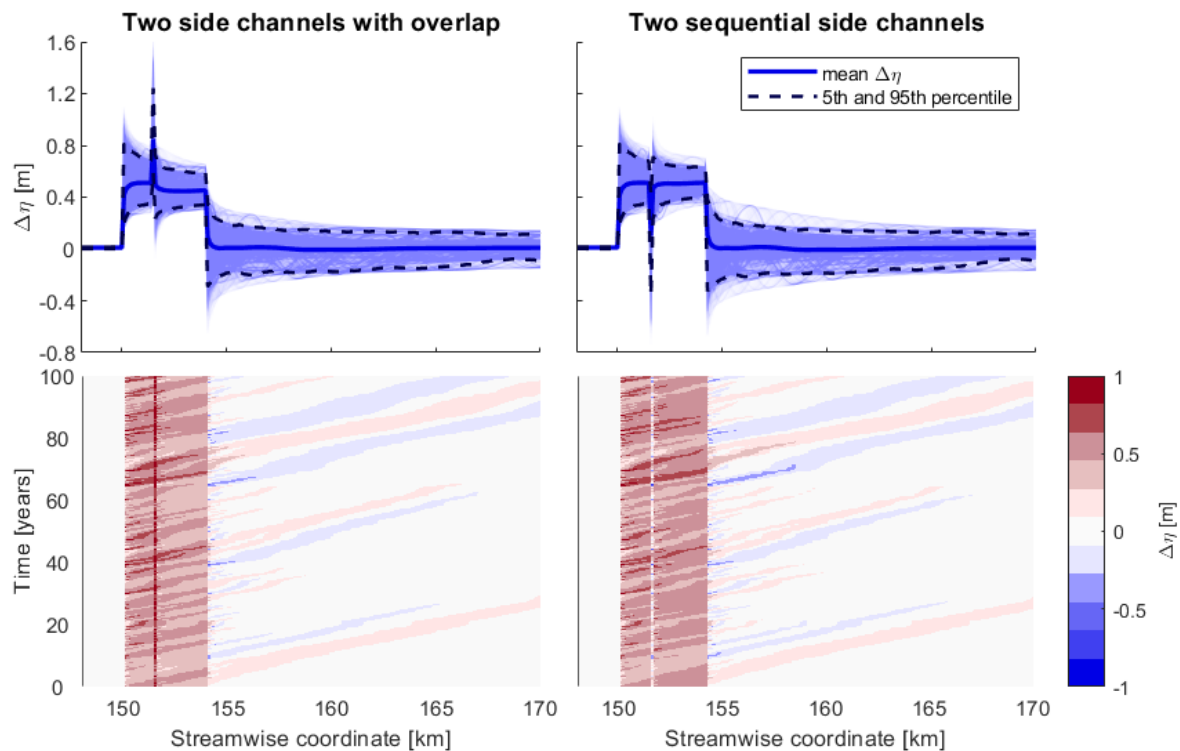


Figure 8.4: Bed level changes caused by two sequential side channels with an overlap of 100 meters (left) and with a gap of 100 meters (right). Top, time-averaged bed level change and the 5th and 95th percentile. Bottom temporal bed level changes over space (x-axis) and time (y-axis)

8.2 Sequential river interventions

We looked at two sequential side channels with a length of 1.5 and 2.5 km, similar to the RfLR project, and distinguished two cases. The two side channels can have an overlap or there is a gap in between both side channels (Fig. 4.10). The idea of sequential river interventions is that the scour hole downstream

of the intervention is compensated by the aggradation upstream of the next intervention. If there is a small overlap between two side channels, a sediment hump arises which can be up to 1.5 meters (Fig. 8.4). By contrast, if there is a small gap between two side channels a scour hole will arise. Most of the time, this hole is smaller than the amount of aggradation caused by the first side channel. Apart from the sediment hump at the location of the overlapping side channels, we see that the bed level fluctuations for two overlapping side channels are smaller than for two side channels with a gap. The time-averaged bed level change caused by the second side channel is almost 5 centimetres larger in the situation of two side channels with a gap in between. Besides, the perturbations in bed elevation that migrate downstream are a few centimetres larger and migrate a few meters further downstream in this situation (Fig. 8.4 bottom).

The explanation of the differences in bed level changes caused by two overlapping side channels and two side channels with a gap in between can be found by the differences in extracted discharge. Figure 8.5 illustrates the discharge in the main channel for both cases with an initial discharge of $1800 \text{ m}^3/\text{s}$ upstream of the intervention. The extracted discharge is determined by the extraction curve and the discharge that flows through the main channel. Due to a difference in location of the second side channel, the amount of discharge in the main channel just upstream of the second side channel is different. This results in a distinction in extracted discharge from the main channel by the second side channel resulting in a difference in bed level fluctuations.

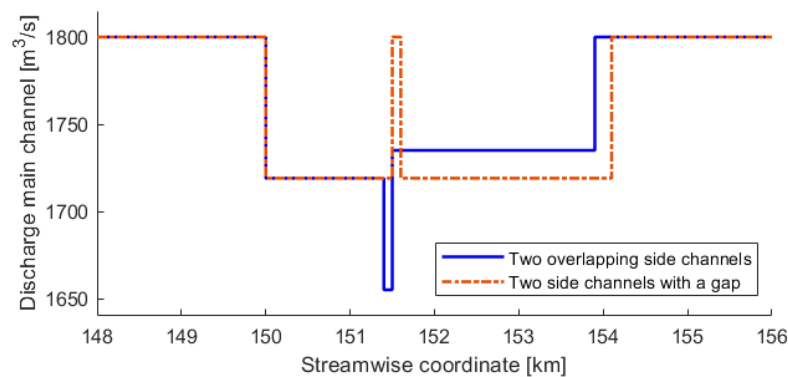


Figure 8.5: Changes in discharge in the main channel caused by two side channels

8.3 Conclusion

We investigated the effect of a combination of a side channel and filling up the groyne fields on the bed elevation. The separated effect at the upstream end of these two interventions is aggradation and degradation, respectively. Also, the temporal changes in bed elevation are inverse. Therefore, combining these two river interventions results in a decrease in bed level fluctuations. So, by combining river interventions which have an opposite effect on the time-averaged bed level change as well as temporal variations in bed elevation, it is possible to decrease the negative morphological effect of river interventions. Whether this combination of river interventions also contributes to the mitigation of the ongoing bed degradation in the Dutch rivers is hard to say since the BWE Model is not able to include the correct initial bed level.

River interventions can also be placed in a row. We looked at two sequential side channel. Two overlapping side channels cause a large sediment hump. In contrast, two side channels with a gap in between cause a scour hole. Besides these sediment hump and scour hole, the temporal fluctuations in bed elevation are also different. Since two overlapping side channels result in less extracted discharge, the changes in sediment transport are less, resulting in smaller bed level fluctuation. So, when looking at the morphological effects of sequential interventions the alignment of these interventions is important.

9 Discussion

In this research, we investigated the effect of several river interventions on the bed elevation. We developed a numerical space-marching model in combination with a Backwater-Exner Model to make rapid calculations of long-term morphological behaviour. The short computation times make it possible to quantify the uncertainties in morphological modelling. In this chapter, we discuss the findings of this research. We reflect on the method that we used including the model choices that we made and look at the reliability of the results. Furthermore, we elaborate on the value of this research for the work field and for future studies.

9.1 Reflection on method & reliability of results

Model choice

In this research, we were looking for a rapid method that can be used in the inventory phase of river projects to make an estimation of the morphological effect of river interventions. We chose an abridged version of the traditional Backwater-Exner Model and assumed that this gives a correct estimation of the equilibrium state. Using the original BWE Model would not meet our criteria of a rapid tool, since the time to compute the dynamic equilibrium of a channel is more than one day. The abridged version of the BWE Model results in a computation time of a couple of minutes. The original BWE Model computes the bed level changes for a cycled hydrograph over a total period of 100 000 years. For the abridged BWE Model, we use only one hydrograph, corresponding to 100 years. So, the abridged version of the BWE Model can be seen as an initial estimation of the equilibrium state. Because the amount of repeated hydrographs is different for the abridged and original BWE model, the model outcomes are also slightly different (Fig. 9.1). The relatively large differences between the abridged BWE Model and the original model at the start of the computation, indicate that the initial condition of the BWE model has not yet reached its equilibrium state. The differences in computed bed elevation between the abridged and original BWE Model is largest at the start of the computation and varies between 5 centimetres at the upstream end of the intervention and -10 centimetres at the downstream end of the intervention. The size of the differences depends on the type of river intervention. It is remarkable that the difference at the downstream end of the river intervention is larger than at the upstream end. The difference between the original and the abridged version of the BWE Model could be a reason for the absence of the scour hole downstream of the river interventions. After 20 years, the error varies between a couple of millimetres (Fig. 9.1).

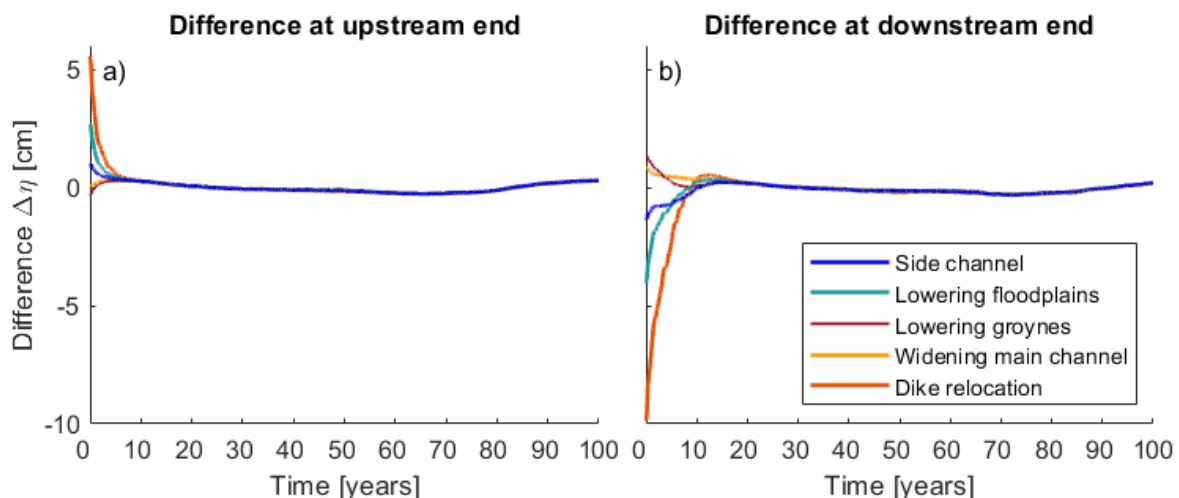


Figure 9.1: Difference between variations in bed elevations calculated with the original and abridged version of the BWE Model at the upstream end (a) and downstream end (b) of the river intervention

The error induced by the use of the abridged BWE Model instead of the original BWE Model is still less than the uncertainty in bed level variations induced by varying discharges. These uncertainties vary between 2 centimetres for the widening of the main channel, up to 10 centimeters for dike relocation. So, by looking at the results of the morphological effect of river interventions one has to keep in mind that for the first 20 years the variation in bed level changes is approximately 10% induced by the error in the model. After 20 years of computation time, it can be assumed that the rapid method reproduces accurate results. It is recommended to use the first 20 years as a kind of run-up time.

Implementation of river interventions

The abridged BWE Model is combined with an extraction tool to schematise the effect of a river intervention. We assume that sediment transport only takes place in the main channel. The lateral discharge to the groyne fields and floodplains is schematised as concentrated water extraction and supply. The amount of extracted and supplied discharge is based on the change in geometry of the cross-section of the river. In reality, this lateral discharge is not concentrated at two points but distributed over the length of the river intervention. Besides, we calculated the fraction curve corresponding to a certain river intervention at the start of the computation. However, bed level fluctuations caused by the river intervention change the water depth of the river. This results in a new fraction curve. So, the discharge extraction is a function of the morphological change in the main channel (Van Vuren, 2005b). An increase in bed elevation in the main channel results in a larger amount of extracted discharge during peak discharges. This leads to even more aggradation. The opposite occurs downstream of an intervention.

Numerical models that consider the effect of distributed discharge and the re-distribution of discharge over the main channel and floodplains as a results of morphological changes show an equilibrium state that differs substantially from the equilibrium state calculated with the equilibrium models that assume concentrated lateral discharge (Fig. 9.2) (Van Vuren, 2005b). Van Vuren (2005b) and Van der Klis (2003) performed computations with a simple analytical tool and a more complex numerical model for lowering of floodplains and narrowing of the main channel. Especially at high discharges a clear difference between both models is seen. This is caused by the re-distribution of the discharge in the main channel. Besides, the numerical model shows a scour hole downstream of the river intervention. The results of the analytical model do not show this scour hole. The difference in shape between both equilibrium states is similar to the difference between the BWE Model and the Delft3D Model of the side channel at Passewaaij.

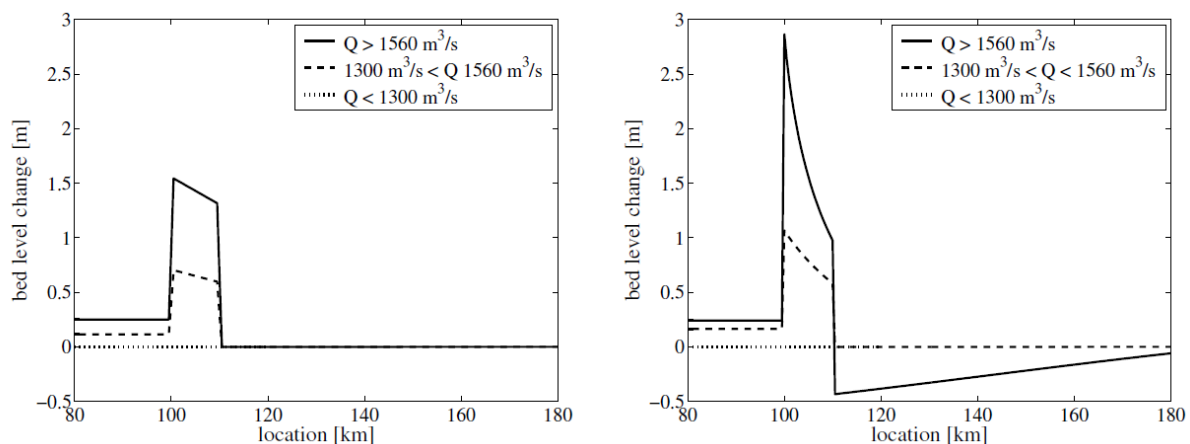


Figure 9.2: (a) Equilibrium state according to an analytical equilibrium model with concentrated extraction and supply. (b) Equilibrium state according to a numerical model with distributed extraction and supply and re-distribution of discharge due to morphological changes (Van Vuren, 2005b)

The effect of the simplification of river intervention as concentrated water extraction and supply from and to the main channel is less visible at the dynamic component of the equilibrium state. The dynamics in bed elevation are strongly related to variations in discharge. With each new discharge, new bottom waves are initiated, which start migrating downstream. High discharges result in accretion peaks upstream of the intervention and erosion peaks downstream. These disturbances propagate downstream and tend to spread out and smooth at low discharges (Van Vuren, 2005b). Lower discharge levels result in less aggradation and degradation. Very low discharges even result in aggradation upstream. This is similar to the findings of previous researches (Van der Klis, 2003; Van Vuren, 2005b). Not a single peak discharge, but the order of flow events affects the location and magnitude of fluctuations. As the time between peak flow events increases, we can expect a larger increase in the magnitude of dynamic bed elevation change. In addition, this research only focuses on the intermediate scale of bed level change. The small scale bed level fluctuations of river dunes might cause additional bed level fluctuations.

Comparing river interventions

We looked at five different types of river interventions: the construction of a side channel, lowering the floodplains, lowering the groyne height, widening the main channel, and dike relocation. To compare these interventions, the size of each intervention is chosen such that all types of river intervention cause an average bed level change of 20 centimetres. For a side channel, groyne lowering and widening of the main channel, this results in realistic values of the size of the intervention. For dike relocation and, to a smaller extent, for the lowering of floodplains, the size of the river intervention is disproportional. Interventions in the floodplains are only activated during peak discharges. Most of the time, the river intervention causes no extra water that is extracted from the main channel. Therefore, the bed level fluctuations are small. Once the discharge reaches bankfull discharge, the floodplains start to inundate. The size of the interventions is relatively large, which results in large amounts of extracted discharge. The larger the changes in discharge the larger the fluctuations in bed elevation. These large fluctuations compensate for the small fluctuations during low discharge levels such that the time-averaged bed level change is 20 centimetres. Because the size of the intervention is disproportional, the results give a distorted view. Since the aim of river interventions in the floodplains is to reduce the water level during peak flows, it would be better to look at the decrease in water level caused by the river intervention instead of the change in bed level. Other options to compare the river interventions are comparing the river interventions by budget, looking at the ecological effects of the river interventions, investigating bottlenecks for shipping, or including the feasibility of the river projects.

Model uncertainties

In this research, we quantified the uncertainties in morphological modelling induced by discharge, sediment feed rate and hydraulic roughness. The variability and uncertainty in future discharge cause the largest uncertainties in bed level changes. We see that for peak discharges, the bed level change tends to reach a limit. However, the hydrographs used for the MCS include only a few peak discharges compared to the base flow and bankfull discharge. If also computations with more frequently peak flows show the exponential behaviour of bed level change, similar to Figure 7.2, predictions of maximum bed level changes at peak flows can be done more accurately. Especially for river interventions that show less sensitivity to varying discharge, the level of confidence increases. The variations in discharge can also be used for future predictions. The set of hydrographs that we used included higher peak flows. This corresponds to the climate change in which more heavy rainfall events are expected. However, climate change will also result in periods of drought. The hydrographs that we used did not include these dry periods. What we see is that the bed level changes are primarily determined by the bankfull discharge and peak discharge. We expect that the dry periods contribute only to a small extent to the bed level fluctuations. However, dry periods result in low water depths that might cause bottlenecks for shipping. For low discharge levels, it is important to not only look at the morphological effect of the river intervention but also at the corresponding water depth.

Another uncertainty in discharge that we did not take into account is the distribution of discharge at the Pannerdense Kop. We assumed a constant fraction of 2/3 of the discharge from the Upper-Rhine that flows into the river Waal. However, at low discharges, this fraction is a bit larger and for high discharges, this fraction is a bit smaller. As a result, the difference between the smallest and largest discharges used in this research gives an overestimation of the real difference. In reality, the computed bandwidth of bed level fluctuations might be smaller.

Besides the discharge, we looked into the variations in yearly sediment transport and hydraulic roughness. However, we did not look into the choice of transport formula and the corresponding parameters. Since the sediment transport formula is the most essential formula in morphological modelling, we must be aware of the choice of formula that we make. In this study, we used the formula of Meyer-Peter and Müller, but the use of another formula, like Engelund-Hansen, might lead to different results. It is very difficult to predict sediment transport in natural rivers. Therefore, it is recommended to look up different transport formulas and evaluate them on the basis of field data before applying the model to case studies in the field (Nakato, 1990). The choice of transport formula is mainly determined by the grain size and shields parameter. Both parameters might be different for different rivers, but also within a river reach. In general, in the upstream segment of a river reach the grain size is larger than in the downstream segment due to downstream fining. In this research, we used the Middle-Waal as a case study with a D_{50} of 1.3 mm. Further downstream the D_{50} becomes smaller and it is recommended to use Engelund-Hansen. The formula of Engelund-Hansen does not include a threshold of motion. Therefore, there is always sediment transport. For larger grain sizes the formula of Meyer-Peter and Müller is recommended.

9.2 Value of this research

Knowledge on river interventions

As rivers fulfil several functions, river management should be focused on improving the river system in such a way that improving one of its functions does not result in a significant loss of another. In addition, we want to make accurate predictions on bed level changes so that we are not faced with unexpected large bed level fluctuations in the future. Therefore, an integrated approach to river management is demanded, with measures that are ecologically responsible and economically maintainable (Van der Brugge et al., 2005; Havinga, 2020). We showed that river interventions in the floodplains result in a large distribution of temporal bed level changes in the main channel. Predicting the effect of these types of river interventions entails large uncertainty. River interventions in the main channel result in smaller bed level fluctuations and show less uncertainty. The river interventions can be used to optimize the river system and mitigate the negative effect of previous interventions, like ongoing bed degradation. To reduce the negative effects of future river interventions, combinations of river interventions can be used. This results in a benefit for one of the functions of the river without harming another (eg. the Room for Living River project).

Application to the field

With simple general rules, like WAQmorf, it is possible to calculate the long-term effect of river interventions on the bed level. However, these simple rules include only the static component of the equilibrium state. As long as the discharge keeps varying, a static equilibrium state will never be reached (Van Vuren, 2005b). We have shown that with an abridged BWE Model with a space-marching model to define the initial condition, it is possible to compute the long-term bed level changes, including the dynamic component of the equilibrium state within a couple of minutes. This BWE Model has some limitations compared to more complex numerical models like WAQUA and Delft3D. For the inventory phase, these limitations are outweighed by the significant reduction of the computation time. The method makes it possible to make quick estimations of the range of bed level variations caused by river interventions. In a more detailed phase, e.g. the design phase, it is recommended to use more complex numerical meth-

ods like WAQUA or Delft3D. With these methods, it is possible to include the existing dynamics in bed elevation and create a more realistic view of bed level fluctuations. In an ideal situation, a river intervention can reduce the existing bottleneck. In the worst-case scenario, the largest bed level fluctuations that are caused by the river intervention are located at the same location as the existing bottleneck. The abridged version of the BWE Model can not be used to investigate bed level changes at a specific time and location since the geometry of the river is strongly simplified. It seems like the model is not able to predict the morphological effect downstream of a river intervention very well. We would expect a scour hole, but the temporal aggradation compensates for the erosion such that the changes in bed elevation are approximately zero at the downstream end of the river intervention. Nevertheless, at the upstream end of the river intervention, the model gives a good estimation of the bed level changes.

In this study, we applied the model to the river Waal. By changing the input variables, like channel width, bed roughness and particle size, the model can be applied to other rivers as well. However, the obtained results in this research are not directly applicable to other rivers. For example, the response time of the river Waal and the river IJssel are different (Van Vuren, 2005b). This affects the size of the boundary layer and the characteristic timescale at which channel equilibrium regarding bed level is defined. In addition, the autocorrelation of discharges is river dependent (Duits, 1997). It is assumed that the uncertainties in bed level changes induced by varying discharges are approximately the same for different river systems, but there might be small differences. These differences will be largest for river interventions in the floodplains, which are most sensitive to variations in discharge.

10 Conclusion & Recommendations

The objective of this research is to gain insight into the long-term effects of river interventions on the bed elevation. A combination of a numerical space-marching model for the static component of the equilibrium state and an abridged version of the Backwater-Exner Model for the dynamic component of the equilibrium state makes it possible to make rapid calculations for the morphological changes due to river intervention. With the insight that we gain by using this rapid method, we can answer the research question:

What is the morphological effect of various types of river interventions, using a rapid method?

In this chapter, we first give the conclusion of this research, answering the main research question. Second, we give recommendations on the use of the rapid method and for further studies to improve the method.

10.1 Conclusion

A space-marching model in combination with the Backwater-Exner Model makes it possible to make rapid computations of bed level changes due to the construction of river interventions. We can use this method to gain insight into the magnitude of aggradation and degradation, in a quick way. In addition, we can quantify the range of uncertainty in bed level fluctuations caused by seasonal variations in discharge, varying yearly sediment supply rates and hydraulic roughness. This enables us to identify possible bottlenecks for shipping at an early stage and make well-considered decisions for future river projects. The size of the bed level fluctuations depends on the location of the river intervention. River interventions in the floodplains cause the largest bed level fluctuations. The floodplains are only inundated a small part of the year. Once the floodplains are inundated, a large fraction of the total discharge is extracted by the floodplains. The large local differences in discharge result in aggradation and degradation of the bed level. This can result in bed level fluctuations of one to several meters. In addition, the fluctuations caused by river interventions in the floodplains entail a large range of uncertainty caused by variations in discharge. The probability of occurrence of peak discharges is small, but the corresponding morphological effect is large. A Monte Carlo Simulation helps us to get insight into the distribution of bed level fluctuations under varying input variables. River interventions in the main channel rarely show fluctuations in bed elevation. The bed level fluctuations vary between a few centimetres up to a maximum of twenty centimetres. The river interventions in the main channel are already active during base flow. Over time, the percentage of discharge extracted from the main channel stays almost the same. There are no large local differences in discharge and therefore the bed level fluctuations are relatively small. The probability of occurrence of base flow is high. A deterministic model approach gives already enough information to make an estimation on bed level fluctuations caused by river interventions in the main channel.

Our knowledge of the morphological effect of separate river interventions can be used to mitigate the negative effects on shipping. Interventions with an opposite morphological effect, like narrowing the main channel and the construction of a side channel, can be combined to reduce the size of bed level fluctuations. The combined river interventions result also in a decrease in time-averaged bed level change. We can use the rapid tool to study the combined effect of a set of river interventions as well as the effect of river interventions on the bed elevation separately. This contributes to a better understanding of the combined effect in complex river projects. The types of river intervention, together with the location of the single interventions determine the size of the morphological effect.

10.2 Recommendations

Based on the findings in this research, we give recommendations on the use of the developed rapid method and look into possibilities for further studies on the topic of morphological modelling of river interventions.

Recommendations on improvements of the rapid method

The method that we used to investigate the morphological effect of river interventions is based on a traditional Backwater-Exner Model. The abridged version of this model showed some small errors. We have seen that the output of Model B+ is similar to the output of the BWE Model but the computation time is almost twice as large. We implemented an extra time-loop to Model B but did not optimise the script. With the optimisation of Model B+, this model could be even quicker than the BWE Model. Thus, we recommend having a look at Model B+ and see whether optimisation can lead to shorter computation times.

Before the method can be applied to river projects it is recommended to extend the model verification. The verification that we have done in this research is very limited. The model is only verified for the construction of a side channel. It is recommended to look at the other types of river interventions to verify whether the implementation of the river intervention, represented by the extraction curve, is accurate. Besides, we suggest to verify the model for combined river interventions to make sure that the combined extraction curves represent the situation well. This verification can be done by the results of Delft3D and WAQUA.

Finally, the schematised geometry of the river can be improved to a certain extent. We use a one-dimensional model with uniform channel width. So, within the assumptions used in this model, it is not possible to include gradients of channel width. However, the natural narrowing of the river can be implemented by a change in the width of the main channel. If needed, the geometry of the floodplains and the width of the groynes can also be changed. It is possible to assign to each grid cell its characteristic width, depth, and roughness height. For the implementation of the river interventions, we used concentrated extraction curves. In further research, the effect of distributed extraction can be investigated. Instead of assigning the extraction curve to one grid cell, the extraction can be distributed over a set of grid cells.

Recommendations on further studies on river interventions

In this research, we studied the effect of river interventions on bed level change. We compared the river interventions by a similar time-averaged increase in bed elevation. For a better understanding of the morphological effect of river interventions, it is recommended to vary the size of the interventions. For a side channel, we used a fixed width-depth ratio of 1/25. This ratio determines the depth of the side channel compared to the bed level of the main channel. Variations in width-depth ratio can result in different outcomes. We have seen that the earlier the river intervention is activated, the smaller are the bed level fluctuations. So, a deeper and smaller side channel can result in smaller bed level variations. Besides, the comparison between river interventions by their time-averaged bed level change resulted in a disproportional size for dike relocation. Therefore, it is recommended to compare the river interventions also by their effect on the water level, especially at peak discharges.

We investigated the effect of five different river interventions that are implemented in the main channel, groynes and floodplains. We have seen that for river interventions in the main channel and groyne field a deterministic model approach gives sufficient information on the morphological behaviour. Using a stochastic model approach has not a significant added value. For river interventions in the floodplains, it is recommended to use a stochastic model approach since the probability of peak discharges that inundate the floodplains is relatively small. However, further studies can look into the possibilities of representative discharges to make it easier to study the effect of river interventions in the floodplains. More than half of the time, the floodplains are not inundated and the effect of the river intervention is not noticeable on the bed level of the main channel. We are not interested in these calculations. For base flows, the time steps could be larger since the morphological effect is very small. This could reduce the computation time and makes it possible to run more hydrographs including more peak discharges without increasing the computation time.

References

- Ahnert, F. (1994). Equilibrium, scale and inheritance in geomorphology. *Geomorphology*, 11(2), 125–140.
- An, C., Fu, X., Wang, G., & Parker, G. (2017). Effect of grain sorting on gravel bed river evolution subject to cycled hydrographs: Bed load sheets and breakdown of the hydrograph boundary layer. *Journal of Geophysical Research: Earth Surface*, 122(8), 1513–1533.
- Arkesteijn, L., Blom, A., Czapiga, M. J., Chavarrías, V., & Labeur, R. J. (2019). The quasi-equilibrium longitudinal profile in backwater reaches of the engineered alluvial river: A space-marching method. *Journal of Geophysical Research: Earth Surface*, 124(11), 2542–2560.
- Barneveld, H., Van Hoven, A., Paarlberg, A., Dagevoorde, R., Spruyt, A., Fujisaki, A., Sloff, K., Ottevanger, W., Van den Bergh, M., & Schielen, R. (2019). *Ruimte voor levende rivieren: Effect grootschalige rivierverruiming op bodemerosie Waal* (tech. rep.). HKV Lijn in water, Deltares; WWF.
- Berends, K. D. (2020). *Human intervention in rivers: Quantifying the uncertainty of hydraulic model predictions*. University of Twente.
- Blom, A., Arkesteijn, L., Chavarrías, V., & Viparelli, E. (2017). The equilibrium alluvial river under variable flow and its channel-forming discharge. *Journal of Geophysical Research: Earth Surface*, 122(10), 1924–1948.
- Bolla Pittaluga, M., Luchi, R., & Seminara, G. (2014). On the equilibrium profile of river beds. *Journal of Geophysical Research: Earth Surface*, 119(2), 317–332.
- Chavarrías, V., Stecca, G., & Blom, A. (2018). Ill-posedness in modeling mixed sediment river morphodynamics. *Advances in Water Resources*, 114, 219–235.
- Colebrook, C. F., Blench, T., Chatley, H., Essex, E., Finnicome, J. R., Lacey, G., Williamson, J., & Macdonald, G. G. (1939). Correspondence. turbulent flow in pipes, with particular reference to the transition region between the smooth and rough pipe laws. (includes plates). *Journal of the Institution of Civil engineers*, 12(8), 393–422.
- De Vriend, H. J. (2002). Model-based morphological prediction: From art to science. *River flow 2002. Proceedings of the international conference on fluvial hydraulics. Louvain-La-Neuve, Belgium*, 4–6.
- De Vries, M. (1975). A morphological time-scale for rivers. *WL publication nr. 147, paper presented at the XVIIth IAHR congress, São Paulo*.
- De Vries, M. (1993). Use of models for river problems. *Studies and reports on Hydrology*, 51.
- Drenthen, M. (2009). Developing nature along dutch rivers: Place or non-place. *New visions of nature* (pp. 205–228). Springer.
- Driessen, T., & De Jong, W. (2011). *Hurwenen - maakbaarheid en vergunbaarheid, hydraulica en morfologie projectontwerp* (tech. rep.). Royal Haskoning.
- Duits, M. T. (1997). *Baggeroptimalisatie in rivierbochten, voorbeeldlocatie waalbocht hulhuizen* (tech. rep.). HKV Lijn in water, TU Delft.
- El kadi Abderrezzak, K., & Paquier, A. (2009). One-dimensional numerical modeling of sediment transport and bed deformation in open channels. *Water Resources Research*, 45(5).
- Exner, F. M. (1920). *Zur physik der dünen*. Hölder.
- Frings, R., Banhold, K., & Evers, I. (2015). *Sedimentbilanz des oberen rheindeltas für den zeitraum 1991–2010* (tech. rep.). Tech. Rep.
- Frings, R., Berbee, B. M., Erkens, G., Kleinhans, M. G., & Gouw, M. J. P. (2009). Human-induced changes in bed shear stress and bed grain size in the river waal (the netherlands) during the past 900 years. *Earth Surface Processes and Landforms*, 34(4), 503–514.
- Havinga, H., Schielen, R. M. J., & Van Vuren, S. (2010). Tension between navigation, maintenance and safety calls for an integrated planning of flood protection measures.
- Havinga, H. (2020). Towards sustainable river management of the dutch rhine river. *Water*, 12(6), 1827.
- Havinga, H., van Adrichem, R., & Paarlberg, A. (2013). The aftermath of room for the river and restoration works: Excessive maintenance dredging. *Proceedings of the 35th IAHR World Congress*.
- Huthoff, F., Van Vuren, S., Barneveld, H., & Scheel, F. (2010). On the importance of discharge variability in the morphodynamic modeling of rivers. *River Flow 2010*, 985–992.
- Jansen, P. P., Van Bendegom, L., Van Den Berg, J. H., De Vries, M. B., & Zanen, A. (1979). *Principles of river engineering: The non-tidal alluvial river*.

- Johnson, P. A. (1996). Uncertainty of hydraulic parameters. *Journal of hydraulic engineering*, 122(2), 112–114.
- Klijn, F., Asselman, N., & Wagenaar, D. (2018). Room for rivers: Risk reduction by enhancing the flood conveyance capacity of the netherlands' large rivers. *Geosciences*, 8(6), 224.
- Lambeek, J. J. P., Jagers, H. R. A., & Van der Klis, H. (2004). Monte carlo method applied to a two-dimensional morphodynamic model. *Proceedings of River Flow*, 1, 191–196.
- Le, T. B., Crosato, A., & Montes Arboleda, A. (2020). Revisiting waal river training by historical reconstruction. *Journal of Hydraulic Engineering*, 146(5), 05020002.
- Manning, R., Griffith, J. P., Pigot, T. F., & Vernon-Harcourt, L. F. (1890). *On the flow of water in open channels and pipes*.
- Meyer-Peter, E., & Müller, R. (1948). Formulas for bed-load transport. *IAHSR 2nd meeting, Stockholm, appendix 2*.
- Morgan, M. G., Henrion, M., & Small, M. (1990). *Uncertainty: A guide to dealing with uncertainty in quantitative risk and policy analysis*. Cambridge university press.
- Nakato, T. (1990). Tests of selected sediment-transport formulas. *Journal of Hydraulic Engineering*, 116(3), 362–379.
- Nikuradse, J. (1933). Stromungsgesetze in rauhen rohren. *VDI-Forschungsheft*, 361, 1.
- Paarlberg, A. (2009). *Verificatie WAQmorf, Vergelijking resultaten WAQmorf en Delft2D en advies gebruik vuistregel* (tech. rep.). HKV Lijn in water.
- Paarlberg, A. (2013). *Aantakking nevengeul Passewaaij: Effecten van de aanleg van een duiker en kade* (tech. rep.). HKV Lijn in water.
- Paarlberg, A., & Schippers, M. (2020). *Inverse modellering evenwichtseffect maatregelen op zomerbedbodem: afleiden dimensies van maatregelen* (tech. rep.). HKV Lijn in water; Witteveen+Bos.
- Paarlberg, A., & Van Lente, J.-W. (2021). *Testen 1d morfologisch model rijntakken: Testcasus plan ruimte voor levende rivieren* (tech. rep.). HKV Lijn in water.
- Papanicolaou, A. T. N., Elhakeem, M., Krallis, G., Prakash, S., & Edinger, J. (2008). Sediment transport modeling review—current and future developments. *Journal of hydraulic engineering*, 134(1), 1–14.
- Pappenberger, F., Matgen, P., Beven, K. J., Henry, J.-B., Pfister, L., et al. (2006). Influence of uncertain boundary conditions and model structure on flood inundation predictions. *Advances in water resources*, 29(10), 1430–1449.
- Parker, G. (2004). Review of 1d open channel hydraulics, chap. 5. *1D sediment transport morphodynamics with applications to rivers and turbidity currents: E-book*.
- Parker, G., Hassan, M., & Wilcock, P. (2007). 10 adjustment of the bed surface size distribution of gravel-bed rivers in response to cycled hydrographs. In H. Habersack, H. Piégay, & M. Rinaldi (Eds.), *Gravel-bed rivers vi: From process understanding to river restoration* (pp. 241–285). Elsevier.
- Ribberink, R. (2011). *River dynamics ii: Transport processes and morphology* (tech. rep.). University of Twente, Enschede.
- Rudolph, M. (2018). *Measures for mitigating the ongoing bed degradation in the rhine river-a first assessment using idealized models of the waal branch*. MSc Thesis, Technical University Delft, Delft, the Netherlands.
- Schielen, R., & Havinga, H. (2010). Long term claims on the dutch river area: Handling climate change, safety, navigation and nature. *River Flow 2010*, 1429–1436.
- Sieben, J. (2011). *Memo methodiek inschatting morfologische effecten in zomerbed door lokale rivieringrepen UPDATE December2011* (tech. rep.). Rijkswaterstaat.
- Sieben, J. (2009). Sediment management in the dutch rhine branches. *International Journal of River Basin Management*, 7(1), 43–53.
- Silva, W., Klijn, F., & Dijkman, J. P. M. (2001). Room for the rhine branches in the netherlands: What the research has taught us. R3294.
- Smit, H. (1985). Het ecosysteem van de nederlandse grote rivieren. *De Levende Natuur*, 86(5), 162–167.
- Straatsma, M., & Huthoff, F. (2011). Uncertainty in 2d hydrodynamic models from errors in roughness parameterization based on aerial images. *Physics and Chemistry of the Earth, Parts A/B/C*, 36(7-8), 324–334.

- Van Alphen, S. (2020). Room for the river: Innovation, or tradition? the case of the noordwaard. *Adaptive strategies for water heritage*, 309.
- Van Asselt, M. B. A., & Rotmans, J. (2002). Uncertainty in integrated assessment modelling. *Climatic change*, 54(1), 75–105.
- Van Denderen, R. P., Kater, E., Jans, L. H., & Schielen, R. M. J. (2020). Changes in the equilibrium river profile due to interventions. *River Flow 2020: Proceedings of the 10th Conference on Fluvial Hydraulics (Delft, Netherlands, 7-10 July 2020)*, 435.
- Van Denderen, R. P., Kater, E., Jans, L. H., & Schielen, R. M. J. (2021). *A wavelet transformation disentangles changes in the river bed profile: The morphological impact of river interventions*.
- Van der Brugge, R., Rotmans, J., & Looibach, D. (2005). The transition in dutch water management. *Regional environmental change*, 5(4), 164–176.
- Van der Klis, H. (2003). *Uncertainty analysis applied to numerical models of river bed morphology*. DUP Science.
- Van Vuren, S. (2006). Development of a 2-d model for sustainable navigation channel improvement in the river rhine. *Proceeding of NCR-days*.
- Van Vuren, S. (2005b). Stochastic modelling of river morphodynamics.
- Van Vuren, S., De Vriend, H. J., Ouwkerk, S., & Kok, M. (2005a). Stochastic modelling of the impact of flood protection measures along the river waal in the netherlands. *Natural Hazards*, 36(1), 81–102.
- Van Vuren, S., Paarlberg, A., & Havinga, H. (2015). The aftermath of “room for the river” and restoration works: Coping with excessive maintenance dredging. *Journal of hydro-environment research*, 9(2), 172–186.
- Van Vuren, S., Van der Klis, H., & De Vriend, H. (2002). Large-scale floodplain lowering along the river waal: A stochastic prediction of morphological impacts. *Proceedings of River Flow*, 2, 903–912.
- Viparelli, E., Gaeuman, D., Wilcock, P., & Parker, G. (2011). A model to predict the evolution of a gravel bed river under an imposed cyclic hydrograph and its application to the trinity river. *Water Resources Research*, 47(2).
- Warmink, J. J., & Booij, M. J. (2015). Uncertainty analysis in river modelling. *Rivers—physical, fluvial and environmental processes* (pp. 255–277). Springer.
- Warmink, J. J., Booij, M. J., Van der Klis, H., & Hulscher, S. J. (2013). Quantification of uncertainty in design water levels due to uncertain bed form roughness in the dutch river waal. *Hydrological processes*, 27(11), 1646–1663.
- Wong, M., & Parker, G. (2006). One-dimensional modeling of bed evolution in a gravel bed river subject to a cycled flood hydrograph. *Journal of Geophysical Research: Earth Surface*, 111(F3).
- Zevenbergen, C., Rijke, J., Van Herk, S., & Bloemen, P. J. T. M. (2015). Room for the river: A stepping stone in adaptive delta management. *International Journal of Water Governance*, 3(1), 121–140.

Appendices

A List of Symbols

| Symbol | Description |
|---------------|---|
| A | Flow area |
| a | Parameter indicating shift in parameter-value |
| B | Width of the channel |
| c_α | Deviation enclosing probability |
| c_f | Bed friction coefficient |
| c_v | Coefficient of variation |
| D | Grain size diameters |
| Fr | Froude Number |
| fc | Floodplain capacity |
| g | Acceleration due to gravity |
| h | Water depth |
| H | Water level |
| k | Nikuradse roughness height |
| L | Total length modelled river reach |
| N | Sample size |
| O | Wetted perimeter |
| p | Percentile of data set |
| Q | Discharge |
| q | Unit discharge |
| q_{bf} | Constant feed rate of sediment transport |
| q_s | Sediment transport per unit width |
| R | Hydraulic radius |
| S | Bed slope |
| S_0 | Initial bed slope |
| \bar{S} | Static component of bed slope |
| S_f | Friction slope |
| S_{yr} | Yearly sediment transport |
| t | Time |
| T_h | Hydrograph duration |
| T_m | Morphological response time |
| u | Flow velocity |
| x | Streamwise coordinate |
| z | Reference bed level |
| α | Degree of accuracy |
| ϵ | Bed porosity |
| \mathcal{E} | Dimensionless time ration |
| δ | Length boundary layer |
| $\Delta\eta$ | Dynamic component of bed level |
| ΔS | Dynamic component of bed slope |
| η | Bed level |
| $\bar{\eta}$ | Static component of bed level |
| λ | Characteristic bed celerity |
| ρ | Auto-correlation |
| ρ_s | Sediment density |
| ρ_w | Water density |

B Study area river Waal

We used the characteristics of the river Waal for our calculations. In addition, we used three case studies of the Waal to verify our model and test the model on a more realistic case study. These three studies are the side channel at Huwenen and Passewaaij and the Room for Living Rivers project from Oosterhout to IJzerdoorn. We looked only at the two side channels at Oosterhout en Beuningen

C Model Testing and Verification

We tested three different models, Model B, Model B+ and the BWE Model. We can compare these models for a normal river reach and one with an intervention. We see that due to the static-slope approximation used in Model B and Model B+, the model is not able to reproduce bed level perturbations that migrate downstream. The BWE Model uses not the static-slope approximations. The results show that this model is able to compute the migrating bed perturbations caused by the upstream boundary.

C.1 Model testing

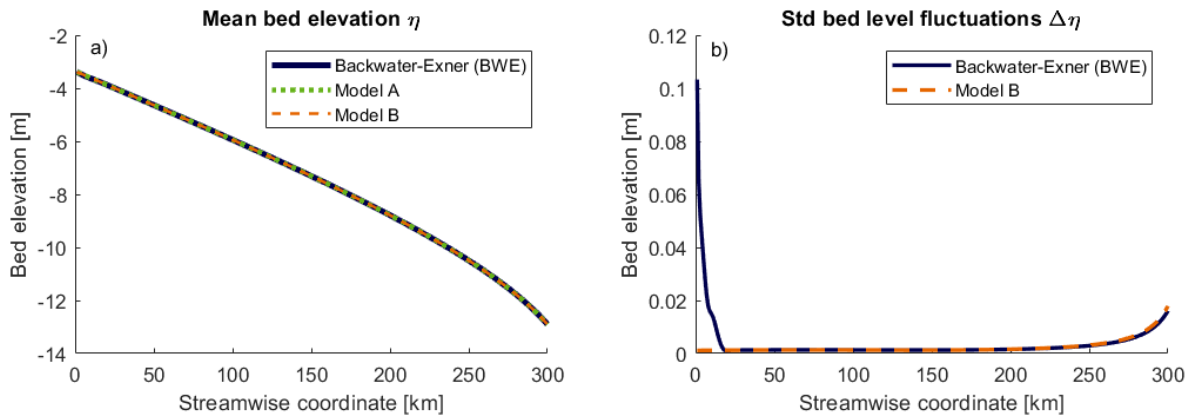


Figure C.1: Comparison BWE Model and Model B for (a) mean bed elevation/static component and (b) standard deviation of bed level fluctuations

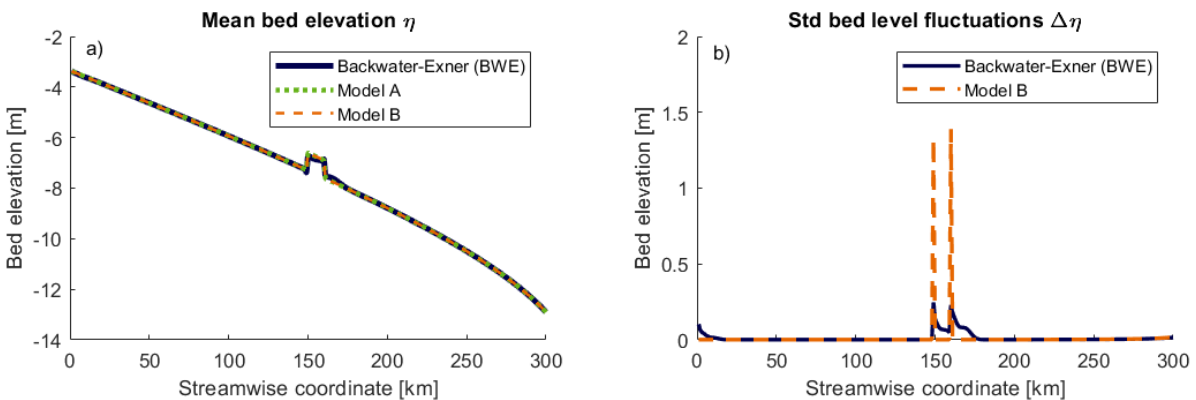


Figure C.2: Comparison BWE Model and Model B with the implementation of a river intervention for (a) mean bed elevation/static component and (b) standard deviation of bed level fluctuations

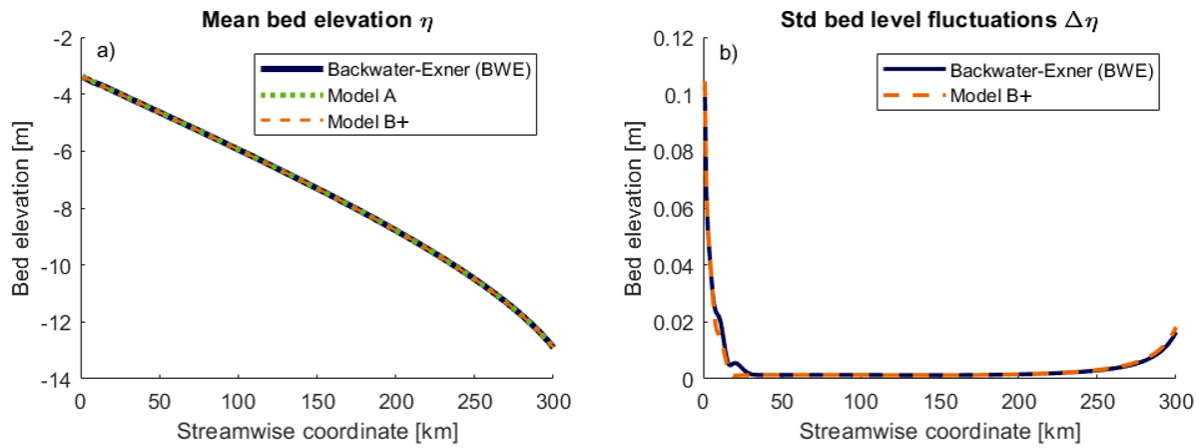


Figure C.3: Comparison BWE Model and Model B+ for (a) mean bed elevation/static component and (b) standard deviation of bed level fluctuations

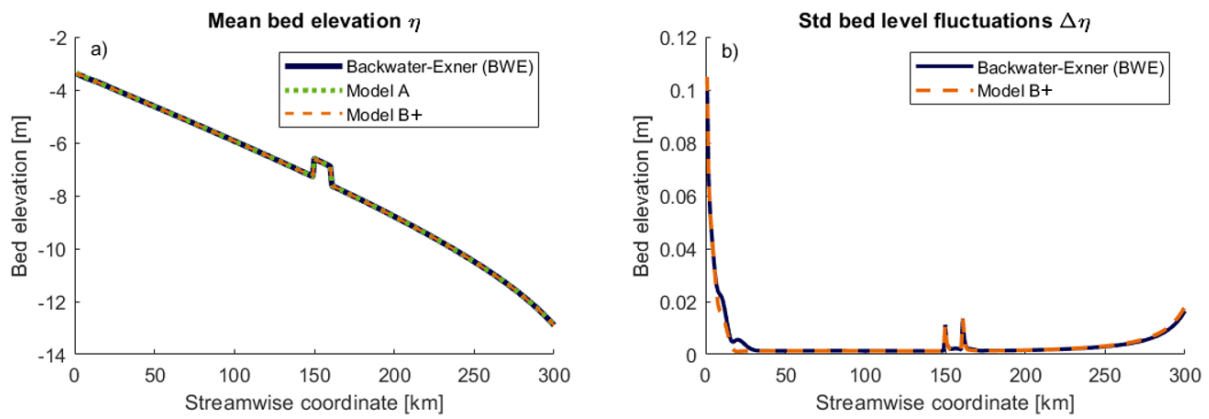


Figure C.4: Comparison BWE Model and Model B+ with the implementation of a river intervention for (a) mean bed elevation/static component and (b) standard deviation of bed level fluctuations

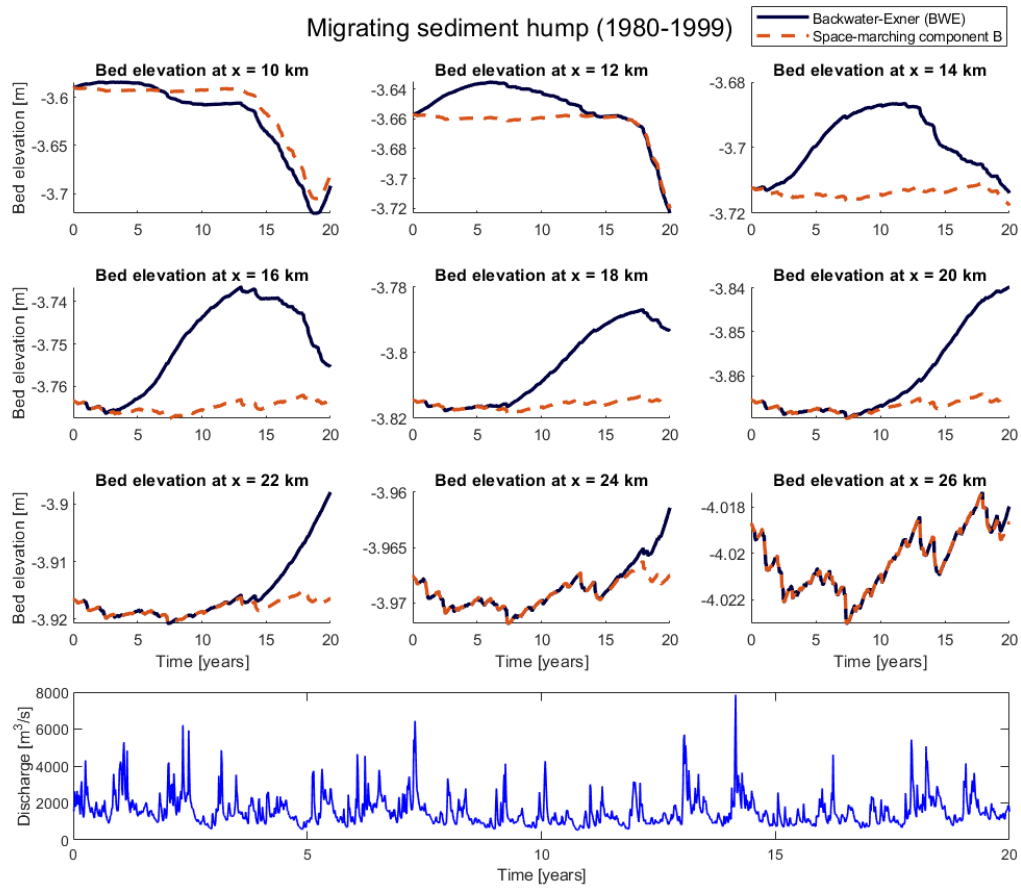


Figure C.5: Migrating sediment hump computed by the BWE Model but not visible with Model B+ due to the static-slope approximation

C.2 Background information Passewaaij

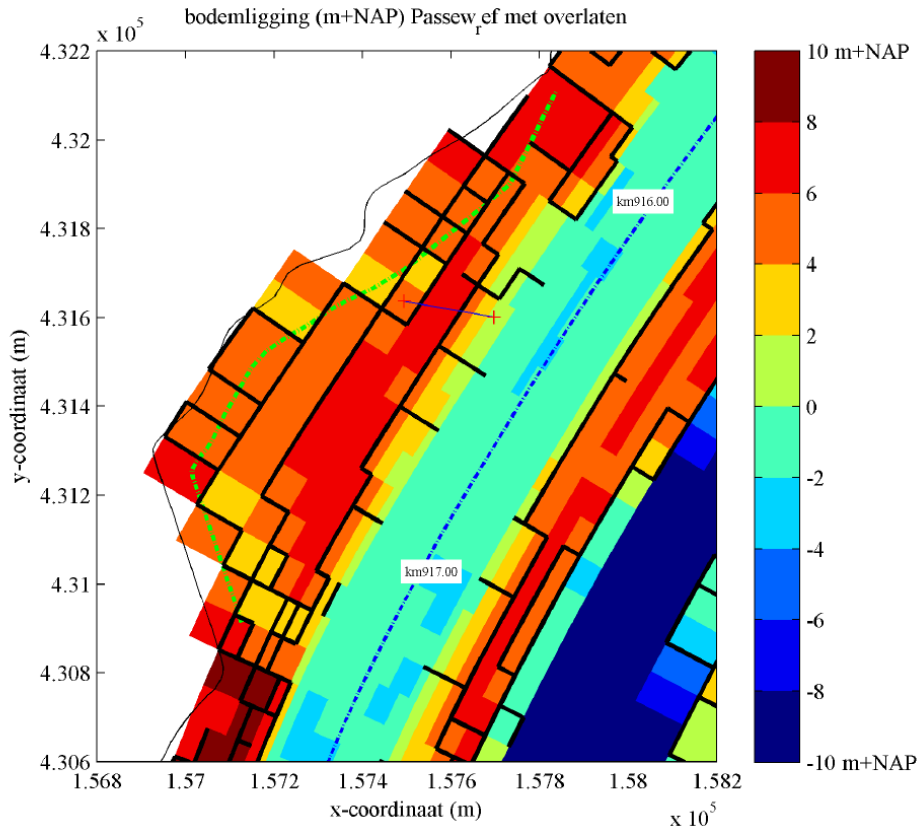


Figure C.6: Reference base line Passewaaij obtained from Baseline (Paarlberg, 2013)

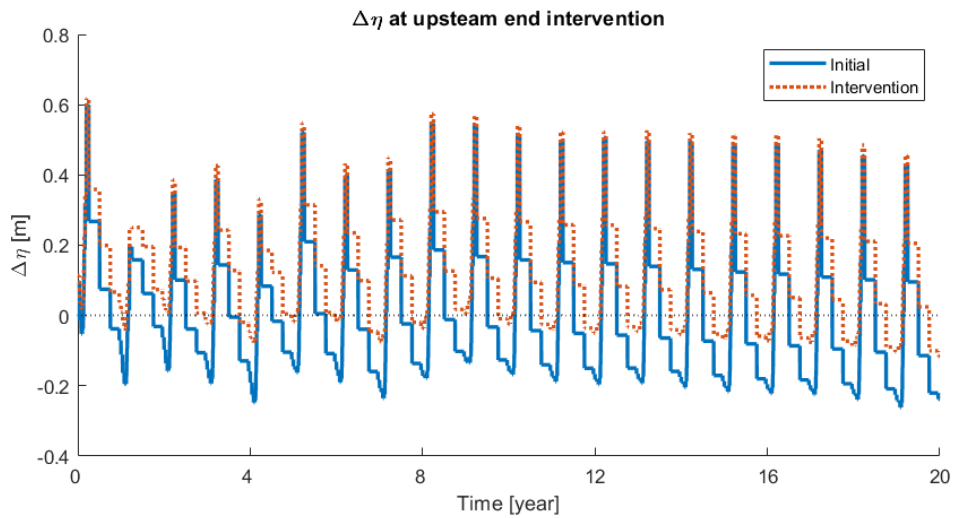


Figure C.7: Delft 3D results of the project at Passewaaij at the upstream end of the side channel on a time scale of 20 years given for the initial situation and the situation with the intervention (Paarlberg, 2013). It can be seen that the bed elevation has reached a quasi-equilibrium state with a small gradient in bed elevation

D Uncertainties in bed level fluctuations

For the Monte Carlo Simulation, we defined 36 decads and found the right values to represent the decad-discharges as log-normal function. This resulted in approximately the same distribution of frequency as the observed data set from 1900-1999. We verified the sample size of 400 sets, which is sufficient for the MCS.

D.1 Generating discharge series

The division of 36 decads:

Decade 1 : 1 of January t/m 10 of January
 Decade 2 : 11 January t/m 20 January
 Decade 3 : 21 January t/m 30 January
 Decade 4 : 31 January t/m 9 February
 Decade 5 : 10 February t/m 19 February
 Decade 6 : 20 February t/m 1 March (Depending whether there is a leap year)
 Decade 7 : 2 March t/m 11 March
 Decade 8 : 12 March t/m 21 March
 Decade 9 : 22 March t/m 31 March
 Decade 10 : 1 April t/m 10 April
 Decade 11 : 11 April t/m 20 April
 Decade 12 : 21 April t/m 30 April
 Decade 13 : 1 May t/m 10 May
 Decade 14 : 11 May t/m 20 May
 Decade 15 : 21 May t/m 31 May
 Decade 16 : 1 June t/m 10 June
 Decade 17 : 11 June t/m 20 June
 Decade 18 : 21 June t/m 30 June
 Decade 19 : 1 July t/m 10 July
 Decade 20 : 11 July t/m 20 July
 Decade 21 : 21 July t/m 31 July
 Decade 22 : 1 August t/m 10 August
 Decade 23 : 11 August t/m 20 August
 Decade 24 : 21 August t/m 31 August
 Decade 25 : 1 September t/m 10 September
 Decade 26 : 11 September t/m 20 September
 Decade 27 : 21 September t/m 30 September
 Decade 28 : 1 October t/m 10 October
 Decade 29 : 11 October t/m 20 October
 Decade 30 : 21 October t/m 31 October
 Decade 31 : 1 November t/m 10 November
 Decade 32 : 11 November t/m 20 November
 Decade 33 : 21 November t/m 30 November
 Decade 34 : 1 December t/m 10 December
 Decade 35 : 11 December t/m 20 December
 Decade 36 : 21 December t/m 31 December

All decads represent a period of ten days. Except for the decads 15, 21, 24, 30 and 36 that consists of 11 days. Decad 6 has 11 days in case of a leap year.

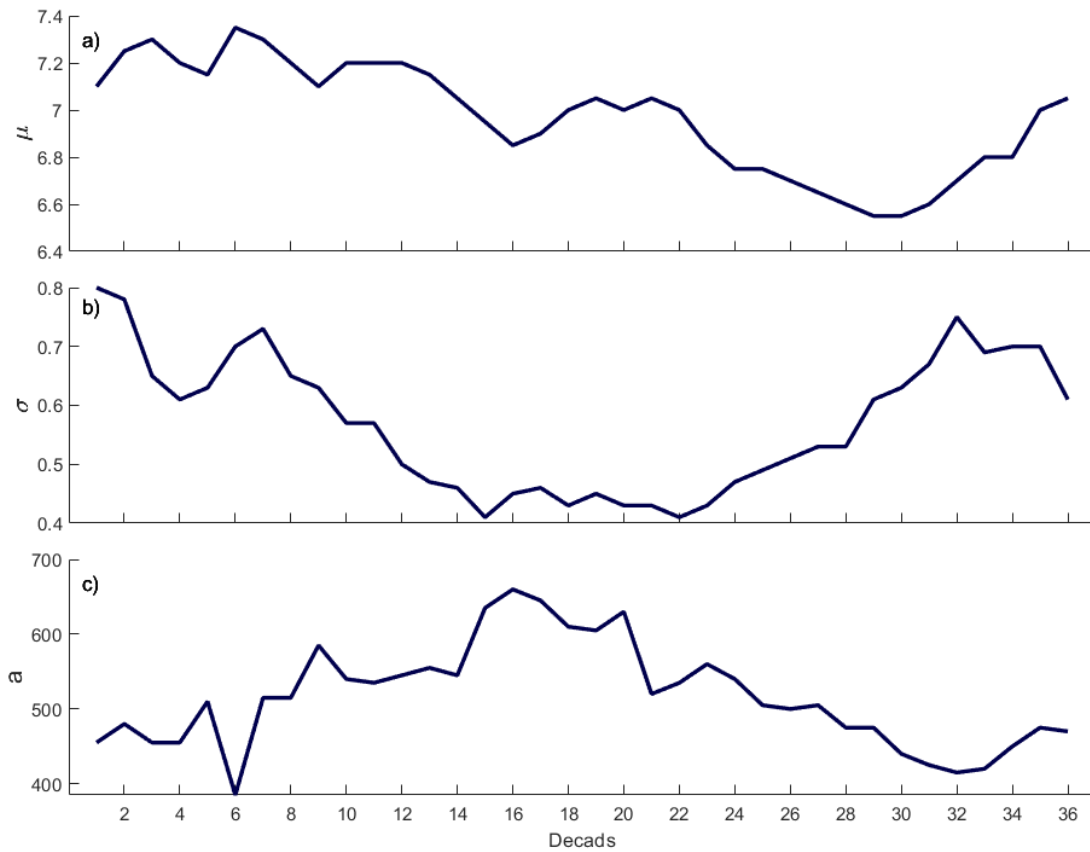


Figure D.8: Input variables for the shifted log-normal distribution of decadal discharges with (a) the mean of the log-normal function, (b) the standard deviation and (c) the parameter for the shift in log-normal function.

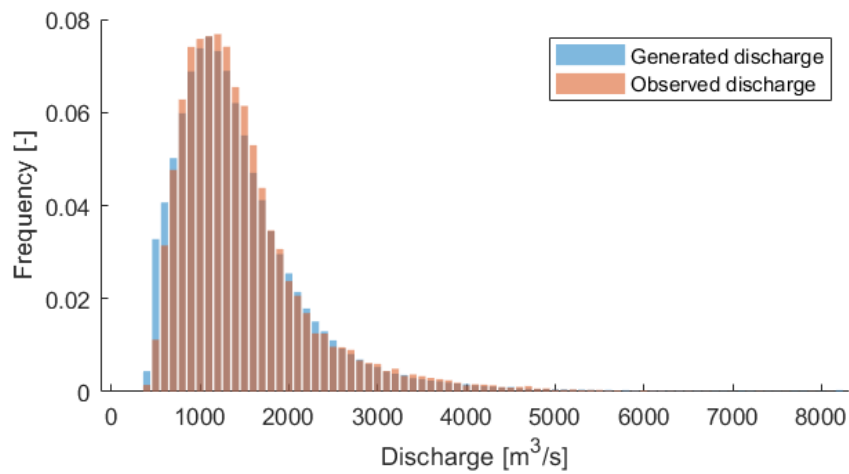


Figure D.9: Generated discharge series compared with observed discharges. Sorted per discharge level

D.2 Accuracy of sample size

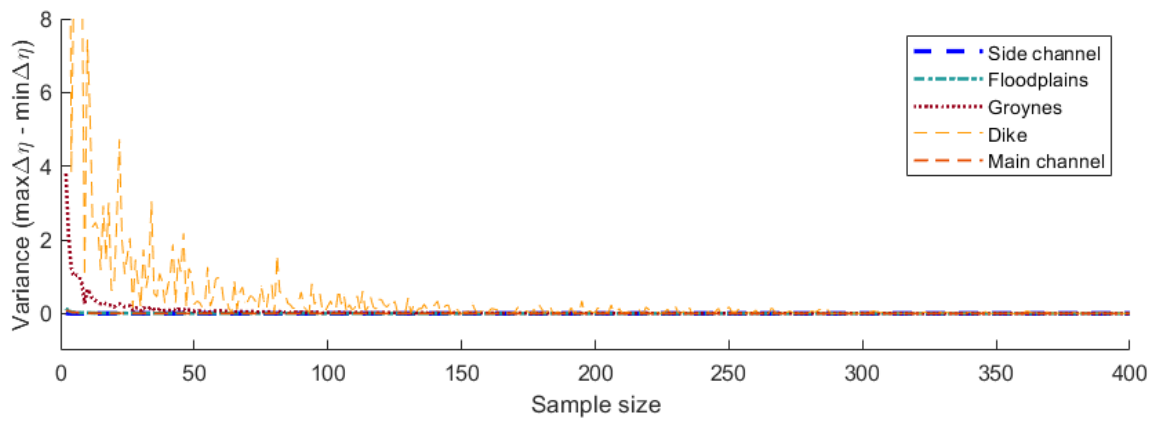


Figure D.10: Variance between maximum accretion at upstream end of the intervention and erosion at the downstream end for a set of sample sizes. For a sample size of 400 there are no changes in variance any more which indicates that a sample size of 400 is accurate

E Combination of river interventions

Results from WAQUA calculations that are used to determine the extraction curves of the side channels. We modified the extraction curves in order to apply them for calculations. The extraction curve of the second side channel is not used.

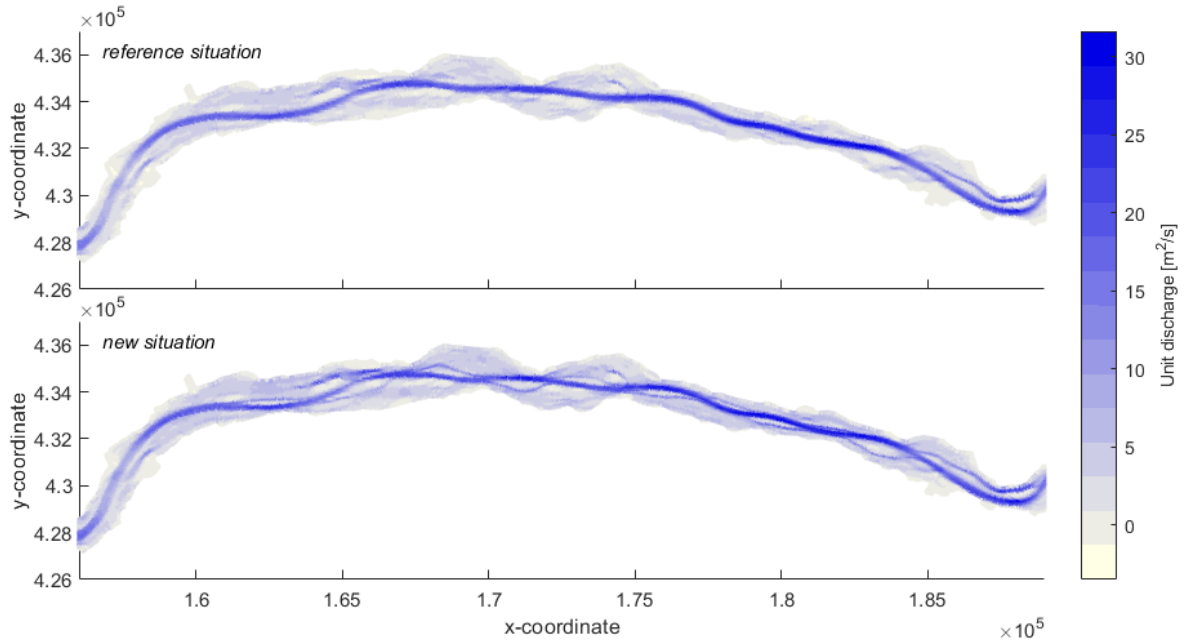


Figure E.11: Unit discharge along the river calculated by WAQUA at the reference situation (top) and the new situation (bottom) with 11 side channels

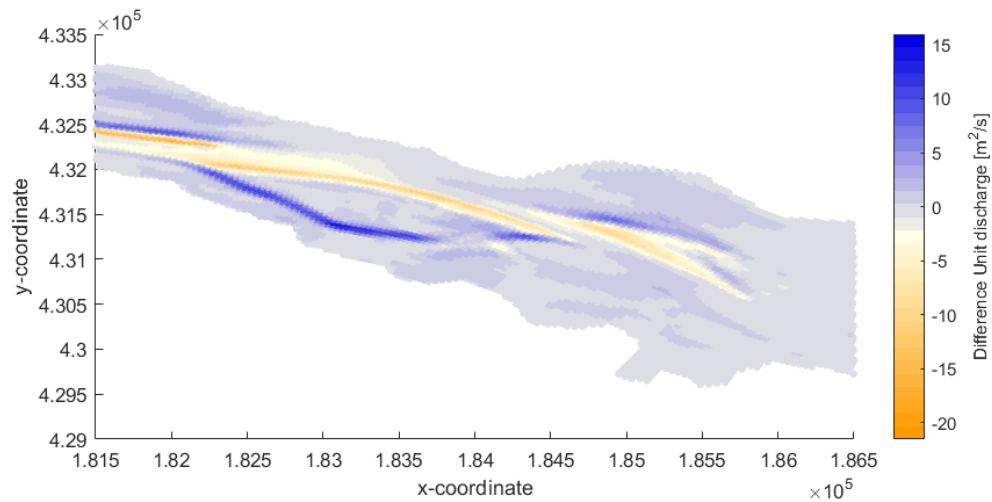


Figure E.12: Difference in unit discharge between the reference situation and the new situation at the location of the first two side channels

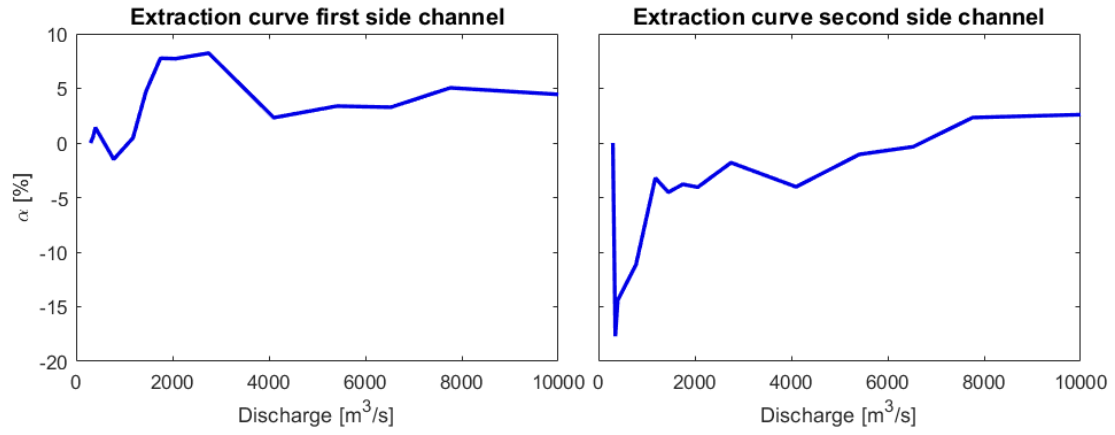


Figure E.13: Extraction curve of the first (left) and second (right) side channel based on unit discharge for the reference and new situation calculated in WAQUA